DOCTORAL DISSERTATION

Continuous Reactor Cascades: an Efficient Toolbox toward Tailor-Made Polymer Materials

Doctoral dissertation submitted to obtain the degree of

Doctor of Science: Chemistry, to be defended by

Evelien Baeten

Promoter: Prof. Dr. Tanja Junkers

Chairman:	Prof. Dr. Jan Colpaert
Promoter:	Prof. Dr. Tanja Junkers
Members of the jury:	Prof. Dr. Wouter Maes
	Prof. Dr. Dirk Vanderzande
	Prof. Dr. Richard Hoogenboom, Ghent University
	Prof. Dr. Philippe Lecomte, University of Liège
	Prof. Dr. Nico Bruns, University of Freiburg

TABLE OF CONTENTS

CHAPTER 1

Introduction

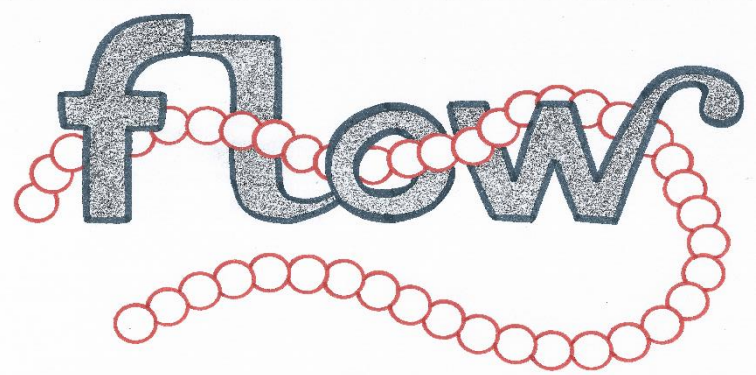

Continuous flow processes – an innovative alternative for conventional batch operations – are associated with many advantages, such as high control over reaction parameters, fast heat exchange, reduced reaction times and high reaction efficiencies. In combination with controlled/"living" polymerization techniques, the polymer field can benefit significantly from microreactor technology and this will lead to a new generation of precise polymer materials. Here, a general introduction will be given on controlled polymerizations, continuous flow processes and the combination of both.

1.1 Polymer chemistry

1.1.1 Polymers – a short history and today's applications

Polymer materials are among the most important substances in our daily life. Some of these materials are inherent to life (like DNA and proteins present in our bodies) or have been provided by nature (such as cotton and rubber).[1] Other polymer materials are synthetic, created by mankind. In 1907, the first synthetic polymer was discovered by Leo Baekeland.[2] This plastic material, bakelite (poly(oxybenzyl methylene glycol anhydride)), became widely-used in every day applications - such as telephone and radio casings. In the 1920s, Hermann Staudinger suggested the term 'macromolecule' for covalently bonded organic molecules with high molecular masses, a revolutionary concept which is often considered as the beginning of the polymer era.[3,4] In 1955, the combined efforts of Karl Ziegler[5] and Giulio Natta[6] led to the use of catalysts in polymerization reactions, boosting polymer applications.[7] Nowadays, only 120 years after the discovery of the first synthetic polymer, polymers have led to unimaginable possibilities: ranging from plastic bottles, coatings and glues, to even medicines and drug carriers.[8-10]

> *"It was very strong and very stiff, unlike anything we had made before. I knew that I had made a discovery. I didn't shout "Eureka!" but I was very excited, as was the whole laboratory excited, and management was excited, because we were looking for something new. Something different. And this was it."*
>
> - Stephanie Kwolek, about the discovery of Kevlar (1965).[9,10]

1.1.2 Polymer molecules vs. macromolecules – definition by IUPAC

Polymer science began with the discovery and synthesis of macromolecules.[11] Yet, originally, the terms 'macromolecules' and 'polymers' (or 'polymer molecules') were not treated as synonyms.[11,12] The term 'macromolecule', originating from the Greek *'makros'* ('large') and the Latin noun *'molecula'* ('small mass')[11] has been suggested in the 1920's by Hermann Staudinger for covalently bonded organic molecules with high molecular masses.[3,4] The term 'polymer' on the other hand can be traced back to the Greek '*polys*' ('many') and *'meros'* ('part').[12] In 1833, the term 'polymerism' was introduced by Jöns Jakob Berzelius to describe the isomerism of two substances with identical relative compositional formulas but with different compositional formulas (such as C_2H_4 and C_4H_8).[12] Strictly speaking, the terms 'macromolecule' and 'polymer' were thus clearly distinctive concepts.[12] The term 'polymer' became a trivialized synonym for 'macromolecules' and both are nowadays considered to be synonyms by IUPAC, where they have been defined as 'a molecule of high relative molecular mass, the structure of which essentially comprises the multiple repetition of units derived, actually or conceptually, from molecules of low relative molecular mass'.[13]

Additionally, a difference can be made between an oligomer and a polymer. The term 'oligomer' can be employed for 'a molecule only existing of a few monomer units', leading to 'a short polymer chain of intermediate relative molecular mass'.[13,14] For a polymer, chain lengths need to be long enough for entanglement to take place. Here, the focus is however directed towards the synthesis of functional materials for biomedical applications, whereby classical polymer properties and polymer entanglement play a minor role. Therefore, a distinction between the terms 'oligomer' and 'polymer' will not further be addressed here.

1.1.3 Step-growth vs. chain-growth polymerizations

To synthesize a macromolecule, monomer molecules are covalently linked during polymerization. Based on the mechanism behind this, a distinction can be made between step-growth and chain-growth polymerizations.[11,15]

Step-growth polymerizations, such as polyaddition and polycondensation reactions, are usually triggered by a catalyst. As its name suggests, the growth of the polymer chain occurs stepwise: monomers first react to form dimers, after which the resulting dimer either reacts with another monomer to form a trimer or reacts with another dimer to form a tetramer, etc. High molecular weight polymers are thus only obtained at high conversions (Figure 1.1).[11,15]

In contrast, chain-growth polymerizations are triggered by an initiator. This initiator reacts with a monomer molecule to form a 'growing polymer chain' (initiation step). This polymer chain can grow upon addition of monomer units to its active site, resulting in the regeneration of the active site (propagation). Hence, high molecular weight polymers can already be obtained at low conversions (free radical and living polymerization, Figure 1.1).[11,16]

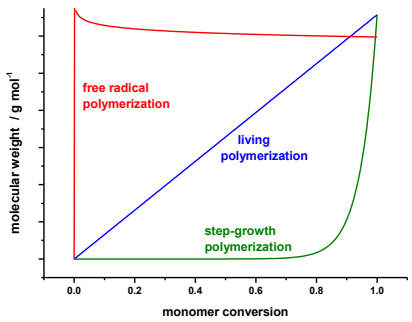

Figure 1.1. Development of molecular weight with increasing monomer conversion for a step-growth, a free radical and a living polymerization.[16]

Depending on the nature (or the functionality) of the active site, chain-growth polymerization can further be divided into different classes: radical, cationic, anionic, and coordination polymerizations. Upon monomer addition, this active site is regenerated. Yet, termination of the active site can also occur by destruction of the reactive center (quenching) or by transfer of its reactive functionality to a different species (chain transfer). These reaction steps are commonly followed in all chain-growth polymerizations. A general mechanism of a free radical polymerization is depicted in Scheme 1.1.[16]

Decomposition	$\mathbf{I_2}$	$\xrightarrow{k_d}$	$\mathbf{2\ I^\bullet}$
Initiation	$\mathbf{I^\bullet + M}$	$\xrightarrow{k_i}$	$\mathbf{R_1^\bullet}$
Propagation	$\mathbf{R_i^\bullet + M}$	$\xrightarrow{k_p}$	$\mathbf{R_{i+1}^\bullet}$
Chain Transfer	$\mathbf{R_i^\bullet + X}$	$\xrightarrow{k_{tr}}$	$\mathbf{P_i + X^\bullet}$
Termination	$\mathbf{R_i^\bullet + R_j^\bullet}$	$\xrightarrow{k_t}$	$\mathbf{P_{i+j}}$ **and/or** $\mathbf{P_i + P_j}$

Scheme 1.1. General mechanism of a free radical polymerization.

In absence of termination or chain transfer reactions, the reactive center of the polymer chain (a radical, anion or cation) stays active for an indefinite period of time.[17,18] Consequently, the polymer keeps on growing until the monomer supply is exhausted. These types of polymerizations were named 'living' polymerizations by Szwarc in 1956 and provide an excellent control over the polymerization.[17,19] The (theoretic) number average molecular weight of the polymer (M_n^{theor}) can thus be controlled and can be predicted via the following equation:

$$M_{\mathrm{n}}^{\mathrm{theor}} = \frac{[M]_0}{[I]_0} \cdot X \cdot M_{\mathrm{M}} + M_{\mathrm{I}} \qquad (1)$$

Hereby, the initial monomer ($[M]_0$) and the initial initiator (or controlling agent) concentration ($[I]_0$) are taken into account, as well as the monomer conversion (X), the molar mass of the monomer (M_{M}) and the molar mass of the initiator (or controlling agent) (M_{I}).[18] Hence, to prove the livingness of the polymerization, a linear relationship between the molecular weight and the conversion should be established, as depicted in Figure 1.1.

The term 'living polymerization' is however often misused in literature. In a recent review, Barner-Kowollik and coworkers addressed this problem by stating the key aspects for a living polymerization process: (i) control over molecular weight by monomer conversion and degree of polymerization (equation 1), (ii) extended lifetime of the propagating chain and (iii) rapid initiation of the initiator or the controlling agent (which often leads to narrow dispersities).[18]

Yet, due to the presence of radical-radical coupling, termination reactions can never be completely avoided in radical polymerizations. The term 'living/controlled radical polymerization' has thus been (mis)used extensively in the past for radical chain-growth polymerization with minimal chain transfer and termination reactions. Therefore, in 2009, IUPAC proposed to use the term 'reversible-deactivation radical polymerizations' (RDRP).[20] Though the terms 'living/controlled radical polymerizations' are still employed nowadays, a clear preference for the official IUPAC term is evident.

1.1.4 Anionic and cationic polymerizations

Ionic chain-growth polymerizations proceed – as its name suggests – via an ionic propagating species: either an anion or a cation. Due to the very strict requirements for the stabilization of this active center, monomer choices are rather limited. Monomers with electron-donating substituents can undergo a cationic polymerization. Monomers possessing electron-withdrawing substituents (or substituents stabilizing a negative charge via delocalization) can undergo an anionic polymerization. Also heterocyclic monomers can undergo an ionic polymerization. These polymerizations occur upon opening of the ring structure, and are called ring-opening polymerizations (ROP). General reaction mechanisms of such an anionic and a cationic ROP are depicted in Scheme 1.2.[16]

Generally, ionic polymerizations proceed as living polymerizations: molecular weights increase linearly with conversion and block copolymers can be synthesized. Ionic polymerizations are extremely sensitive to the presence of impurities. Hence, living characteristics – and thus the absence of early termination reactions – can be reached by providing high reagent purities and inert reaction conditions.[16]

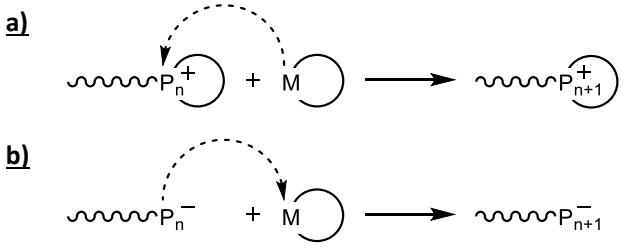

Scheme 1.2. Propagation step of a cationic ring-opening polymerization (CROP) (a) and an anionic ring-opening polymerization (AROP) (b).

1.1.5 Reversible deactivation radical polymerizations

Next to ionic chain-growth, control over a chain-growth polymerization can also be achieved via reversible deactivation radical polymerizations (RDRP). This type of polymerization is a well-established polymerization technique, employable on a daily basis for advanced material synthesis. The fundamental principle of RDRP is the existence of an equilibrium between an active radical and a dormant species, providing control over molecular weight in function of the monomer conversion and the degree of polymerization – which is the key aspect for living chain-growth polymerizations (1.1.3). To establish such an equilibrium over the polymerization reaction, three different 'deactivation' strategies can be followed: deactivation by catalyzed reversible coupling, by spontaneous reversible coupling or by degenerative chain transfer. Anticipating on these strategies, a distinction can be made between atom transfer radical polymerization (ATRP), nitroxide-mediated polymerization (NMP) and reversible addition-fragmentation chain transfer (RAFT) polymerization, respectively. Alternatives based on these fundamental techniques exist as well.

The existence of the equilibrium between an active radical and a dormant species also explains the increased lifetime of a propagating chain. Yet, in contradiction to the living ionic polymerizations, it is not possible to eliminate all chain transfer and termination reactions for radical polymerizations – therefore the term reversible deactivation radical polymerizations (RDRP) is preferred over 'living' or controlled radical polymerizations. The complete absence of transfer and termination reactions is thus never entirely true for radical polymerizations, though these processes are strongly reduced for ATRP and NMP.

Atom transfer radical polymerization (ATRP) – the reversible deactivation radical polymerization whereby the deactivation of the active species occurs via a catalyzed reversible coupling – was independently discovered by Matyjaszewski et al.[21] and Higashimura et al.[22] in 1995. Generally, ATRP employs a transition metal complex Mt/L as catalyst and an alkyl halide R-X as initiator. As depicted in Scheme 1.3, the metal complex Mt^Z/L (the 'activator') can abstract the halogen atom from the dormant polymer species P_n-X (or in an earlier stage from the ATRP initiator R-X) yielding the active radical species $P_n^\bullet$ and the corresponding high oxidation state metal complex $X\text{-}Mt^{Z+1}/L$. By retransferring the halogen to the radical species, the dormant polymer species P_n-X and the low oxidation state metal complex Mt^Z/L can be regenerated, leading to an equilibrium between the active and the dormant polymer species.[23]

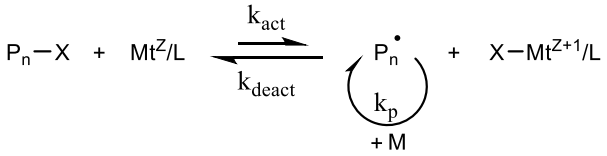

Scheme 1.3. Main equilibrium between active and dormant species during ATRP.

Various metals and ligands have been successfully employed as ATRP catalysts, though copper complexes with *N*-containing ligands are most often used. Nevertheless, classical ATRP requires a high amount of the copper catalyst – a major drawback of this technique. Not only an extra purification step for catalyst removal is required (leading to an increase of the production costs), also the toxicity of the catalyst is detrimental for applicability of ATRP in certain applications (such as biomedical applications).[23]

Hence, different activator regeneration techniques have been proposed as alternatives to classical ATRP to reduce the catalytic amount to only a few ppm. Initiators for continuous activator regeneration (ICAR) ATRP for example employs radical initiators – such as azobisisobutyronitrile (AIBN) – to reactivate the metal complex. In activators regenerated by electron transfer (ARGET) ATRP on the other hand, reducing agents – such as ascorbic acid, glucose, etc. – are used to regenerate the active metal complex by reduction.[23] (Chapter 5)

Nitroxide-mediated polymerizations (NMP) on the other hand, are reversible deactivation radical polymerizations whereby the deactivation of the active species occurs via spontaneous reversible coupling. In 1960, the stable nitroxide radical (2,2,6,6-tetramethylpiperidin-1-yl)oxyl (TEMPO) led to the discovery of NMP.[24] Later, alternatives such as *N*-*tert*-butyl-*N*-[1-diethylphosphono-(2,2-dimethylpropyl)]nitroxide (SG1)[25] and 2,2,5-trimethyl-4-phenyl-3-azahexane-3-nitroxide (TIPNO)[26] have been proposed. As depicted in Scheme 1.4, NMP is thus a rather simple process, occurring in the absence of metal catalysts. The nitroxide radical can trap the active radical species to obtain the dormant species. Upon release of the nitroxide radical, the dormant species is converted to an active radical species.[23]

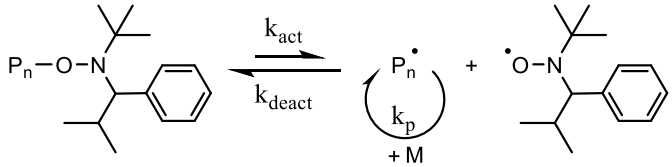

Scheme 1.4. Main equilibrium between an active and dormant species during NMP, when employing TIPNO as radical trapping agent.

The most versatile reversible deactivation radical polymerizations are however the reversible addition-fragmentation chain transfer (RAFT) polymerizations.[27,28] RAFT has many advantages compared to other RDRP methods, due to its suitability to polymerize a broad diversity of monomers within a wide range of reaction conditions. The equilibrium between an active radical and a dormant species is based on the deactivation of the active radical species via degenerative transfer. An active radical species can interact with a RAFT agent, leading to the formation of a (dormant) macroRAFT agent $S=C(Z)SP_m$ and an active radical species $R^{\bullet}$ (pre-equilibrium) (Scheme 1.5a). The released radical species $R^{\bullet}$ will act as initiator for the formation of a new polymer chain. After consumption of the RAFT agent, a symmetrical equilibrium will be established between the propagating radical $P_n^{\bullet}$ and the dormant macroRAFT agent $S=C(Z)SP_n$ (main equilibrium) (Scheme 1.5b).[18,29]

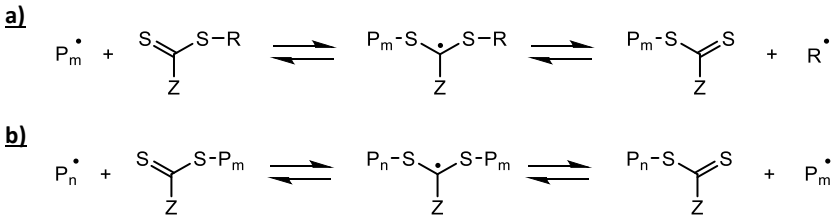

Scheme 1.5. General reaction mechanism of a RAFT polymerization with a) the pre-equilibrium and b) the main equilibrium.

The key aspect here is the rapid consumption of the RAFT agent and thus the rapid conversion of the initial RAFT agent (S=C(Z)SR) to the macroRAFT agent ($S=C(Z)SP_m$). The RAFT agent should thus be chosen carefully, to promote the release of the active radical species $R^{\bullet}$ in preference to the propagating species

$P_m^{\bullet}$. The nature of the RAFT agent is thus crucial for the success of the RAFT polymerization. Its effectiveness is determined by the R and Z substituents, hence the RAFT agent should be selected based on the activity of the monomer. Monomers are therefore divided into two classes: the more activated monomers (MAM) (such as methacrylates, acrylates, acrylamides, styrene, etc.) and the less activated monomers (LAM) (such as vinyl acetate, *N*-vinylpyrrolidone, etc.).[30,31] This also has an important effect on the formation of block copolymers. The RAFT agent, especially the Z-group of the RAFT agent, must be appropriate to control the polymerization of all monomers that comprise the block copolymer. Besides the selection of the RAFT agent, also the order of monomer addition has to be taken into account when targeting block copolymers via RAFT. The first block will serve as macroRAFT agent when polymerizing the second block, hence this dormant species must be a better leaving group than the second monomer (similar to the preferential cleavage of the $R^{\bullet}$ compared to $P_m^{\bullet}$ when targeting homopolymers). Thus, more activated monomers should be introduced before less activated monomers (methacrylates >> styrenes, acrylates, acrylamides > vinyl acetates, *N*-vinylpyrrolidone).[23,29]

Next to the monomer order requirement, also the effect of initiator concentration plays an important role when targeting block copolymers via RAFT. The initiator concentration directly determines the speed of the reaction but it has a tremendous influence on the end group fidelity of the polymer. The more initiator is added, the more dead chains are formed and thus a low end group fidelity of the ω end group ('the end of the polymer chain') is achieved. In fact, employing 1/0.01 ratio between the RAFT agent and initiator leads to 99% livingness L, as can be calculated at any point in time (t) via the following equation:

$$L = \frac{[CTA]_0}{[CTA]_0 + 2\,f\,[I]_0\,(1 - \mathrm{e}^{-k_d t})(1 - \frac{f_c}{2})} \qquad (2)$$

Hereby, the RAFT agent concentration $[CTA]_0$, the initiator concentration $[I]_0$, the initiator efficiency f and the initiator dissociation constant k_d are taken into account. Also radical-radical coupling is taken into account by the term $1 - \frac{f_c}{2}$ as the number of chains produced by bimolecular termination (with f_c the coupling factor = 1 for combination and f_c = 0 for disproportionation).[32,33]

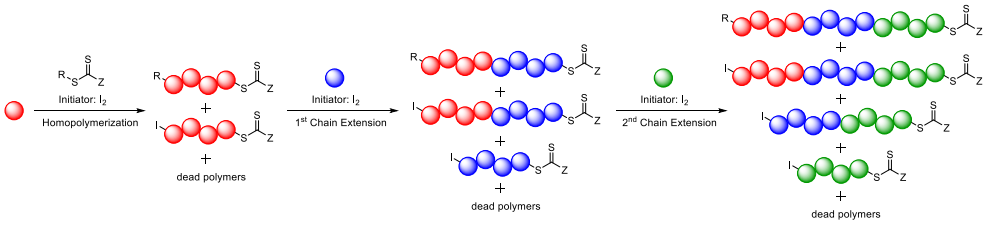

Figure 1.2: Influence of the α and ω end group functionality on the polymer product when targeting multiblock copolymers via RAFT.

On first glance, this seems the most important information to access multiblock copolymers via chain extension. Yet, also the other chain end, the α chain end ('the start of the polymer chain') plays an important role (Figure 1.2). The mechanism of a RAFT polymerization (Scheme 1.5) suggests a bimodal existence for this α chain end for every RAFT polymer. The majority of the polymers carries the 'R-group', while some polymers were initiated by the initiator ('I-group') as α chain end. Hence, when targeting block copolymers, also the α chain end has tremendous effects, as will also later be seen in Chapter 4.[29,33]

1.1.6 Polymer architectures

The physical properties of a polymer are determined by its macromolecular architecture. Due to the use of advanced polymerization techniques, different complex polymer architectures are accessible and control over melting point, solubility and critical solution temperature can be achieved. In addition, macromolecular architecture also influences the mechanical properties, and thus directly determines the possible applicability of the final product. The architecture of a polymer is mainly determined by its composition, its functionality and its topology (Figure 1.3).

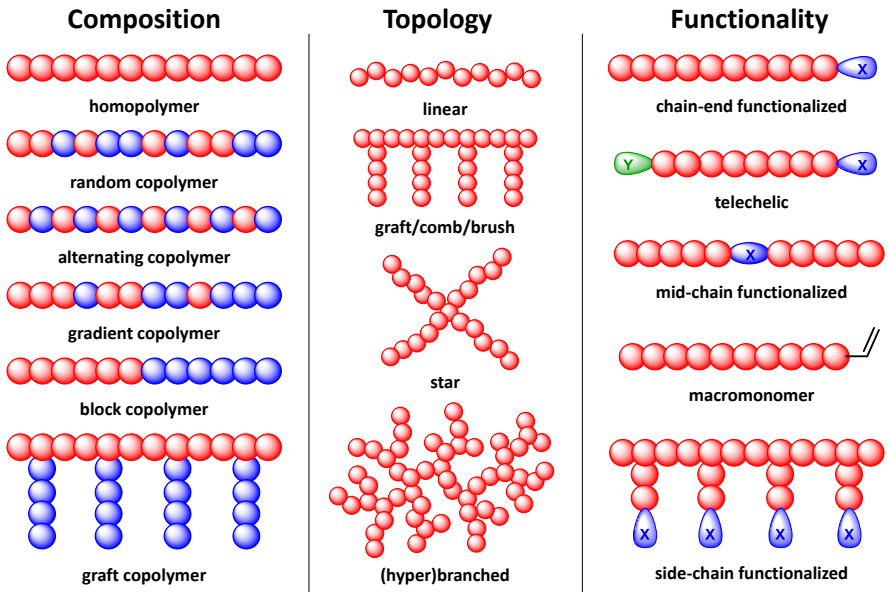

Figure 1.3. Overview of different polymer architectures, divided into 3 categories: polymer composition, polymer topology and polymer functionality.

'Polymer composition' is basically the order of monomer units along the backbone of the polymer. The simplest composition – a homopolymer – only consists of one type of monomer units. Copolymers – consisting of at least two different monomers – can exhibit different compositions, depending on the distribution of the different monomer units along the backbone (random/alternating/block-like/graft-like/gradient).

'Polymer topology' on the other hand is related to the shape of the polymer structure. A linear polymer chain can be considered as the simplest topology. Yet, more complex shapes can be obtained as well. By using multifunctional initiators, star polymers can be synthesized. Crosslinking leads to (hyper)branched structures and polymer networks. Grafted/comb/brush polymers can be obtained via chemical modifications on the polymer side chains or via the use of macromonomers.

The last criteria, the 'polymer functionality', is the possible presence (and the position) of a chemical functionality. Functional groups can be introduced at the beginning or at the end of a polymer chain by using a functional initiator or termination agent (quench). Yet, these functionalities can also be located at the polymer side chains or at the center of the polymer chain.

1.1.7 Perspectives of polymer chemistry

Polymers can be found nearly everywhere in our daily life, for example in plastic usables, vehicles and city routes. These 'plastic' materials are also the main concern and thus the major income of the traditional polymer industry. Yet, different applications are still sought and found by the polymer field. More and more polymers inspired by nature are investigated nowadays, to mimic biological activity or to be used in biomedical applications.

In addition, the focus of polymer research is also directed towards precise control over molecular architecture, enabling the synthesis of more specialized materials via the use of controlled/living polymerization techniques.[34] Still, fundamental mechanistic and kinetic studies are needed to gain a deeper understanding of the correlation between the molecular structure of a polymer and its macroscopic properties – and how to control both.[34,35] The use of flow chemistry might be the ideal tool for these investigations, as discussed further.

1.2 Flow chemistry

Traditionally, organic reactions and (controlled) polymerizations are carried out in round-bottom flasks and standardized glassware. Such batch approach is still commonly used in research laboratories worldwide.[36] Yet, optimization and tuning of reaction conditions in batch processes is usually very time and energy consuming and the ability to upscale reactions from milligram to gram-scale is severely limited.[37] Due to these issues regarding optimization and upscaling, alternatives to batch processes are sought. The use of microreactor technology (MRT) has been proposed as alternative since it features many advantages in comparison to batch-wise chemistry,[36] which will further be discussed. First, the material and flow characteristics of MRT will be elucidated, followed by a brief comparison to batch chemistry and a short outlook.

1.2.1 Characteristics of microfluidic set-ups

As the name suggests, microreactor technology employs miniaturized flow reactors to carry out a continuous flow process. These microfluidic reactors essentially consist of well-defined three-dimensional structured reactor channels (with inner diameter of less than 1 mm in size), often embedded in a flat 'reactor chip'.[37-40] The reactor chips itself can be made of a variety of materials, such as silicon, glass, metals and polymers.[37,38] Yet, glass reactor chips are the most popular due to their chemical inertness towards most reagents and solvents and their transparency allowing for visual inspection of a reaction.[37] Glass microreactors are usually produced via photolithography, though other fabrication methods exist depending on the employed material.[38]

Various commercial microreactors are available nowadays. Within the scope of this thesis, a Labtrix® Start set-up was employed as a continuous flow process at microscale (Figure 1.4 – 1.5, Chapter 2-3). This microreactor system is commercially available, features a high versatility and is equipped with changeable reactor chips that can be operated in a broad window of reaction conditions. Reactor chips can be chosen based on the volume (1 μL – 19.5 μL) and number of fluidic input connections (2 to 5), enabling an easy switch to a completely different reaction set-up depending on the requirements of a certain reaction. Additionally, reaction conditions can easily be controlled. Temperatures can be varied between –20°C and 195°C, up to pressures of 25 bar, while residence times on the other hand can be varied from 1.2 s to 97.5 min (depending on the reactor volume and the flow rate).[41]

Figure 1.4. Commercially available Labtrix® Start set-up.

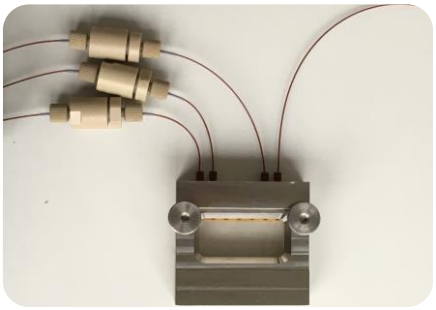

Figure 1.5. The microreactor unit of a Labtrix® Start set-up.

When larger residence times, or larger reactor volumes, are required, a switch to larger reactor systems can be made. Again, various commercial systems are available. Yet, within the scope of this thesis, a home-made tubular reactor was employed (Figure 1.6 – 1.7) (Chapter 4 and 6). Often, the term 'meso-reactor' is employed when internal volumes are situated in the milliliter range (ID reactor channel ~ mm).[42,43] The use of tubular reactors allows for a very simple building-block or modular approach, whereby every part of the set-up (micromixers, fittings, back pressure regulators, etc.) can be exchanged or modified. Thereby, different tubular reactors can easily be connected together, as independent self-contained units, allowing for multistep reactions. This feature makes tubular reactor systems even more attractive.

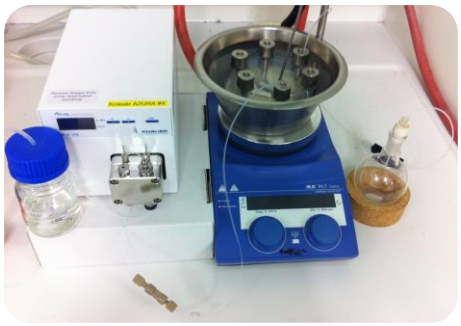

Figure 1.6. Home-made tubular reactor set-up.

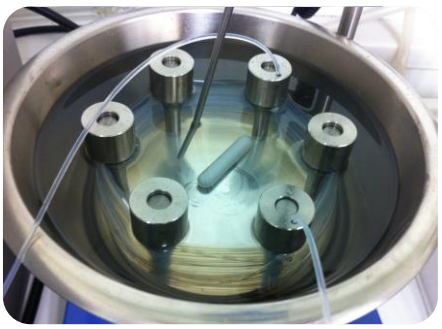

Figure 1.7. Tubular reactor, with reactor channels of 0.75 mm inner diameter.

1.2.2 Flow Characteristics

An important aspect of microreactors is the hydrodynamic flow in the microchannels.[39] The dimensionless Reynold's number (Re) can be used to predict flow patterns in fluid dynamics. Flow profiles can either be laminar ($\mathrm{Re} < 2300$) or turbulent (> 4000). For tubular reactors, Reynold's number is defined by:

$$\mathrm{Re} = \frac{Q\,D}{\nu\,A} \qquad (3)$$

whereby the volume flow rate $Q\ \left(\frac{\mathrm{m}^3}{\mathrm{s}}\right)$, the hydrodynamic diameter $D\ (\mathrm{m})$, the kinematic viscosity $\nu\ \left(\nu = \frac{\mu}{\rho}\right)\ \left(\frac{\mathrm{m}^2}{\mathrm{s}}\right)$ and the cross-sectional area $A\ (\mathrm{m}^2)$ are taken into account. Microfluidic systems have a Reynold's number below 1000, often even below 100, and thus a laminar flow profile.[39,40] Hereby, the fluid passes through the tubing in layers parallel to flow direction, without any lateral mixing. Essential to control the residence time of a fluid element inside a reactor (and thus its 'reaction time') is its residence time distribution.[39] To assure the same residence time for every fluid element, a plug flow would be ideal for a microfluidic reactor.[44] All fluid elements in the solution at a certain cross-section of the reactor should then have the same velocity while back mixing would not occur. Hence, microfluidic reactors provide a laminar plug profile in the ideal case, as depicted in Figure 1.8, allowing fluid to flow in parallel layers with the same velocity. Naturally, in practice, any shape deviation (turn, mixer unit, fitting, etc.) in the reactor unit might give a deviation from this ideal case.[44]

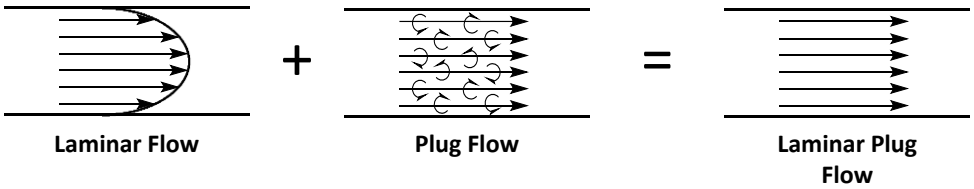

Figure 1.8. Laminar plug flow pattern in a microfluidic reactor.

1.2.3 Beneficial features of microreactors

The most beneficial feature of a microreactor is a **high surface-to-volume ratio**, due to its intrinsic small and well-defined reactor channels. The surface-to-volume ratio for a microreactor is situated between 10 000 – 50 000 m^2/m^3 compared to 100 – 1000 m^2/m^3 for batch reactors.[39,40] This difference results in a better thermal heat transfer when compared to batch, leading to a uniform temperature distribution in the microreactor. Especially for highly endo- or exothermic reactions, these isothermal conditions (absence of hot spots) result in the suppression of undesirable side reactions leading to higher yields, less product impurities and in case of polymers a better definition of the obtained material.[45,46] By working under slightly elevated pressure, unconventional temperature regimes above the boiling point of the solvent can be reached.[47] Combined with an improved mass transport, due to the short diffusion lengths in microreactors, reactions can thus largely be accelerated and full conversions can be reached in shorter reaction times when compared to batch processes.[39,47]

Next, MRT provides a very **precise control over different reaction parameters**. Temperature, pressure and the reactor residence time can easily be adjusted, allowing for a simple screening and optimization of reaction conditions.[46-48] Chosen reaction conditions are also highly reproducible and allow for very stable operation over extended periods of time.[43,47] The intrinsic small volume, and the ability to perform multistep reactions in a closed system, also assures a lower hazard potential and higher safety when working with strongly exothermic reactions, explosive reactions or toxic substances.[45,46,48]

Furthermore, **upscaling** optimized continuous flow processes employing MRT is much simpler than upscaling batch processes. To simply increase the amount of obtained product, longer reaction run times can be employed for continuous processes – the so-called 'scale-out' principle.[47,48] This way, a larger amount of product can be obtained, though the production rate (amount/h) is kept constant. To really upscale a production process, an increase of the output flow can be provided. A questionable upscale-method, is the "numbering-up", a principle where several reactors are placed in parallel assuring identical modes. "Numbering-up" can either be done externally, by placing whole reactor set-ups (reactor + pumping system + process control) in parallel, or internally by sharing the pumping system and process control over several reactors.[43,49] It has been claimed that the latter is more economically feasible. However, the key aspect for internal "numbering-up" – the distribution of the reaction streams over the different reactors – is still challenging from a technical point of view.[36,37,40]

Naturally, a more straightforward approach can be followed by adapting an existing flow procedure to larger continuous flow reactors (with a bigger reactor volume).[48] As an example, a procedure applicable for a Labtrix® Start system (mg to g scale) can be adapted to a KiloFlow® (kg scale) or Plantrix® (tons scale) system without the need for extensive re-optimizations.[41] Naturally, this commercially available series of Chemtrix BV is only one example and many more possibilities exist. A microfluidic procedure can for example also be upscaled to a home-made tubular reactor set-up. Yet, upscaling to a larger reactor unit might be more challenging than it seems, due to changes in the thermal and mass transportation properties or safety reasons.[48]

1.2.4 Challenges of microreactor technology

The potential of microfluidic reactors has already been explored extensively. Yet, given their characteristics, microfluidic reactors also have their restrictions. The reaction time range is rather limited due to the intrinsic small reactor volumes.[37,46] To obtain a significant amount of product or to produce a certain amount of product, collection times are extensive (time/yield). Equipment costs are rather high. Yet, these disadvantages can be overcome quite easily. To use longer reaction times or to obtain more product outcome, a bigger reactor might be useful, while equipment costs might be compensable by production costs.

In fact, microreactor technology has only one major disadvantage: its limited applicability to only those reactions compatible with the continuous nature of chemistry.[46] The formation of solids or highly viscous substances must be avoided at all times.[37] The presence of precipitates, dust particles or even the increase in product viscosity, will inevitably lead to an internal pressure increase.[46] Any of these can lead to reactor fouling or reactor clogging, causing a disruption of the continuous flow[46] (an example of a clogged reactor chip is shown in Figure 1.9). The major challenge of microreactor technology is thus dealing with this disadvantage. Often, reaction conditions can be adjusted accordingly.[46] Yet, specialized reactor set-ups have been designed as well, to deal with the formation of precipitates.[50,51]

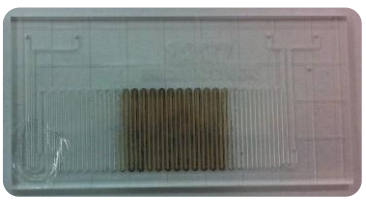

Figure 1.9. Example of a clogged Labtrix® 3227 reactor.

1.2.5 Perspectives of flow chemistry

In most research laboratories worldwide, chemical investigations still take place in batch-wise approaches. Usually only chemical considerations are taken into account (on laboratory scale), while technical aspects are neglected. Yet, terms like "industrialization" and "automation" are the major driving forces in industry.[36]

By implementing flow chemistry in research laboratories, large scale-production can be mimicked on laboratory scale, slowly bridging the gap between academic research and industry.[42] The enormous industrial interest[52-56] and multiple industrial projects in academia[57] support that thought. Flow chemistry research on the other hand, should not only focus on proof-of-concept demonstrations, but also on its future: its applicability as practical technology.[58]

Figure 1.10. Old-fashioned batch ~~alchemy~~ chemistry.[59]

1.3 Continuous polymerization processes

1.3.1 Microreactor technology in polymer science

Many beneficial features of microreactor technology (MRT) have been described above. Especially the high surface-to-volume ratio – and thus the excellent thermal heat transfer – makes MRT an interesting tool for polymerization reactions.[45,46] Still, MRT did not become an area of broad interest for polymer chemistry until the late 1990s, mostly due to the challenges arising from inherently high viscosities of polymer solutions.[46] Nowadays, MRT represents an emerging field in polymer science.[40] Microreactors have already been employed for all kind of polymerizations, as also will be demonstrated throughout this thesis.

1.3.2 Continuous polymerizations

The first 'living' anionic polymerizations were investigated in 1956, by Swarc and coworkers (as mentioned before).[17] In 1962, the same research group built one of the first continuous set-ups.[60] Concurrently, Schulz and coworkers also conducted kinetic studies on the anionic polymerization of styrene in a continuous flow reactor.[61,62] Despite its success, the area remained almost dormant in academic research until the late 1990s.[40,46] Picked up by Müller and co-workers, the anionic polymerization of methyl methacrylate was shown as an elegant example in 1997. Narrow polydispersities were reached ($1.04 \leq Đ \leq 1.08$), illustrating the potential of continuous flow for anionic polymerizations.[63]

This pioneering work on continuous anionic polymerization was the start of the era of continuous polymerizations. Cationic polymerizations in flow were first reported in 2004 by Yoshida and coworkers, whereby a 'cation pool' (generated in a microfluidic electrochemical system) was employed as effective initiator.[64-68] Free radical polymerizations have also been carried out in microreactors. The superior heat and mass transfer, as well as the use of low viscosities in MRT, suppresses the Trommsdorff effect (or the so-called gel effect), leading to better control over the molecular weight distribution.[11,69] Next to free radical polymerizations, also reversible-deactivation radical polymerizations (RDRP) benefit from MRT. Continuous atom transfer radical polymerizations (ATRP)[70-74] and derivatives such as activator regenerated by electron transfer (ARGET) ATRP[74,75] have already been carried out. Single electron transfer living radical polymerizations (SET-LRP) on the other hand can employ a copper tubing as reactor and catalyst source simultaneously.[76,77] Nitroxide-mediated polymerizations (NMP)[78-80] and reversible addition-fragmentation chain transfer (RAFT)[47,81-83] polymerizations have also been carried out continuously. Continuous photopolymerizations have attracted a lot of interest as well, due to the improved illumination in a microflow reactor (related to the shortened optical path lengths). For example, the photo-induced copper-mediated polymerization (photoCMP) can be carried out in microflow, by directly activating the active copper catalyst by UV-light.[84-86]

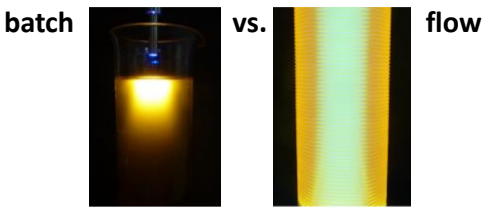

Figure 1.11. Improved illumination in a microfluidic reactor.[84]

1.3.3 Continuous polymer conjugations and modifications

Besides polymerizations, also polymer-polymer conjugations can be carried out under continuous conditions. For example, continuous copper catalyzed azide-alkyne 1,3-dipolar cycloaddition (CuAAC) reactions have first been investigated for small molecules,[87] but can also be employed to chemically link two well-defined polymers.[88] Additionally, microfluidic reactors can be employed for end group modification of a well-defined polymer as well. For example, in-situ aminolysis of well-defined polymers obtained via RAFT can be carried out in a microreactor chip, followed by a base-catalyzed thiol-ene reaction in one-pot.[88,89]

1.3.4 Outlook

In summary, the polymer field can benefit tremendously from microreactor technology (MRT). Many polymerizations have been found to proceed faster and with better control when performed in flow, which is a significant advantage in the realm of precision polymer design. Naturally, this introduction was only meant to give a rough idea on the potential of MRT for the polymer field. A more complete overview is given in some excellent reviews and can thus be found elsewhere.[40,46,90] A lot of progress has been made during the last decade. Still, most polymerizations performed in MRT so far were carried out as proof of concept rather than for the continuous synthesis of larger amounts of functional materials. Yet, as Frey and coworkers[46] noted: "microreactor technology has only begun to show its eminent potential for controlled polymerizations".

1.4 Aim and outline of the thesis

The aim of the research presented in this thesis is the development of microfluidic reactor cascades as a polymer toolbox to synthesize more specialized polymer materials. Different polymerization techniques (anionic, cationic, free radical, ATRP, NMP, RAFT, …) were already investigated under continuous conditions. Based on these experiments and the beneficial features of MRT for these reactions, these different polymerization techniques were used to synthesize complex polymer materials to be used in biomedical applications. Yet, going for more precise and more specialized polymer materials, different polymerization or modification steps have to be carried out. By connecting several reactors in tandem – and thus employing a so-called reactor cascade – these polymerization and modification steps can be carried out in one go. The use of such connected reactor cascades allows for continuous production of the specialized material, and thus for a simple production route for future applications.

In **Chapter 2**, cationic ring-opening polymerizations of 2-oxazolines were investigated in continuous microflow reactors. The homopolymerizations of 2-ethyl-2-oxazoline and 2-*n*-propyl-2-oxazoline were investigated, aiming for full monomer conversions. Well-defined diblock and triblock copolymers were targeted in a later stage, employing a microfluidic reactor cascade.

Chapter 3 describes the anionic ring-opening polymerization of cyclic phosphates, directly enabling the continuous synthesis of linear poly(phosphoester)s. The polymerization of 2-isobutoxy-2-oxo-1,3,2-dioxaphospholane was optimized,

employing two organocatalytic systems. Next, 2-butenoxy-2-oxo-1,3,2-dioxaphospholane, containing an alkene functionality in the side chain, was polymerized and continuously post modified via a UV-induced radical thiol-ene reaction in a two-stage reactor set-up.

Chapter 4 focuses on the synthesis of well-defined acrylate-based multiblock copolymers via reversible addition-fragmentation chain transfer (RAFT) polymerization in a fully continuous multireactor cascade. Based on theoretical considerations, reactor volumes and reactant concentrations were optimized. A broad variety of homo-, diblock, triblock and tetrablock copolymers was obtained.

In **Chapter 5**, continuous enzymatic controlled radical polymerizations were investigated. Therefore, a reversible immobilization route of hemoglobin (Hb) towards an enzyme-immobilized microreactor was developed, in order to perform enzyme-catalyzed controlled radical polymerizations. Secondly, the continuous homogeneous polymerization of 4-acryloylmorpholine (AcMo) – via the use of Hb as catalyst – was investigated. In a later stage, the Hb-immobilized reactor chips were tested to carry out the enzyme-catalyzed radical polymerization of AcMo.

Chapter 6 describes the preparation of cyclic polymers via a ring-closure strategy carried out in a looped flow reactor. First, a looped flow procedure was developed in order to increase the reaction efficiency and to reduce the amount of solvent. Afterwards, the intramolecular coupling of the chain ends of the linear precursor was investigated under continuous flow conditions. In a later stage, cyclic polymers were prepared via the use of a looped flow reactor.

All experimental details of the work in this thesis have been compiled in **Chapter 7**, including the materials and characterization methods, followed by a general summary and outlook in **Chapter 8**.

1.5 References

(1) Heinrich, M. T. *Kunststoffen vandaag en morgen* **1986**.

(2) Roosens, L.; Lepoivre, J. A.; Schrooten, J. *Essay voor het Chemie-Onderwijs (EChO) - 11 Reuzenmoleculen - Art 01 Baekeland*.

(3) Staudinger, H. *Berichte der deutschen chemischen Gesellschaft (A and B Series)* **1924**, *57*, 1203.

(4) Mülhaupt, R. *Angewandte Chemie International Edition* **2004**, *43*, 1054.

(5) Ziegler, K.; Holzkamp, E.; Breil, H.; Martin, H. *Angewandte Chemie* **1955**, *67*, 541.

(6) Natta, G.; Pino, P.; Corradini, P.; Danusso, F.; Mantica, E.; Mazzanti, G.; Moraglio, G. *Journal of the American Chemical Society* **1955**, *77*, 1708.

(7) Deelstra, H.; Lepoivre, J. A.; Schrooten, J. *Essay voor het Chemie-Onderwijs (EChO) - 11 Reuzenmoleculen - Art 03 Ziegler en Natta*.

(8) De Cock, Y.; Lepoivre, J. A.; Schrooten, J. *Essay voor het Chemie-Onderwijs (EChO) - 11 Reuzenmoleculen - Art 05 Plastics*.

(9) *http://www.dupont.com/products-and-services/fabrics-fibers-nonwovens/fibers/articles/joel-westfahl-story.html, retrieved on 21-06-2017.*

(10) *'Women in Chemistry: Stephanie Kwolek' (video file) https://www.youtube.com/watch?v=L1pepaAdkWA, retrieved on 21-06-2017.*

(11) Elias, H.-G. *An introduction to polymer science*; 1 ed., 1996.

(12) Jensen, W. B. *Journal of Chemical Education* **2008**, *85*, 624.

(13) Jenkins, A. D.; Jones, R. G.; Moad, G. In *Pure And Applied Chemistry* 2009; Vol. 82, p 483.

(14) Naka, K. In *Encyclopedia of Polymeric Nanomaterials*; Kobayashi, S., Müllen, K., Eds.; Springer Berlin Heidelberg: Berlin, Heidelberg, 2014, p 1.

(15) Elias, H.-G. *Macromolecules - Volume 1: Chemical structures and syntheses*; Wiley-VCH Verlag Gmbh & Co. KGaA, Weinheim, 2005.

(16) Odian, G. *Principles of polymerization*; fourth edition ed.; John Wiley & Sons, 2004.

(17) Szwarc, M. *Nature* **1956**, *178*, 1168.

(18) Stenzel, M. H.; Barner-Kowollik, C. *Materials Horizons* **2016**, *3*, 471.

(19) Szwarc, M. *Polymer Chemistry* **1998**, *36*, 9.

(20) Jenkins, A. D.; Jones, R. G.; Moad, G. *Pure And Applied Chemistry* **2010**, *82*, 483.

(21) Wang, J.-S.; Matyjaszewski, K. *Journal of the American Chemical Society* **1995**, *117*, 5614.

(22) Kato, M.; Kamigaito, M.; Sawamoto, M.; Higashimura, T. *Macromolecules* **1995**, *28*, 1721.

(23) *Aldrich - Controlled Radical Polymerization Guide*.

(24) Kermagoret, A.; Gigmes, D. *Tetrahedron* **2016**, *72*, 7672.

(25) Benoit, D.; Grimaldi, S.; Finet, J. P.; Tordo, P.; Fontanille, M.; Gnanou, Y. In *Controlled Radical Polymerization*; American Chemical Society: 1998; Vol. 685, p 225.

(26) Benoit, D.; Chaplinski, V.; Braslau, R.; Hawker, C. J. *Journal of the American Chemical Society* **1999**, *121*, 3904.

(27) Chiefari, J.; Chong, Y. K.; Ercole, F.; Krstina, J.; Jeffery, J.; Le, T. P. T.; Mayadunne, R. T. A.; Meijs, G. F.; Moad, C. L.; Moad, G.; Rizzardo, E.; Thang, S. H. *Macromolecules* **1998**, *31*, 5559.

(28) Chong, Y. K.; Le, T. P. T.; Moad, G.; Rizzardo, E.; Thang, S. H. *Macromolecules* **1999**, *32*, 2071.

(29) Keddie, D. J. *Chemical Society Reviews* **2014**, *43*, 496.

(30) Chiefari, J.; Mayadunne, R. T. A.; Moad, C. L.; Moad, G.; Rizzardo, E.; Postma, A.; Thang, S. H. *Macromolecules* **2003**, *36*, 2273.

(31) Chong, Y. K.; Krstina, J.; Le, T. P. T.; Moad, G.; Postma, A.; Rizzardo, E.; Thang, S. H. *Macromolecules* **2003**, *36*, 2256.

(32) Gody, G.; Maschmeyer, T.; Zetterlund, P. B.; Perrier, S. *Nature Communications* **2013**, *4*, 2505.

(33) Vandenbergh, J.; Junkers, T. *Macromolecules* **2014**, *47*, 5051.

(34) Braunecker, W. A.; Matyjaszewski, K. *Progress in Polymer Science* **2007**, *32*, 93.

(35) Destarac, M. *Macromolecular Reaction Engineering* **2010**, *4*, 165

(36) Jas, G.; Kirschning, A. *Chemistry – A European Journal* **2003**, *9*, 5708.

(37) Geyer, K.; Codée, J. D. C.; Seeberger, P. H. *Chemistry – A European Journal* **2006**, *12*, 8434.

(38) Fletcher, P. D. I.; Haswell, S. J.; Pombo-Villar, E.; Warrington, B. H.; Watts, P.; Wong, S. Y. F.; Zhang, X. *Tetrahedron* **2002**, *58*, 4735.

(39) Jähnisch, K.; Hessel, V.; Löwe, H.; Baerns, M. *Angewandte Chemie International Edition* **2004**, *43*, 406.

(40) Tonhauser, C.; Natalello, A.; Löwe, H.; Frey, H. *Macromolecules* **2012**, *45*, 9551.

(41) *Labtrix, Kiloflow and Plantrix Brochures, distributed by Chemtrix BV.*

(42) Wegner, J.; Ceylan, S.; Kirschning, A. *Advanced Synthesis & Catalysis* **2012**, *354*, 17.

(43) Cambié, D.; Bottecchia, C.; Straathof, N. J. W.; Hessel, V.; Noël, T. *Chemical Reviews* **2016**, *116*, 10276.

(44) Davis, M. E.; Davis, R. J. *Fundamentals of chemical reaction engineering*; McGraw-Hill Higher Education , New York, NY., 2003.

(45) Jensen, K. F. *Chemical Engineering Science* **2001**, *56*, 293.

(46) Wilms, D.; Klos, J.; Frey, H. *Macromolecular Chemistry and Physics* **2008**, *209*, 343.

(47) Vandenbergh, J.; de Moraes Ogawa, T.; Junkers, T. *Journal of Polymer Science Part A: Polymer Chemistry* **2013**, *51*, 2366.

(48) Wiles, C.; Watts, P. *European Journal of Organic Chemistry* **2008**, 1655.

(49) Su, Y.; Kuijpers, K.; Hessel, V.; Noel, T. *Reaction Chemistry & Engineering* **2016**, *1*, 73.

(50) Hartman, R. L. *Organic Process Research & Development* **2012**, *16*, 870.

(51) Fernandez Rivas, D.; Cintas, P.; Gardeniers, H. J. G. E. *Chemical Communications* **2012**, *48*, 10935.

(52) Hessel, V. *Chemical Engineering & Technology* **2005**, *28*, 243.

(53) Roberge, D. M.; Ducry, L.; Bieler, N.; Cretton, P.; Zimmermann, B. *Chemical Engineering & Technology* **2005**, *28*, 318.

(54) Markowz, G.; Schirrmeister, S.; Albrecht, J.; Becker, F.; Schütte, R.; Caspary, K. J.; Klemm, E. *Chemical Engineering & Technology* **2005**, *28*, 459.

(55) Kirschneck, D.; Tekautz, G. *Chemical Engineering & Technology* **2007**, *30*, 305.

(56) Roberge, D. M.; Zimmermann, B.; Rainone, F.; Gottsponer, M.; Eyholzer, M.; Kockmann, N. *Organic Process Research & Development* **2008**, *12*, 905.

(57) *Persmededeling 28-10-2016, by Essencia Vlaanderen and FISCH-Flanders*.

(58) Whitesides, G. M. *Nature* **2006**, *442*, 368.

(59) Pont, J. *Chemistry Today* **2009**, *27*, 3.

(60) Geacintov, C.; Smid, J.; Szwarc, M. *Journal of the American Chemical Society* **1962**, *84*, 2508.

(61) Barnikol, V. W. K. R.; Schulz, G. V. *Die Makromolekulare Chemie* **1963**, *68*, 211.

(62) Löhr, G.; Schmitt, B. J.; Schulz, G. V. *Zeitschrift für Physikalische Chemie* **1972**, *78*, 177.

(63) Baskaran, D.; Müller, A. H. E. *Macromolecules* **1997**, *30*, 1869.

(64) Yoshida, J.-i.; Suga, S.; Suzuki, S.; Kinomura, N.; Yamamoto, A.; Fujiwara, K. *Journal of the American Chemical Society* **1999**, *121*, 9546.

(65) Suga, S.; Suzuki, S.; Yamamoto, A.; Yoshida, J.-i. *Journal of the American Chemical Society* **2000**, *122*, 10244.

(66) Yoshida, J.-i.; Suga, S. *Chemistry – A European Journal* **2002**, *8*, 2650.

(67) Nagaki, A.; Kawamura, K.; Suga, S.; Ando, T.; Sawamoto, M.; Yoshida, J.-i. *Journal of the American Chemical Society* **2004**, *126*, 14702.

(68) Yoshida, J.; Nagaki, A.; Iwasaki, T.; Suga, S. *Chemical Engineering & Technology* **2005**, *28*, 259.

(69) Iwasaki, T.; Yoshida, J.-i. *Macromolecules* **2005**, *38*, 1159.

(70) Shen, Y.; Zhu, S.; Pelton, R. *Macromolecular Rapid Communications* **2000**, *21*, 956.

(71) Shen, Y.; Zhu, S. *AIChE Journal* **2002**, *48*, 2609.

(72) Wu, T.; Mei, Y.; Cabral, J. T.; Xu, C.; Beers, K. L. *Journal of the American Chemical Society* **2004**, *126*, 9880.

(73) Müller, M.; Cunningham, M. F.; Hutchinson, R. A. *Macromolecular Reaction Engineering* **2008**, *2*, 31.

(74) Hu, X.; Zhu, N.; Fang, Z.; Li, Z.; Guo, K. *European Polymer Journal* **2016**, *80*, 177.

(75) Chan, N.; Boutti, S.; Cunningham, M. F.; Hutchinson, R. A. *Macromolecular Reaction Engineering* **2009**, *3*, 222.

(76) Chan, N.; Cunningham, M. F.; Hutchinson, R. A. *Macromolecular Rapid Communications* **2011**, *32*, 604.

(77) Burns, J. A.; Houben, C.; Anastasaki, A.; Waldron, C.; Lapkin, A. A.; Haddleton, D. M. *Polymer Chemistry* **2013**, *4*, 4809.

(78) Enright, T. E.; Cunningham, M. F.; Keoshkerian, B. *Macromolecular Reaction Engineering* **2010**, *4*, 186.

(79) Zitlalpopoca-Soriano, A. G.; Vivaldo-Lima, E.; Flores-Tlacuahuac, A. *Macromolecular Reaction Engineering* **2010**, *4*, 599.

(80) Zitlalpopoca-Soriano, A. G.; Vivaldo-Lima, E.; Flores-Tlacuahuac, A. *Macromolecular Reaction Engineering* **2010**, *4*, 516.

(81) Diehl, C.; Laurino, P.; Azzouz, N.; Seeberger, P. H. *Macromolecules* **2010**, *43*, 10311.

(82) Hornung, C. H.; Nguyen, X.; Kyi, S.; Chiefari, J.; Saubern, S. *Australian Journal of Chemistry* **2013**, *66*, 192.

(83) Li, Z.; Chen, W.; Zhang, L.; Cheng, Z.; Zhu, X. *Polymer Chemistry* **2015**, *6*, 5030.

(84) Wenn, B.; Conradi, M.; Carreiras, A. D.; Haddleton, D. M.; Junkers, T. *Polymer Chemistry* **2014**, *5*, 3053.

(85) Chuang, Y.-M.; Wenn, B.; Gielen, S.; Ethirajan, A.; Junkers, T. *Polymer Chemistry* **2015**, *6*, 6488.

(86) Railian, S.; Wenn, B.; Junkers, T. *Journal of Flow Chemistry* **2016**, *6*, 260.

(87) Bogdan, A. R.; Sach, N. W. *Advanced Synthesis & Catalysis* **2009**, *351*, 849.

(88) Vandenbergh, J.; Tura, T.; Baeten, E.; Junkers, T. *Journal of Polymer Science Part A: Polymer Chemistry* **2014**, *52*, 1263.

(89) Vandenbergh, J.; Junkers, T. *Polymer Chemistry* **2012**, *3*, 2739.

(90) Junkers, T. *Macromolecular Chemistry and Physics* **2017**, *218*, 1600421.

CHAPTER 2

Continuous triblock copolymer synthesis of poly(2-oxazoline)s

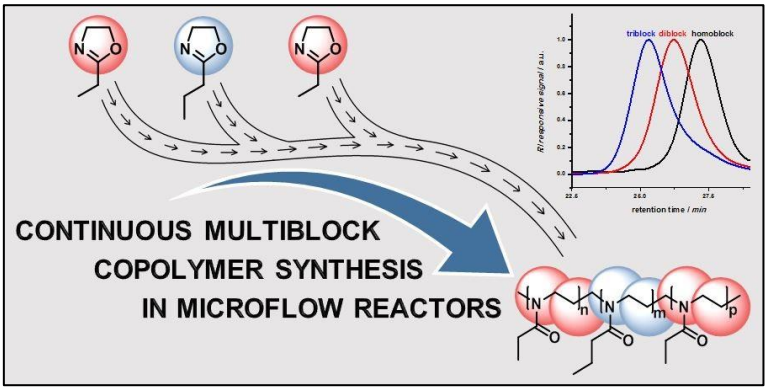

Cationic ring-opening polymerizations (CROP) of 2-oxazolines were investigated in continuous microflow reactors. Fast homopolymerizations of 2-ethyl-2-oxazoline (EtOx) and 2-*n*-propyl-2-oxazoline (*n*PropOx) were carried out up to 180°C, yielding well-controlled polymers. Also well-defined diblock and triblock copolymers were produced in a microfluidic reactor cascade, demonstrating the high value of microflow synthesis for the built-up of advanced poly(2-oxazoline)-based polymers.

(collaboration with Supramolecular Chemistry Group, UGent)
E. Baeten, B. Verbraeken, R. Hoogenboom, T. Junkers,
Chemical Communications **2015**, *51*, 11701.

2.1 Poly(2-oxazoline)s

Poly(2-oxazoline)s are an emerging class of biocompatible and non-toxic polymer materials, making them an interesting alternative for poly(ethylene glycol).[1,2] Properties of poly(2-oxazoline)s can be finetuned by simply varying the side chains.[3] Short side chains, such as methyl, ethyl, or *n*-propyl groups result in water-soluble and thermoresponsive polymers.[3,4] Longer side chains result in hydrophobic polymers, which in combination with the living nature of the polymerization provide direct access to amphiphilic (multi)block copolymers.[2,3,5] Such non-ionic amphiphilic polymers are interesting for a wide variety of applications as, e.g. carriers for drugs[6,7] and pigment dispersants in inks,[8] or as replacement of pluronics.[9]

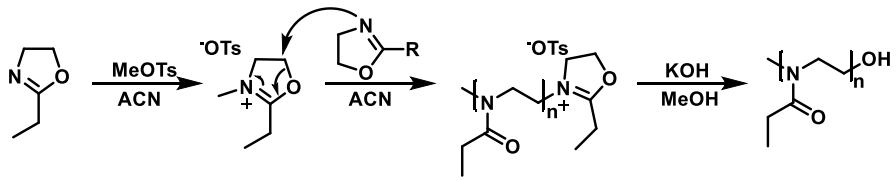

Scheme 2.1. Reaction mechanism of the cationic ring-opening polymerization of 2-ethyl-2-oxazoline (EtOx).

In 1966, the first polymerizations of 2-oxazolines were reported, enabling the synthesis of poly(2-alkyl/aryl-2-oxazoline)s (PAOx).[10-14] A cationic ring-opening mechanism was proposed, as depicted in Scheme 2.1.[15,16] Due to the cationic nature of the reaction, monomer side chains are limited to non-nucleophilic moieties. Via an oxazolinium cation as active species, the polymerization occurs in a living manner, in the absence of termination or chain transfer reactions.[14]

Yet, defined poly(2-oxazoline)s have so far not found widespread commercial application, originally due to extended polymerization times in batch (> 10 h) and immanent problems regarding the upscale of their synthesis.[10,16,17] Reaction times could however already be significantly reduced via pressurized batch reactors[18] or via microwave-assisted polymerizations (< 1 min at 200°C; although side reactions were observed above 140°C).[15,16,19,20] Microwave-assisted chemistry also offers several beneficial features over batch chemistry.[21] (Though beyond the scope of this project, a short overview of these beneficial features is given in Figure 2.1.) Still, scale-up in batch is limited due to the strong exothermic nature of the reaction and microwave chemistry leads to severe temperature gradients throughout the reaction.[22,23] Furthermore, integration of consecutive reaction steps is difficult to achieve for batch processes due to the very high sensitivity of the reactions towards water. Therefore, the use of microflow techniques seems to be an ideal alternative where a similar reduction of reaction time is expected, while providing an easy and safe scale-up of the polymerization in a hermetically sealed and hence chemically inert environment.

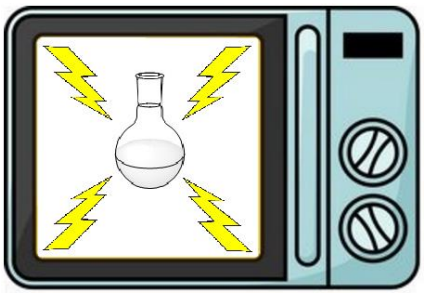

Rapid Heating

High Throughput

Shorter Reaction Times

Higher Temperature Range

High Control Reaction Conditions

Figure 2.1 Advantages of microwave-assisted chemistry (compared to batch).

The possibility for scale-up and the inert reaction conditions are not the only advantage of employing flow chemistry towards high-added value polymer synthesis. By combining several inlets into a specific reactor, entire reaction sequences can be carried out, allowing to target specialized polymer architectures in a one-step procedure. It is at this point that continuous flow unfolds its largest potential when compared to classical synthesis. At present, poly(2-oxazoline)s with many different polymer architectures have been synthesized in batch mode.[2] Several block copolymers[19,24] as well as brush[25,26] and star-shaped copolymers[25,27] are known.

The preparation of multiblock copoly(2-oxazoline) sequences is, however, challenging as during each monomer addition step extreme care must be taken to not introduce any moisture in the reactors, which unavoidably leads to termination. Furthermore, such a multistep batch synthesis of multiblock copolymer is labor intensive and tedious. By using microreactor technology (MRT), these hurdles can be overcome via direct preparation of such complex polymer structures in an integrated continuous flow process. Here, the cationic ring-opening polymerization of 2-oxazolines is evaluated with regards to reaction temperature for 2-ethyl-2-oxazoline (EtOx) and 2-*n*-propyl-2-oxazoline (*n*PropOx), followed by the continuous synthesis of multiblock copolymers consisting of various combinations of EtOx and *n*PropOx blocks in a one-step fashion by utilizing a reactor cascade in which consecutive blocks are polymerized directly after each other.

2.2 Continuous homopolymerization of 2-oxazolines

2.2.1 Homopolymerization of 2-ethyl-2-oxazoline

In a first step, the homopolymerization of 2-ethyl-2-oxazoline (EtOx) was carried out in a 19.5 μL microreactor to screen the kinetics of the process and to identify optimal process windows for further block copolymer synthesis. A typical stock solution – composed of EtOx (4 M, target degree of polymerization (DP) 60) and methyl tosylate in acetonitrile – was prepared under nitrogen atmosphere. By injecting this solution at a chosen flow rate, residence times were varied between 15 s and 20 min at reactor temperatures between 120°C and 180°C (note that reactions were carried out at 20 bar using a back pressure regulator). Due to the small volumes required for the flow reactions, a full set of kinetic data (depicted in Figure 2.3) is accessed in a simple fashion within 24 hours using only 10 mL of stock solution. The molecular weight is linearly related to the monomer conversion, indicating the livingness of the polymerization (Figure 2.2).[16] Practically full monomer conversions were obtained after 12 min 30 s at 140°C, 5 min at 160°C and 2 min at 180°C. (Note: all characterization details and experimental procedures can be found in Chapter 7.)

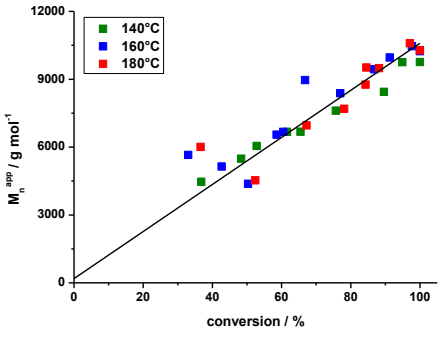

Figure 2.2. Development of molecular weight with the monomer conversion.

140°C

Residence Time	Conversion / %	M_n^{app} / g · mol^{-1}	Đ
2 min	36.8	4470	1.12
2 min 30 s	48.3	5490	1.14
3 min	52.8	6050	1.10
3 min 30 s	61.6	6670	1.09
4 min	65.5	6680	1.12
5 min	75.7	7610	1.19
7 min 30 s	89.6	8440	1.17
10 min	94.9	9750	1.14
12 min 30 s	100.0	9760	1.15

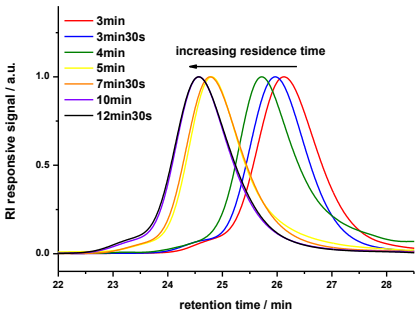

160°C

Residence Time	Conversion / %	M_n^{app} / g · mol^{-1}	Đ
40 s	33.0	5650	1.09
50 s	42.7	5140	1.08
1 min	50.3	4380	1.08
75 s	58.6	6550	1.08
80 s	60.5	6670	1.10
100 s	66.8	8960	1.10
2 min	77.0	8380	1.10
2 min 30 s	86.8	9440	1.10
3 min	91.3	9960	1.10
4 min	97.7	10460	1.10
5 min	100.0	10240	1.11

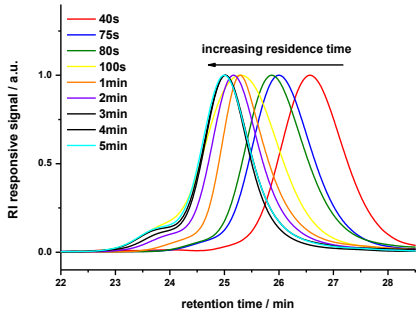

180°C

Residence Time	Conversion / %	M_n^{app} / g · mol^{-1}	Đ
20 s	36.6	6010	1.09
30 s	52.4	4530	1.08
40 s	67.2	6960	1.12
50 s	78.1	7690	1.12
1 min	84.3	8760	1.11
75 s	88.2	9490	1.11
80 s	84.5	9520	1.11
100 s	97.1	10590	1.11
2 min	100.0	10280	1.12

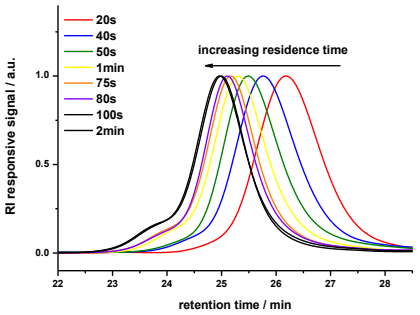

Figure 2.3. Results of the EtOx homopolymerizations at 140°C, 160°C and 180°C. The tables includes conversions, molecular weights and polydispersities for different residence times. Overlays of SEC elugrams are shown as well for the same conditions.

To investigate these reactions for ideal living polymerization behavior, a first order kinetic plot was constructed from the obtained kinetic data (Figure 2.4a). When the concentration of actively propagating chains remains constant throughout the polymerization, linearity should be observed in the logarithmic plot with respect to monomer concentration (first order). From the slope of the plots, the overall propagation rate coefficient of the polymerization at the respective temperature can be obtained. An almost identical Arrhenius relation of the propagation rate coefficient is obtained for the microflow polymerization (Figure 2.4b) in comparison to the microwave-assisted polymerization. Deduced activation energies for EtOx are in excellent agreement (73.5 ± 3.8 kJ mol^{-1} in microflow vs 73.4 ± 0.5 kJ mol^{-1} in microwave synthesis), and also frequency factors between both techniques match very well taking error margins into account [(1.4 ± 0.4)·10^8 L mol^{-1} s^{-1} in microflow vs (2.0 ± 0.9)·10^8 L mol^{-1} s^{-1} in microwave synthesis)].[16] Furthermore, the low scatter of the data in Figure 2.4a underpins that the flow reactor is indeed performing very well with respect to reaction stability, batch-to-batch variation and synthesis precision.

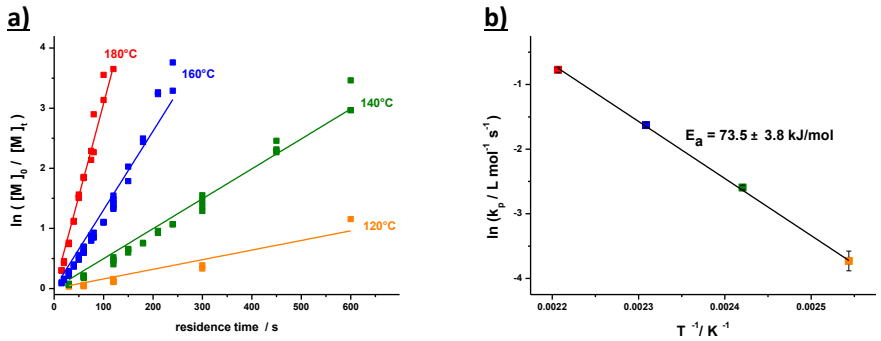

Figure 2.4. a) First order kinetic plot of the homopolymerization of EtOx at 120°C, 140°C, 160°C and 180°C. b) Arrhenius plot of the homopolymerization of EtOx.

	Residence Time	*Conversion / %*	M_n^{app} / g · mol^{-1}	*Đ*
DP 15	2 min	36.8	4470	1.12
DP 30	2 min 30	48.3	5490	1.14
DP 60	3 min	52.8	6050	1.10
DP 120	12 min 30	100.0	9760	1.15

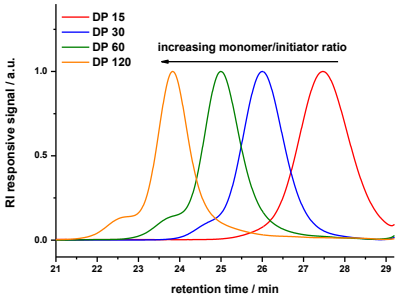

Figure 2.5. Results of the homopolymerization of EtOx at 160°C with an increasing degree of polymerization. The table includes conversions, molecular weights and polydispersities. An overlay of SEC elugrams is shown as well.

Different molecular weights could be targeted by varying the monomer/initiator ratio. Closer inspection of the resulting molecular weight distributions reveals that some transfer reactions were occurring at high conversions and high temperatures since a shoulder appears at the high molecular weight side in the SEC elugrams (Figure 2.5). Even though this observation is in line with literature, the effect appears to be less when performing the reaction in flow.[15,16] The dispersities of the obtained polymers are well below 1.2, indicating a high control over the polymerization process at all instances. Less transfer reactions are apparent when targeting lower molecular weights (DP 15 and DP 30), still allowing for full monomer conversions within 5 min at 160°C (Figure 2.5).

2.2.2 Homopolymerization of 2-*n*-propyl-2-oxazoline

In a similar approach, the homopolymerization of 2-*n*-propyl-2-oxazoline (*n*PropOx) was investigated as well. The kinetics of both homopolymerizations are rather similar and full conversions were also obtained after 12 min 30 s at 140°C, 5 min at 160°C and 2 min at 180°C (Figure 2.7). Furthermore, a first order kinetic plot could be constructed from the obtained kinetic data (Figure 2.6a). The deduced activation energy and frequency factor of the *n*PropOx polymerization (70.9 ± 8.2 kJ mol^{-1} and (0.68 ± 0.12) 10^8 $L \cdot mol^{-1} \cdot s^{-1}$, respectively) are well-aligned with the results of the EtOx polymerization (Figure 2.6b).

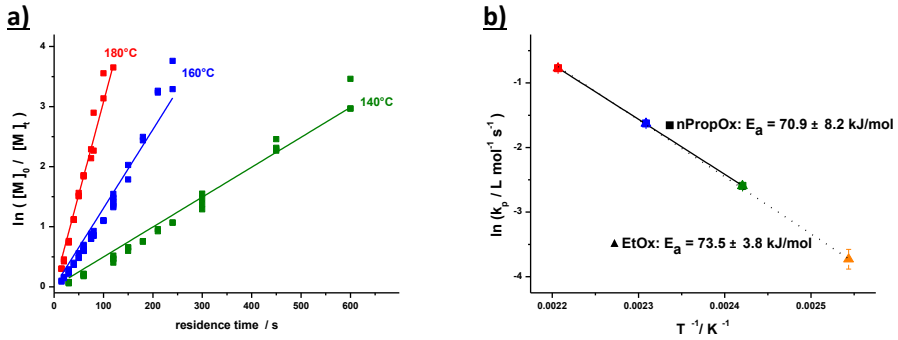

Figure 2.6. a) First order kinetic plot of the homopolymerization of *n*PropOx at 140°C, 160°C and 180°C. b) Arrhenius plot of the homopolymerization of *n*PropOx (solid line) in comparison to EtOx (dotted line).

Microfluidic reactors thus provide a high control over the homopolymerization of 2-oxazolines, and provide conditions to target polymers with full monomer conversions within few minutes of reaction time. For further investigations, 160°C was chosen as optimal reaction temperature as reasonable reaction times could be achieved while keeping transfer reactions at a tolerable level.

140°C

Residence Time	*Conversion / %*	M_n^{app} / g · mol^{-1}	*Đ*
3 min	52.0	4290	1.22
4 min	65.7	5590	1.18
5 min	76.1	7680	1.15
7 min 30 s	91.0	8720	1.20
10 min	96.2	8560	1.26
12 min 30 s	99.3	8950	1.24

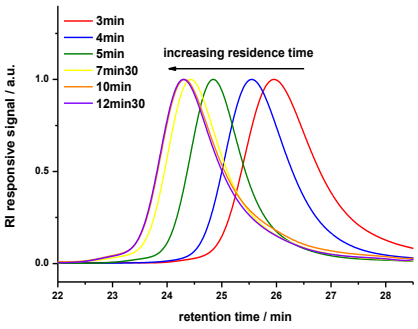

160°C

Residence Time	*Conversion / %*	M_n^{app} / g · mol^{-1}	*Đ*
1 min	41.6	4210	1.19
2 min	76.6	6610	1.18
3 min	91.0	7880	1.18
4 min	97.1	7770	1.22
5 min	100	8170	1.23

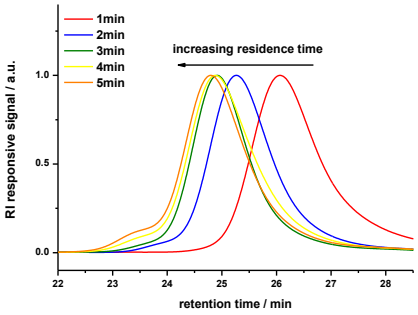

180°C

Residence Time	*Conversion / %*	M_n^{app} / g · mol^{-1}	*Đ*
30 s	54.6	5360	1.13
40 s	68.1	6800	1.12
50 s	75.0	7010	1.14
1 min	85.1	7010	1.19
75 s	92.8	7580	1.19
80 s	93.8	7790	1.19
100 s	98.4	8530	1.18
2 min	99.5	9240	1.16

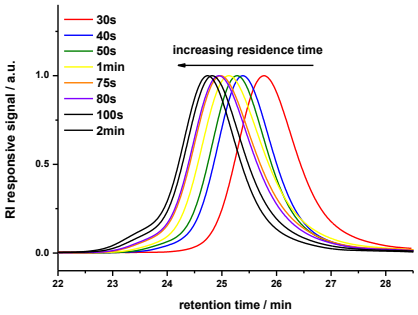

Figure 2.7. Results of *n*PropOx homopolymerizations at 140°C, 160°C and 180°C. The tables includes conversions, molecular weights and polydispersities for different residence times. Overlays of SEC elugrams are shown as well for the same conditions.

2.3 Continuous diblock copolymerization

2.3.1 EtOx-*b*-*n*PropOx diblock copolymerization

After optimization of the homopolymerizations, diblock copolymers were targeted in a direct continuous flow set-up. Therefore, a 15 μL microfluidic multi-compartment reactor chip was employed, containing an additional reactor inlet at 1/3 of the reactor, hence dividing the chip into two reactor compartments: the first with 5 μL internal volume – where the first monomer can be polymerized – and a second part with 10 μL internal volume where the second block is attached. A schematic representation can be found in Figure 2.8. The increase in reactor volume compensates the increase of total flow rate in the reactor and thus allows the use of a similar residence time for both blocks. Reaction times can thus be kept nearly constant in both reactor parts. To assure full monomer conversions for the first block, optimized conditions at 160°C of the homopolymerization were applied to the first reactor part. The polymerization stock solutions were injected at a total flow rate of 1 μL min^{-1} leading to 5 min residence time and thus full monomer conversions. The second monomer was directly injected without dilution.

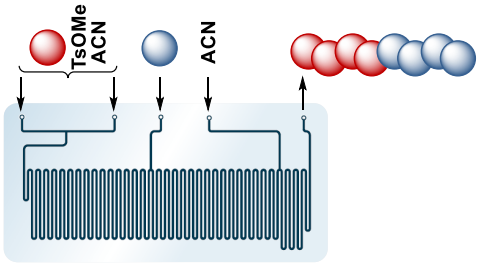

Figure 2.8. Schematic representation of the multicompartment microreactor chip.

In this way, a flexible set-up is obtained where changing the flow rate of the second monomer leads to a change in the ratio of monomer 1 to monomer 2 and thus block copolymer composition. A change in individual block lengths can thus be realized simply by adjusting flow rates, and does not require any change in the preparation of reaction solutions. By targeting different molecular weights for the first block as well, a variety of diblock copolymers was prepared: 30/15, 30/30, 30/60, 15/15 and 15/30 (DP EtOx/nPropOx) (Table 2.1).

Table 2.1. Results of the EtOx-*b*-*n*PropOx diblock copolymerizations, including residence times for every polymerization step, conversions of the *n*PropOx block, molecular weights, polydispersities and observed EtOx/*n*PropOx ratios.

Targeted DP EtOx / nPropOx	***residence time EtOx block***	***residence time nPropOx block***	***conversion nPropOx block***	M_n^{app} / g · mol^{-1}	*Đ*	M_p^{app} / g · mol^{-1}	***Observed EtOx / nPropOx***
30 / -	5 min	-	-	6830	1.08	7160	1 / -
30 / 15	5 min	8 min 08 s	100 %	8030	1.18	9720	1 / 0.49
30 / 30	5 min	6 min 48 s	100 %	9370	1.19	12890	1 / 1.10
30 / 60	5 min	5 min 08 s	91 %	11230	1.31	17400	1 / 2.07
15 / -	5 min	-	-	3510	1.10	3790	1 / -
15 / 15	5 min	6 min 48 s	100 %	6140	1.12	7130	1 / 0.96
15 / 30	5 min	5 min 08 s	76%	9350	1.13	11710	1 / 5.15

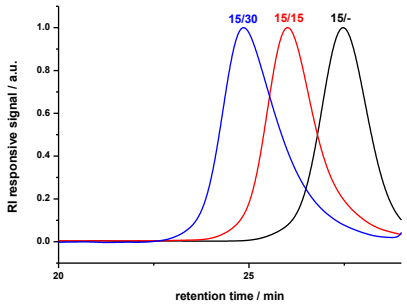

Figure 2.9. Overlay of the SEC elugrams of the EtOx homopolymer and the EtOx-*b*-*n*PropOx diblock copolymers in different EtOx/*n*PropOx ratios (DP 15 /…).

The SEC elugrams of the 15/15 and 15/30 diblock copolymers are shown in Figure 2.9, together with the EtOx (DP 15)(15/-) homopolymer (note that distributions overlap on the low molecular weight shoulder with the employed quench solutions that are used to stop the polymerizations directly at the reactor end and thus are cut off slightly). A clear shift of the distributions towards higher retention times is observed with increasing *n*PropOx block length, indicating the pristine nature of the block copolymers and high re-initiation rate that is achieved in the second reactor compartment. Diblock copolymers with an EtOx block of DP 60 were not targeted since some transfer reactions were already observed for the DP 60 homopolymerization.

2.3.2 *n*PropOx-*b*-EtOx diblock copolymerization

In a similar approach, *n*PropOx-*b*-EtOx diblock copolymers were targeted, namely 30/15, 30/30, 30/60, 15/15, 15/30 and 15/60 (DP *n*PropOx/EtOx) (Table 2.2 and Figure 2.10).

Table 2.2. Results of the *n*PropOx-*b*-EtOx diblock copolymerizations, including residence times for every polymerization step, conversions of the EtOx block, molecular weights, polydispersities and observed *n*PropOx/EtOx ratios.

Targeted DP nPropOx / EtOx	*residence time nPropOx block*	*residence time EtOx block*	*conversion EtOx block*	M_n^{app} / g · mol^{-1}	*Đ*	M_p^{app} / g · mol^{-1}	*Observed nPropOx / EtOx*
30 / -	5 min	-	-	6510	1.09	7130	1 / -
30 / 15	5 min	8 min 20 s	100 %	6670	1.21	9230	1 / 0.53
30 / 30	5 min	7 min 09 s	95 %	10670	1.16	13640	1 / 1.05
30 / 60	5 min	5 min 33 s	100 %	13640	1.23	16040	1 / 2.22
15 / -	5 min	-	-	3940	1.09	4220	1 / -
15 / 15	5 min	7 min 09 s	100 %	5540	1.17	6490	1 / 1.18
15 / 30	5 min	5 min 33 s	100 %	7690	1.17	9340	1 / 2.24
15 / 60	5 min	3 min 51 s	100 %	17360	1.13	17450	1 / 5.80

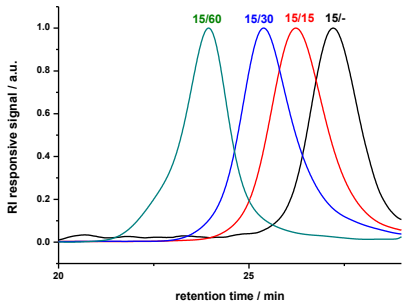

Figure 2.10. Overlay of the SEC elugrams of the *n*PropOx homopolymer and the *n*PropOx-*b*-EtOx diblock copolymers in different *n*PropOx/EtOx ratios.

Diblock copolymers could thus directly be synthesized with high accuracy without any isolation step being required in between. Since variations of flow rates are easily realized, the reactor can be adjusted in very short time to produce a block copolymer with a composition of choice (typically about twice the reactor residence time is required to reach stable continuous flow conditions). In principle, such setup can thus be used for high-throughput synthesis of libraries of block copolymers.

2.4 Continuous triblock copolymerization

Encouraged by the success of the diblock copolymerizations, the reactor setup was extended by a second reactor chip to also target the direct continuous flow synthesis of triblock copolymers. Therefore, the multi-compartment 15 μL microfluidic system was coupled to a second, independently thermostated microreactor of 19.5 μL featuring a single reaction channel. This way, a hermetically sealed microreactor cascade is obtained, consisting of three sequential reactor parts with increasing internal volumes (Figure 2.11). The first reactor chip was used for the diblock copolymerizations as described above, while the third reactor was used to attach a third polymer block.

In this way, a EtOx-*b*-*n*PropOx-*b*-EtOx triblock copolymer (15/15/15) in a 2/1.02 EtOx/*n*PropOx ratio could be obtained, with an apparent molecular weight of 7400 g mol^{-1} and a dispersity of 1.25. Also its mirror image, the *n*PropOx-*b*-EtOx-*b*-*n*PropOx triblock copolymer was developed in a 2/1.11 *n*PropOx/EtOx ratio with a molecular weight of 7320 g mol^{-1} and a dispersity of 1.21. The corresponding molecular weight distributions and molecular weights are shown in Figure 2.11, in comparison to the homo- and diblock copolymers discussed above.

Triblock copolymers with longer block lengths (DP 30 for each block) were likewise targeted. Results are included in Table 2.3 and Table 2.4. Overall, some broadening of the molecular weight distributions is observed during the attachment of the third block. Nevertheless, overall dispersities are relatively low and the reaction outcome can be seen as very successful. The broadening that is observed may stem from slight impurities being entered into the reactor by the multiple injection points, but can also be due to diffusion (back mixing) occurring during transfer of the reaction solutions from reactor 1 to 2, where a short piece of non-heated PEEK tubing was used.

Table 2.3. Results of a EtOx-*b*-*n*PropOx-*b*-EtOx (30/30/30) triblock copolymerization. The table includes residence times for every polymerization step, molecular weights, polydispersities and observed EtOx/*n*PropOx ratios.

Targeted DP	***residence time EtOx block***	***residence time nPropOx block***	***residence time 2nd EtOx block***	M_n^{app} / g · mol^{-1}	***Đ***	M_p^{app} / g · mol^{-1}	***Observed EtOx / nPropOx***
30 homoblock	5 min	-	-	6830	1.08	7150	1 / -
30 / 30 diblock	5 min	6 min 48	-	9370	1.19	12900	1 / 1.10
30 / 30 / 30 triblock	5 min	6 min 48	6 min 48	9850	1.33	14970	2 / 0.98

Table 2.4. Results of a *n*PropOx-*b*-EtOx-*b*-*n*PropOx (30/30/30) triblock copolymerization. The table includes residence times for every polymerization step, molecular weights, polydispersities and observed *n*PropOx/EtOx ratios.

Targeted DP	***residence time nPropOx block***	***residence time EtOx block***	***residence time 2nd nPropOx block***	M_n^{app} / g · mol^{-1}	***Đ***	M_p^{app} / g · mol^{-1}	***Observed nPropOx / EtOx***
30 homoblock	5 min	-	-	6510	1.09	7130	1 / -
30 / 30 diblock	5 min	7 min 09	-	10670	1.16	13640	1 / 1.05
30 / 30 / 30 triblock	5 min	7 min 09	6 min 48	11410	1.29	16650	2 / 1.11

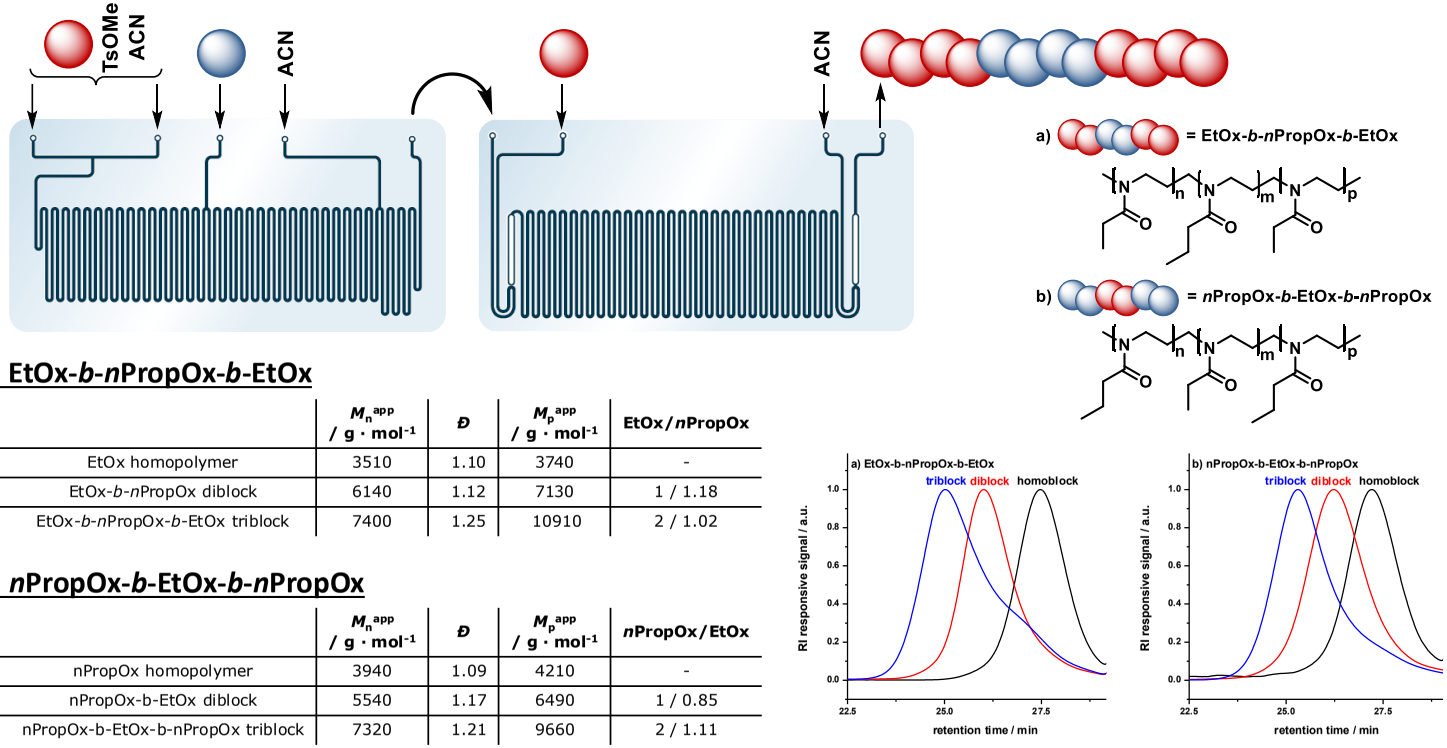

a) EtOx-*b*-*n*PropOx-*b*-EtOx

	M_n^{app} / g · mol^{-1}	Đ	M_p^{app} / g · mol^{-1}	EtOx/*n*PropOx
EtOx homopolymer	3510	1.10	3740	-
EtOx-*b*-*n*PropOx diblock	6140	1.12	7130	1 / 1.18
EtOx-*b*-*n*PropOx-*b*-EtOx triblock	7400	1.25	10910	2 / 1.02

b) *n*PropOx-*b*-EtOx-*b*-*n*PropOx

	M_n^{app} / g · mol^{-1}	Đ	M_p^{app} / g · mol^{-1}	*n*PropOx/EtOx
nPropOx homopolymer	3940	1.09	4210	-
nPropOx-b-EtOx diblock	5540	1.17	6490	1 / 0.85
nPropOx-b-EtOx-b-nPropOx triblock	7320	1.21	9660	2 / 1.11

Figure 2.11. Schematic representation of the microfluidic cascade consisting of a two-stage 15 μL and a 19.5 μL microreactor. a) EtOx-*b*-*n*PropOx-*b*-EtOx: 5 min + 6 min 48 s + 6 min 58 s. b) *n*PropOx-*b*-EtOx-*b*-*n*PropOx: 5 min + 7 min 09 s + 6 min 58 s.

2.5 Conclusions

Poly(2-oxazoline) triblock copolymers were successfully synthesized by the use of a microreactor cascade consisting of two commercially available microreactor systems. First, the homopolymerizations of EtOx and *n*PropOx were investigated in detail with respect to changing reaction temperature. The use of microfluidic reactors provides high control over the homopolymerization of these 2-oxazolines and full monomer conversions are obtained after 12 min 30 at 140°C, 5 min at 160°C and 2 min at 180°C for both monomers. Via operation at 160°C, diblock copolymers were directly synthesized in a two-compartment reactor chip without any additional isolation step in between the individual polymerizations. A large variety of diblock copolymers could be obtained by simply varying the flow rate of the second monomer. Afterwards, the microfluidic system was coupled to a second microreactor, resulting in a hermetically sealed microreactor cascade where triblock copolymers of the structure EtOx-*b*-*n*PropOx-*b*-EtOx and *n*PropOx-*b*-EtOx-*b*-*n*PropOx could successfully be obtained in one step. The use of such microreactor cascades demonstrates the high potential that continuous flow chemistry has for precision synthesis of complex macromolecules. Cationic ring opening polymerizations are – due to their high sensitivity to water – not easy to be carried out conventionally and the above work shows how microfluidics can help to overcome a significant synthetic hurdle – while still providing conditions that intrinsically allow for facile scale-up of the reactions.

2.6 Outlook

The first polymerization of 2-oxazolines was already reported in 1966.[10-14] Yet, due to the extended polymerization times, the popularity of these polymers remained rather poor.[16] Later, the use of microwave-assisted polymerizations allowed the application of high temperatures, reducing the polymerization times to minutes.[14,16] Despite the bloom in scientific publications, the use of microwave synthesizers is limited to 1 L reactor vessels, due to the low penetration depth of microwaves. In addition, the polymerization of 2-oxazolines is highly exothermic, complicating temperature and pressure control at elevated temperatures.

As shown in this chapter, microreactor technology is an extremely useful tool to overcome these complications. The high control of reaction parameters allows for a safe and stable operation over extended periods of time. Yet, the reactors employed here are rather small and only allow production at g scale. Hence, as continuation of this project, the upscale of an EtOx homopolymerization was further investigated for which a patent was filed. Similar poly(2-oxazoline) products are now commercially available via Sigma-Aldrich.[28]

2.7 References

(1) Barz, M.; Luxenhofer, R.; Zentel, R.; Vicent, M. J. *Polymer Chemistry* **2011**, *2*, 1900.

(2) Adams, N.; Schubert, U. S. *Advanced Drug Delivery Reviews* **2007**, *59*, 1504.

(3) Hoogenboom, R.; Schlaad, H. *Polymers* **2011**, *3*, 467.

(4) Hoogenboom, R.; Thijs, H. M. L.; Jochems, M. J. H. C.; van Lankvelt, B. M.; Fijten, M. W. M.; Schubert, U. S. *Chemical Communications* **2008**, 5758.

(5) Persigehl, P.; Jordan, R.; Nuyken, O. *Macromolecules* **2000**, *33*, 6977.

(6) Luxenhofer, R.; Schulz, A.; Roques, C.; Li, S.; Bronich, T. K.; Batrakova, E. V.; Jordan, R.; Kabanov, A. V. *Biomaterials* **2010**, *31*, 4972.

(7) Luxenhofer, R.; Han, Y.; Schulz, A.; Tong, J.; He, Z.; Kabanov, A. V.; Jordan, R. *Macromolecular Rapid Communications* **2012**, *33*, 1613.

(8) Ma, S.-H.; Rodriguez-Parada, N. 1998; Vol. US5854331.

(9) Kobayashi, S.; Igarashi, T.; Moriuchi, Y.; Saegusa, T. *Macromolecules* **1986**, *19*, 535.

(10) Kagiya, T.; Narisawa, S.; Maeda, T.; Fukui, K. *Journal of Polymer Science Part B: Polymer Letters* **1966**, *4*, 441.

(11) Tomalia, D. A.; Sheetz, D. P. *Journal of Polymer Science Part A-1: Polymer Chemistry* **1966**, *4*, 2253.

(12) Seeliger, W.; Aufderhaar, E.; Diepers, W.; Feinauer, R.; Nehring, R.; Thier, W.; Hellmann, H. *Angewandte Chemie International Edition in English* **1966**, *5*, 875.

(13) Bassiri, T. G.; Levy, A.; Litt, M. *Journal of Polymer Science Part B: Polymer Letters* **1967**, *5*, 871.

(14) Verbraeken, B.; Lava, K.; Hoogenboom, R. In *Encyclopedia of Polymer Science and Technology*; John Wiley & Sons, Inc.: 2002.

(15) Wiesbrock, F.; Hoogenboom, R.; Abeln, C. H.; Schubert, U. S. *Macromolecular Rapid Communications* **2004**, *25*, 1895.

(16) Wiesbrock, F.; Hoogenboom, R.; Leenen, M. A. M.; Meier, M. A. R.; Schubert, U. S. *Macromolecules* **2005**, *38*, 5025.

(17) Aoi, K.; Okada, M. *Progress in Polymer Science* **1996**, *21*, 151.

(18) Hoogenboom, R.; Fijten, M. W. M.; Paulus, R. M.; Thijs, H. M. L.; Hoeppener, S.; Kickelbick, G.; Schubert, U. S. *Polymer* **2006**, *47*, 75.

(19) Wiesbrock, F.; Hoogenboom, R.; Leenen, M.; van Nispen, S. F. G. M.; van der Loop, M.; Abeln, C. H.; van den Berg, A. M. J.; Schubert, U. S. *Macromolecules* **2005**, *38*, 7957.

(20) Litt, M.; Levy, A. H., J. *Journal of Macromolecular Science: Part A - Chemistry* **1975**, *5*, 703.

(21) Lidström, P.; Tierney, J.; Wathey, B.; Westman, J. *Tetrahedron* **2001**, *57*, 9225.

(22) Hoogenboom, R.; Paulus, R. M.; Pilotti, Å.; Schubert, U. S. *Macromolecular Rapid Communications* **2006**, *27*, 1556.

(23) Paulus, R. M.; Erdmenger, T.; Becer, C. R.; Hoogenboom, R.; Schubert, U. S. *Macromolecular Rapid Communications* **2007**, *28*, 484.

(24) Trinh, L. T. T.; Lambermont-Thijs, H. M. L.; Schubert, U. S.; Hoogenboom, R.; Kjoniksen, A.-L. *Macromolecules* **2012**, *45*, 4337.

(25) Lach, C.; Hanselmann, R.; Frey, H.; Mülhaupt, R. *Macromolecular Rapid Communications* **1998**, *19*, 461.

(26) Zhang, N.; Luxenhofer, R.; Jordan, R. *Macromolecular Chemistry and Physics* **2012**, *213*, 1963.

(27) McAlvin, J. E.; Fraser, C. L. *Macromolecules* **1999**, *32*, 1341.

(28) de la Rosa, V. R.; Van Den Bulcke, A.; Hoogenboom, R. *Material Matters - Aldrich Materials Science* **2016**, *11*, 75.

CHAPTER 3

Functional poly(phosphoester)s via continuous UV-modification

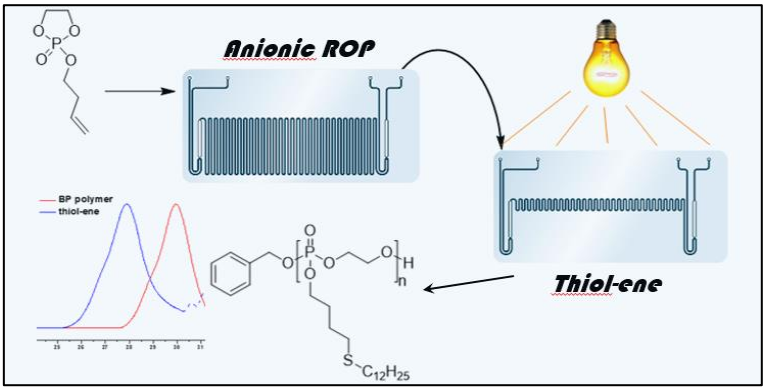

Anionic ring-opening polymerizations (AROP) of cyclic phosphates to yield linear poly(phosphoester)s (PPEs) were investigated in a microfluidic chip reactor. The homopolymerization of 2-isobutoxy-2-oxo-1,3,2-dioxaphospholane (iBP) has been investigated employing two organocatalytic systems. After optimization, 2-butenoxy-2-oxo-1,3,2-dioxaphospholane (BP) – with an alkene functionality in the side chain – was polymerized and directly post modified via a UV-induced radical thiol-ene reaction in a two-stage reactor setup with a high efficiency.

(collaboration with Center for Education and Research on Macromolecules, ULg)
E. Baeten, S. Vanslambrouck, C. Jérôme, P. Lecomte, T. Junkers,
European Polymer Journal **2016**, *80*, 208.

3.1 Poly(phosphoester)s

Next to poly(2-oxazoline)s, also other polymers can be investigated as alternatives for poly(ethylene glycol) (PEG) for biomedical applications.[1-5] One of the latest upcoming materials, next to poly(2-oxazoline)s, are poly(phosphoester)s (PPEs). Due to their structural similarity to biomolecules such as naturally occurring nucleic acids, PPEs are biocompatible and hemocompatible.[6,7] The inherent phosphoester backbone makes the PPEs (bio)degradable through hydrolysis and possibly enzymatic digestion.[6] The side chains of PPEs are structurally versatile and can be functionalized on request,[6] leading to four subclasses of polymers: poly(alkylene H-phosphonate)s, poly(phosphate)s, poly(phosphoramidate)s and poly(phosphonate)s, as depicted in Scheme 3.1.[4] Depending on their structure, PPEs can be water soluble, with an LCST (e.g. thermoresponsive poly(phosphate)s)[7,8] or without an LCST (e.g. flame-retarding poly(phosphonate)s).[9]

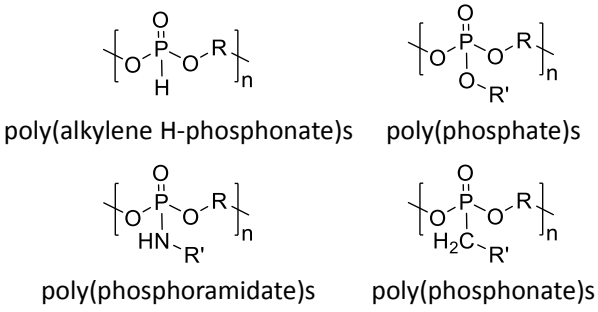

Scheme 3.1. Four subclasses of poly(phosphoester)s.

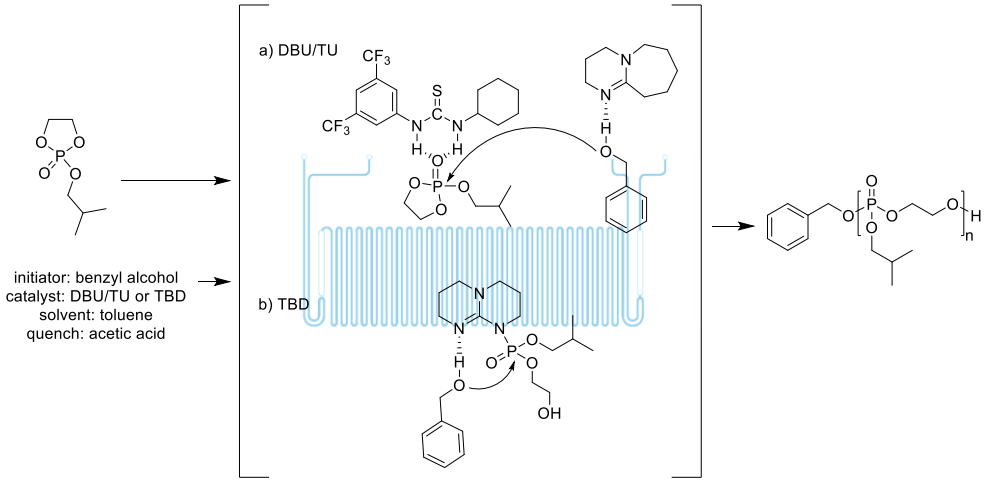

Scheme 3.2. Synthetic pathway for the AROP of 2-isobutoxy-2-oxo-1,3,2-dioxaphospholane (iBP) via the organocatalytic system DBU/TU (a) or TBD (b).

Commonly, PPEs are synthesized via anionic ring-opening polymerizations (AROP),[10] polycondensations,[11] transesterifications[12] or enzymatic polymerizations,[13] of which the AROP is a well-established process to produce linear PPEs with predictable molecular weights and narrow molecular weight distributions.[6] A catalytic system is required to activate the alcoholic chain end of the propagating chain (thus resembling an oxygen anion). Many cytotoxic metal-catalytic systems have been reported, such as triisobutylaluminum (iBu$_3$Al)[7] or tin octanoate (Sn(Oct)$_2$).[14] Yet, organocatalytic alternatives have been provided by Hedrick et al. for the ROP of lactones towards polyesters.[15-17] The efficiency of these organocatalysts has also been proven for PPEs using 1,8-diazobicyclo[5.4.0]undec-7-ene (DBU), 1,5,7-triazobicyclo-[4.4.0]dec-5-ene (TBD) and DBU/TU (with TU as a functionalized thiourea) as an organocatalytic system.[6] AROP towards PPEs with DBU as organocatalyst is, however, slow and

transesterification reactions occur due to the activation of the propagating alcoholic chain end. The use of a cocatalyst such as TU, which activates the monomer, in combination with DBU leads to an acceleration of the reaction (Scheme 3.2a). On the other hand, the use of TBD as bifunctional catalyst, remarkably speeds up the reaction by simultaneous activation as hydrogen-bond donor to the monomer and as hydrogen-bond acceptor to the hydroxyl proton of the initiator or the propagating alcohol, as depicted in Scheme 3.2b.[6]

In addition, due to the anionic nature of PPE polymerization, stringent reaction conditions must be provided during synthesis, leading to considerable batch-to-batch variation and difficulty to scale up reactions. The use of microstructured continuous flow reactors can overcome these problems. In addition, the uniform temperature distribution in microreactors is beneficial for the AROP of cyclic phosphates by avoiding the occurrence of unwanted transesterification reactions, even though only low temperature regimes need to be employed (0°C to 40°C) for PPE synthesis.[6] Thereby, the ease of upscaling optimized flow processes makes the use of microreactor technology very interesting for industrial applications.[18-20] This, in combination with a reproducible and uniform reaction product, makes the synthesis and side-chain modification of poly(phosphate)s via a straightforward flow process extremely rewarding for further biomedical and pharmaceutical applications – also because MRT is inherently favored for good manufacturing practices (GMP) by the FDA.[21,22]

3.2 Project objectives

In this project, the anionic ring-opening polymerization of cyclic phosphates was carried out in a microfluidic chip reactor. To the best of our knowledge, a continuous (anionic) polymerization to produce linear poly(phosphate)s (or any other PPE) has not yet been reported. First, the polymerization of the cyclic phosphate 2-isobutoxy-2-oxo-1,3,2-dioxaphospholane (iBP) was carried out in a commercially available microreactor (Scheme 3.2). After optimization of this process, an alkene-functionalized PPE was targeted, based on the cyclic monomer 2-butenoxy-2-oxo-1,3,2-dioxaphospholane (BP).

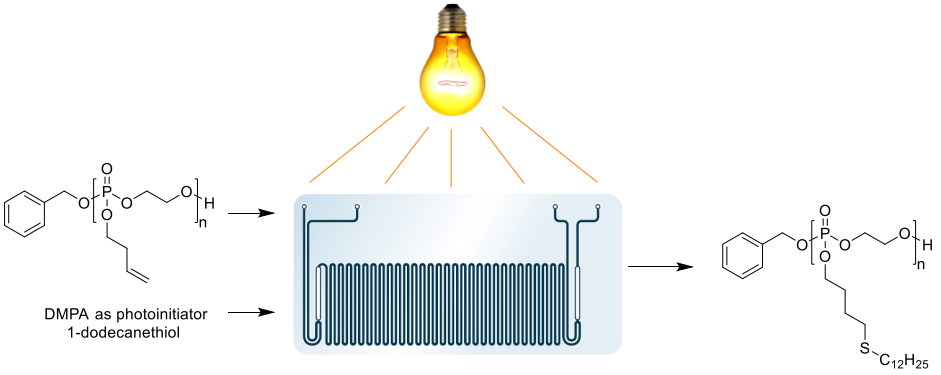

Scheme 3.3. Reactor scheme of the UV-induced radical thiol-ene reaction as post functionalization of an alkene-functionalized BP polymer.

The obtained BP polymer could then be used for a UV-induced radical thiol-ene postpolymerization modification with a thiol, as depicted in Scheme 3.3. This type of thiol-ene reactions – in contrast to the base catalyzed thiol-ene reaction – is known as an efficient conjugation tool, but usually fail in the sense of a 'click

reaction' for polymer-polymer conjugations, probably due to diffusion limitations.[23,24] However, its synthetic value has been proven in numerous applications[25-27] especially for post functionalization of vinyl-functional polymers.[26-28] Also for photoreactions, MRT can play a beneficial role, due to better illumination and hence less absence of light intensity gradients when compared to batch reactors.[29] In fact, any light-induced reaction is inherently difficult to scale up, which is directly overcome by applying MRT – making flow processing and photoreactions an almost ideal couple. Few examples for the combination of thiol-ene chemistry with flow have recently been introduced,[30-32] but to date, the reaction has not yet been applied for the continuous post functionalization of linear polymers.

Performing such UV-induced post modification in flow is by itself interesting, yet the largest potential is obtained when such reaction is coupled with the polymerization. Via the direct coupling of two microreactor systems into a microreactor cascade, consecutive flow reactions can be carried out in one-step allowing the polymerization to take place in one reactor while the post modification can consequently be carried out in a second stage without any isolation of material between the two reactors.[5,33] This combination of a thermal and a photochemical reaction in a one-step procedure can be highly rewarding and leads to accelerated material synthesis due to the ability to produce a relatively broad range of materials with a single procedure.

3.3 Polymerization of iBP

3.3.1 Preliminary results

In a first step, the anionic polymerization of the cyclic phosphate monomer 2-isobutoxy-2-oxo-1,3,2-dioxaphospholane (iBP) was explored. iBP is an ideal monomer to test under which conditions the cyclic phosphate polymerizations can be performed. Previous batch experiments have already demonstrated that the reactions proceed under homogeneous conditions.[6] Absence of any precipitation during the polymerization process is crucial to avoid blockages inside the microreactor. Therefore, the viscosity of the final polymerization mixture has to be taken into account as well, to avoid reactor clogging. The use of lower monomer concentrations (higher dilution) might avoid interference of viscosity. Yet, lower concentrations also lead to lower polymerization rates, which is unfavorable. Thus, several polymerizations with different iBP concentrations were carried out in microflow, and an optimum for the time-conversion relation without noticeable viscosity problems was found for a monomer concentration of 2.5 $mol \cdot L^{-1}$.

Viscosity is not only determined by polymer concentration, but also by the overall chain length of the polymer. Three different chain lengths (degree of polymerization, DP) were explored likewise without any viscosity problems: DP 30, 60 and 120. However, in order to reach longer chain lengths, less initiator and catalyst were employed, resulting in somewhat slower polymerizations. Hence, in the following we focused mostly on experiments with a target DP of 30 to retain high polymerization rates. Results will be extrapolatable to longer chains and behave similarly, especially with respect to the UV-induced postpolymerization.

Regarding the rate of polymerization, further tests were carried out in order to identify the optimal solvent for the polymerization. Thereby, deceleration of the propagation was observed in polar media, most likely due to a less effective catalytic activation of the monomer and the propagating alcoholic chain end. Hence, the apolar solvent toluene was chosen for all further experiments, also to avoid transesterification reactions during polymerization.

3.3.2 iBP polymerization – optimization

The organocatalytic systems, DBU/TU and TBD, were tested in more detail for the iBP polymerization. The AROP of iBP via DBU/TU was first carried out in toluene at 0°C, as given in entries 1-5 in Table 3.1. The molecular weight is linearly related to the monomer conversion, indicating the livingness of the polymerization (Figure 3.1a). A first order kinetic plot is depicted in Figure 3.1b, indicating a high control over the polymerization at 0°C. Almost full conversions (93%) were obtained after a residence time of 20 min. (Conversions of 94% were reached after 40 min reaction time in batch, for a DP 100 polymer.[6]) Molecular weight distributions were measured via THF-SEC, giving low dispersities (< 1.15) and molecular weights around 2400 g mol^{-1} (deviating from the expected molecular weight of 5400 g mol^{-1} due to the SEC calibration based on polystyrene). In order to speed up the reaction, the reaction temperature was increased to 40°C. Yet, a loss of livingness is observed at higher conversions (Figure 3.1). Higher reaction temperatures were avoided to prevent the occurrence of side reactions. Flow conditions (due to the inherently good thermal stability) do allow to use such temperatures, which is much more difficult to achieve in batch reactions, where cooling usually must be foreseen. At 40°C, 95% conversion could be obtained after only 10 min reaction time. Again monomodal molecular weight distributions

with $Đ$ < 1.20 and M_n^{app} ~ 2400 g mol^{-1} were observed (Table 3.1), showing that 40°C is a still suitable temperature with respect to distortion of the polymer product distribution.

Table 3.1. iBP polymerization via DBU/TU as catalytic system at 0°C and 40°C.

Entry	***Reaction Temperature***	***Residence Time***	***Conversion / %***	***M_n^{app} / g · mol^{-1}***	***Đ***
1	0°C	5 min	42	1100	1.13
2	0°C	7 min 30 s	60	1520	1.14
3	0°C	10 min	71	1820	1.15
4	0°C	15 min	85	2230	1.12
5	0°C	20 min	93	2440	1.10
6	40°C	1 min	29	920	1.16
7	40°C	2 min	52	1720	1.12
8	40°C	3 min	73	2190	1.12
9	40°C	4 min	82	2580	1.09
10	40°C	5 min	88	2710	1.10
11	40°C	7 min 30 s	93	2870	1.13
12	40°C	10 min	95	3250	1.09

*** M_n^{app} was determined via THF-SEC based on polystyrene standards.**

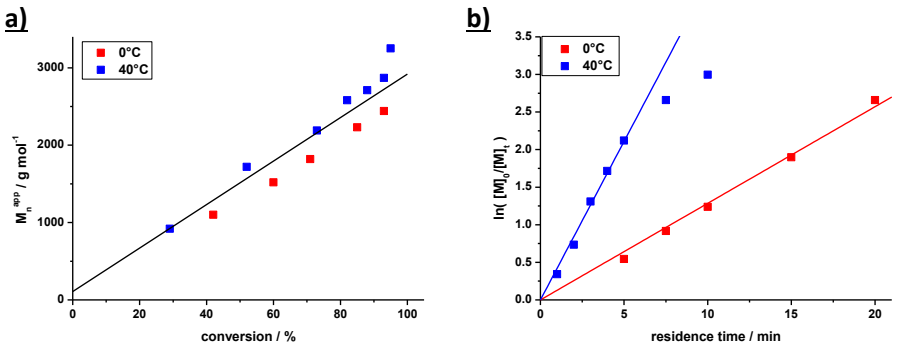

Figure 3.1. a) Development of molecular weight with the monomer conversion and b) the first order kinetic plot for the homopolymerization of iBP, employing DBU/TU as catalytic system, at 0°C and 40°C.

For the alternative catalyst, TBD, first tests were also carried out in toluene at 0°C. The amount of TBD needed to be lowered to 0.15 eq in comparison to original batch experiments, in which 1 eq of catalyst was employed,[6] in order to gain better control over the polymerization. At these concentrations, a monomer conversion of 84% could already be reached after 3 min of residence time, as depicted in Figure 3.2. A further increase of monomer conversion was not observed for longer residence times, for which the exact reason is not known at this stage. Also the molecular weight did not significantly change anymore at longer residence times, which suggested a premature ending of the polymerization. However, narrow and monomodal molecular distributions were obtained, indicating that polymerizations with this catalyst also occurred in absence of significant transesterification reactions.

Residence Time	*Conversion / %*	M_n^{app} / g · mol^{-1}	*Đ*
1 min	49	1840	1.15
2 min	75	2460	1.12
3 min	84	2650	1.11
4 min	84	2700	1.12

*** M_n^{app} was determined via THF-SEC based on polystyrene standards.**

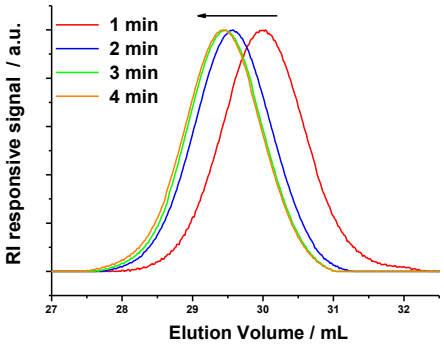

Figure 3.2. Results of the iBP polymerization via TBD as catalytic system at 0°C.

As indicated above, both catalytic systems follow a somewhat different mechanism, as given in Scheme 3.2. While DBU only activates the propagating alcoholic chain end and TU activates the monomer, TBD simultaneously activates the monomer and the propagating alcoholic chain end, which explains the faster

propagation kinetics for polymerizations employing TBD. This trend was already observed in batch experiments,[6] but is for flow polymerizations more noticeable as residence times are fixed, in contrast to batch experiments, where often longer reaction times are applied than actually necessary to reach full conversions.

3.4 Polymerization of BP

After optimization of the AROP of iBP in microflow, similar kinetic tests were performed on the cyclic phosphate 2-butenoxy-2-oxo-1,3,2-dioxaphospholane (BP). Via the use of this monomer, an alkene-functionalized PPE can be obtained, which allows for a later post functionalizing step via a thiol-ene reaction. Hence, the AROP of BP via DBU/TU was carried out at 0°C and 40°C, employing similar conditions as for the iBP polymerization. Due to the structural similarity between the iBP and the BP monomer, similar reaction kinetics could be expected. However, small changes in the cyclic phosphate monomer structure can in some cases have a tremendous influence on the kinetics of the polymerization. As shown in Table 3.2, indeed similar results were obtained for the functional monomer. Yet, since only high conversions were obtained in even short reaction times, the livingness of the polymerization can not as nicely be proven by a linear relationship between the molecular weight and the monomer conversion (Figure 3.3a). Thereby, more variation can be seen in the first order kinetic plot, indicating less control over the BP polymerization (Figure 3.3b) than over the iBP polymerization (Figure 3.1b). Still, a BP polymer could be synthesized with high monomer conversions, monomodal molecular weight distributions and low polydispersities.

Table 3.2. BP polymerization via DBU/TU as catalytic system at 0°C and 40°C.

Entry	*Reaction Temperature*	*Residence Time*	*Conversion / %*	M_n^{app} / g · mol^{-1}	*Đ*
1	0°C	5 min	11	1400	1.08
2	0°C	7 min 30 s	67	2460	1.15
3	0°C	10 min	75	2200	1.14
4	0°C	15 min	87	3040	1.14
5	0°C	20 min	95	3580	1.15
6	40°C	3 min	67	1710	1.13
7	40°C	4 min	75	2020	1.14
8	40°C	5 min	84	2440	1.16
9	40°C	7 min 30 s	89	3130	1.21
10	40°C	10 min	93	2800	1.20

*** M_n^{app} was determined via DMF-SEC based on polystyrene standards.**

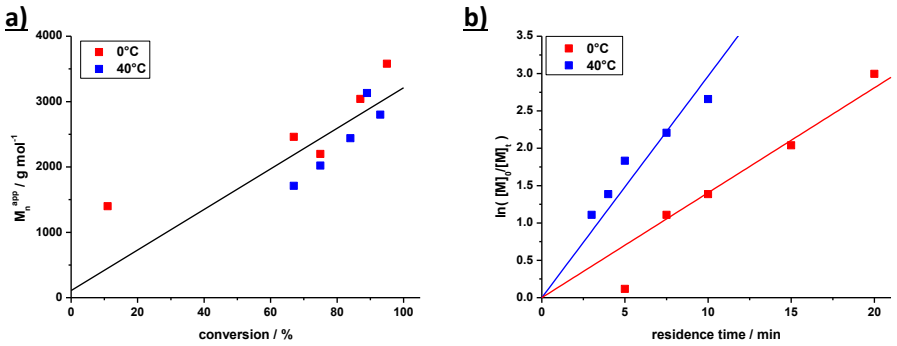

Figure 3.3. a) Development of molecular weight with the monomer conversion and b) the first order kinetic plot for the homopolymerization of iBP, employing DBU/TU as catalytic system, at 0°C and 40°C.

At 0°C, almost full conversions were obtained after 20 min residence time, with narrow and monomodal molecular weight distributions. At 40°C, the reaction – in very good agreement to the iBP system – came close to completion (93%) within 10 min. The obtained dispersities were slightly higher for BP (*Đ* ~ 1.20), causing

a small decrease of the molecular weight, although well-defined monomodal distributions were generally obtained.

Consequently, the anionic ROP of BP was also tested via the use of TBD as catalyst. On first glance surprisingly, the polymerization of BP via TBD was rather unsuccessful and no BP polymer could be obtained. The presence of the alkene functionality of the BP monomer has thus clearly an effect on the catalytic activity of the TBD system, though further NMR studies are required to determine the exact reason behind the unsuccesfull polymerization via TBD. This observation was in line with literature reports that describe that not all cyclic phosphate monomers can be polymerized via both organocatalytic systems. For example, 2-isopropyl-1,3,2-dioxaphospholane can not be catalyzed by DBU due to steric reasons.[4] Hence, catalyst activity must be in all cases be tested for each individual monomer, for which microflow offers an economic pathway due to the low amounts of material required for a complete test series. Yet, with respect to BP, the DBU/TU acts as a good catalytic system, making also this flow polymerization successful. Employing the conditions of entry 10 (Table 3.2), a significant amount of BP (~ 0.3 g) could be isolated during a continuous flow synthesis of 7 h 30 min.

3.5 UV-induced post modification of poly(BP)

The obtained alkene-functionalized poly(BP) has been described before in batch to be an efficient material for post functionalization via UV-induced thiol-ene reactions. As described above, thiol-ene reactions have been carried out in flow before, yet not much data is to date available for polymer reactions in homogenous solution. UV-induced radical thiol-ene reactions are known to proceed relatively quickly in batch. However, due to the absorption of light by the UV-chromophore, light gradients are created that lead to the situation that only at the reactor surface (towards the light source) a reaction may occur.[29] Hence, if the entire solution was illuminated equally, faster conversions could be obtained. Microreactors allow for such conditions as the flow channels have very short optical path lengths. To accommodate for UV reactions, the same microreactor set-up as employed for the polymerization reactions was fitted with an Omnicure UV lamp with a spectral emission between 320 and 500 nm (maximum emission at 365 nm). It should be noted that the microreactor chip was made of borosilicate glass, and hence a cut-off in the UV range of 330 nm applies. The whole reaction chip is more or less homogenously illuminated, allowing to perform highly efficient thiol-ene reactions.

To test the postpolymerization modification reaction, the alkene-functionalized polymer (isolated after prior synthesis) was reacted with various thiols. The reaction was followed by ^{1}H NMR via the presence/absence of the characteristic alkene peaks (1H, 5.84 ppm and 2H, 5.18 ppm), as depicted in Figure 3.4 for the modification with *n*-dodecanethiol. Full conversions were already observed after

1 min of residence time, when employing the photoinitiator 2,2-dimethoxy-2-phenylacetophenone (DMPA) as a radical source. In principle, thiol-ene reactions can also self-activate in the absence of an exogenous radical source, but proceed at a reduced rate. Further optimization of the thiol-ene reaction may allow to shorten the reaction time even further. Yet, within the aims of the envisaged reactor coupling, a further rate increase is not required (as in that case the residence time on the second reactor stage is pre-determined by the first reactor, in which the polymerization is carried out at significantly longer residence times and hence lower flow rates).

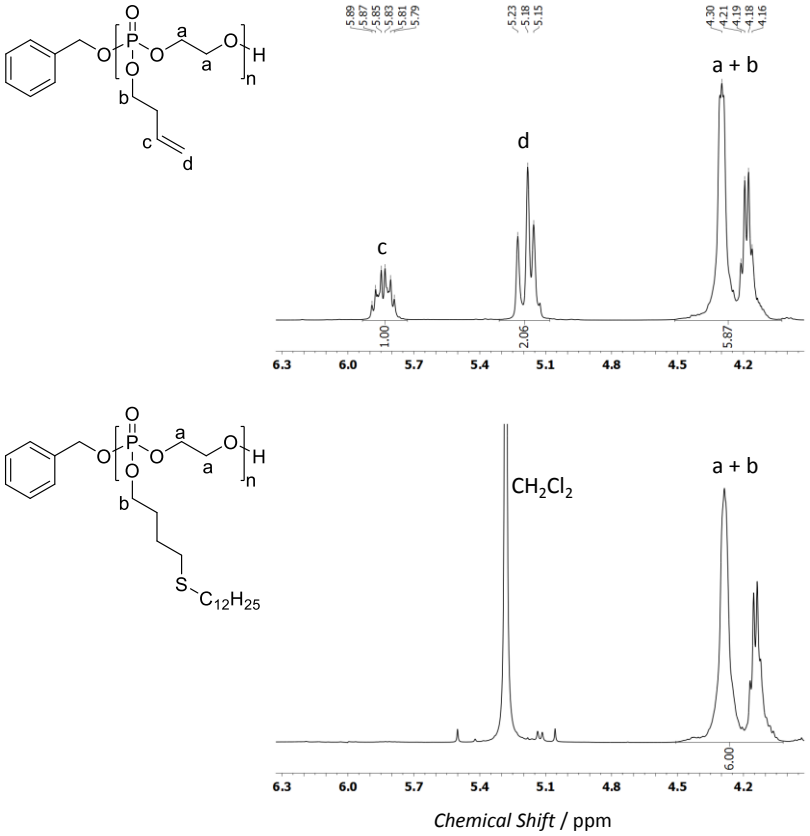

Figure 3.4. ^{1}H NMR spectra of the alkene-functionalized BP polymer (top) and the post functionalized polymer (bottom) via a UV-induced thiol-ene reaction.

3.6 Direct post functionalization in a microfluidic cascade

So far, the polymerization of BP and its UV-induced post functionalization of the alkene functionality were separately carried out and were proven successful. Hence, by coupling both reactors, a cyclic phosphate monomer such as BP can directly be polymerized and post functionalized in one step. The possibility of connecting two microreactors to perform sequential polymer reactions was already shown in Chapter 2.[5,33] Yet, a thermal reaction that is followed by a UV reaction has not been described for polymer reactions before. Such coupling of two reaction modes is highly attractive, as separation of activation modes allows in principle for reduction of possible side reactions. To achieve this aim in the present case, the polymerization was carried out in a 19.5 μL microreactor at 40°C. The UV reaction was then performed in a 5 μL microreactor. In this way, residence times in the second reactor stage could be kept relatively short to avoid over-exposure of the material to UV light. A pressure monitor was placed in between both reactors to monitor viscosity fluctuations at an early stage. Also an additional check valve was employed to prevent any backflow from the second to the first reactor. A representation of this reactor cascade can be found in Figure 3.5, while a schematic overview is given in Figure 3.6. Flow rates for the polymerization were preset at 0.73 μL min^{-1} for BP and 1.22 μL min^{-1} for the DBU/TU stock solution, leading to a polymerization time of 10 min. Flow rates for the second reactor are carefully chosen, providing molar equivalences in the reactor chip of $[BP]_0$ / $[BzOH]_0$ / $[DBU]_0$ / $[TU]_0$ / $[DMPA]_0$ / [thiol] equal to 30 / 1 / 1.5 / 1.5 / 1.5 / 45. With the given 10 min residence time in the first reactor, this results in a residence time of 65 seconds in the 5 μL UV reactor.

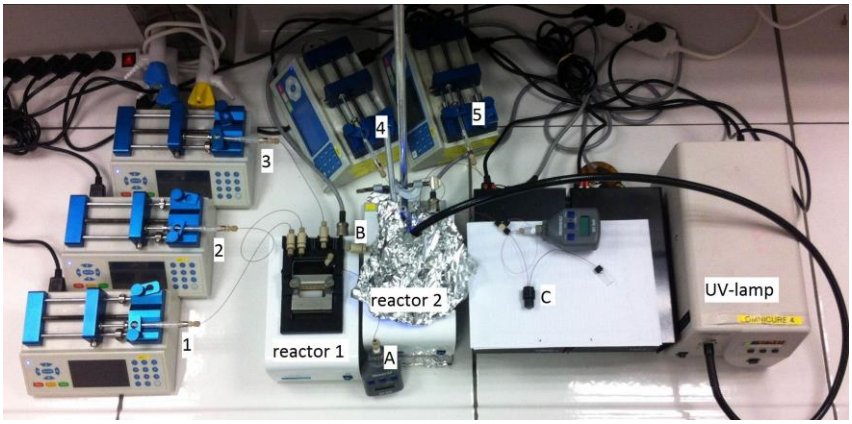

Figure 3.5. Setup of the two-stage microreactor cascade for consecutive polymerization and post modification (numbers 1-5: inlet flows; A: inline manometer, B: inline check-valve; C: pre-set back pressure regulator).

An aliquot at the outlet of the first reactor was taken to test the completion of the polymerization, for the coupled reactor, within the given residence time. Full monomer conversion was observed with $Đ$ = 1.23 and M_n^{app} of 2060 g mol^{-1} (Figure 3.6). Without stopping the polymerization, the reactor was coupled to the second reactor for the post functionalization step. No isolation or in-flow purification of the polymer was required as in principle no other species were present in the product mixture after polymerization than solvent, catalyst and polymer. The coupled system was allowed to run for 3 h. The results of this coupling are shown in Figure 3.6. A clear shift of the distribution was observed (low molecular weight material is present in the final product due to catalyst and residual thiol) with an increase of the apparent molecular weight of around 4000 g mol^{-1}, which fits well to the theoretical expectation for this particular thiol. In addition, the absence of alkene peaks in NMR indicated 100% conversion of the alkene towards a thioether.

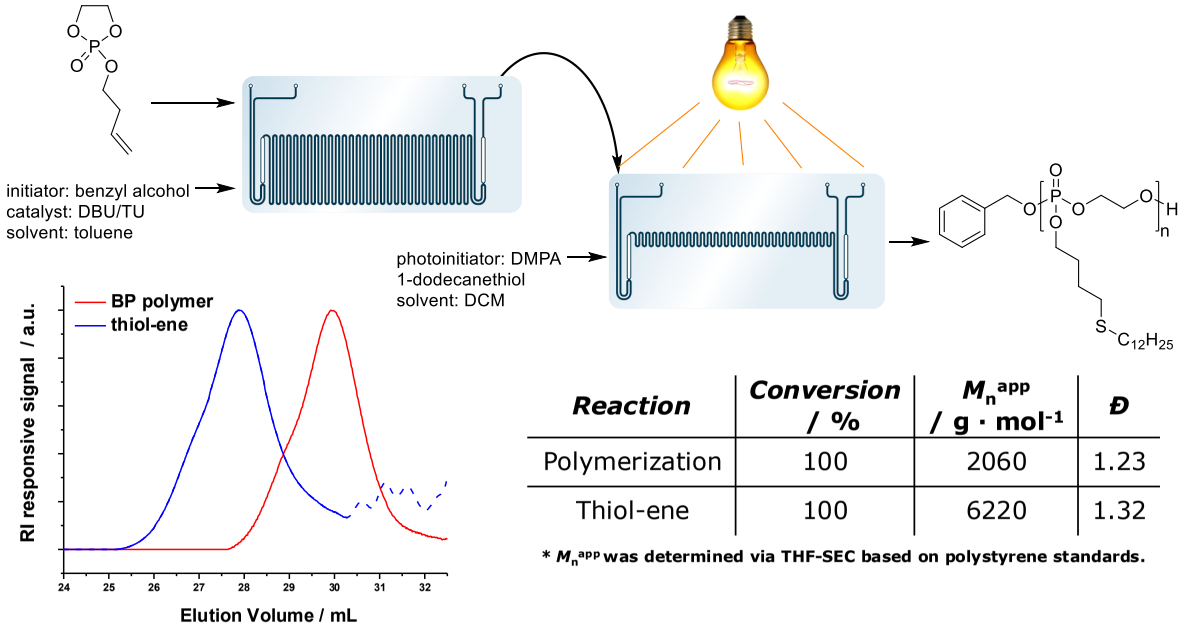

Reaction	Conversion / %	M_n^{app} / g · mol^{-1}	Đ
Polymerization	100	2060	1.23
Thiol-ene	100	6220	1.32

* M_n^{app} was determined via THF-SEC based on polystyrene standards.

Figure 3.6. Schematic representation of the microfluidic cascade consisting of a two stage 19.5 μL and 5 μL microreactor. An alkene-functionalized BP polymer is formed in the first reactor, after which the polymer is directly functionalized via a UV-induced thiol–ene reaction.

3.7 Conclusions

The anionic ring-opening polymerization of the cyclic phosphate 2-isobutoxy-2-oxo-1,3,2-dioxaphospholane (iBP) was optimized for continuous flow processing in a chip-based microreactor. Narrow monomodal molecular weight distributions were obtained for the organocatalysts DBU/TU and TBD. Following the optimization of the polymerization protocol, the technique was adapted for the polymerization of the alkene-functionalized cyclic phosphate 2-butenoxy-2-oxo-1,3,2-dioxaphospholane (BP), which yields a PPE with one alkene group available for postpolymerization modification per monomer unit. Postpolymerization modification was achieved, likewise under flow conditions, via a UV-induced radical thiol-ene reaction. UV-induced thiol-ene reactions in flow have been described before, but to date not for modification of polymers in homogeneous solution. While the polymerizations are carried out on the timescale of minutes to reach high monomer conversions, the UV reactions were already finished within one minute. Via the direct coupling of two microreactors, the polymerization and the UV-induced post functionalization could be carried out in a single step, without isolation or in-line purification of the intermediate polymer. In this way, a straightforward flow process was developed to synthesize a large variety of functional polyphosphates that could in future allow for precise engineering of PPE materials with specific chemical functionality and LCST behavior.

3.8 Outlook

Poly(phosphoester)s (PPEs) are a novel class of polymer materials, interesting for biomedical applications. Besides studies on their structural similarities to biomolecules and related advantages towards biocompability and degradability, efforts have been made to evaluate their potential towards drug delivery. PPEs have proven to be a promising candidate for micellar drug delivery systems for intravenous injection.[34] Still, further investigations are necessary before PPEs can actually be applied in industrial applications. The developed flow process can be an effective tool to synthesize a large variety of functional polyphosphates.

Here, no intentions were directed towards the upscale of the polymerization, since only minor polymer amounts (mg scale) are required for micellar testing. Yet, the major difficulty to be overcome in the field of PPEs is related to the upscale of a process, namely the upscale of the monomer synthesis. The cyclic phosphate monomers, as employed in this project, are prepared from a condensation of an alcohol and 2-chloro-2-oxo-1,3,2-dioxaphospholane (COP).[35] The reaction itself is quite efficient and can be carried out in continuous conditions. Yet, the work-up of the resulting monomer is quite time-consuming due to the extreme sensitivity of the monomer species towards oxygen, acid and water residues. Hence, towards the industrial applicability of PPEs, investigations should focus on the improvement of the monomer synthesis: either by more efficient (perhaps even continuous) work-up procedures or by transfer to a more stable monomer class (such as phosphonates, depicted in Scheme 3.1).[9]

3.9 References

(1) Webster, R.; Didier, E.; Harris, P.; Siegel, N.; Stadler, J.; Tilbury, L.; Smith, D. *Drug Metabolism & Disposition* **2007**, *35*, 9.

(2) Barz, M.; Luxenhofer, R.; Zentel, R.; Vicent, M. J. *Polymer Chemistry* **2011**, *2*, 1900.

(3) Ulbricht, J.; Jordan, R.; Luxenhofer, R. *Biomaterials* **2014**, *35*, 4848.

(4) Wolf, T.; Steinbach, T.; Wurm, F. R. *Macromolecules* **2015**, *48*, 3853.

(5) Baeten, E.; Verbraeken, B.; Hoogenboom, R.; Junkers, T. *Chemical Communications* **2015**, *51*, 11701.

(6) Clément, B.; Grignard, B.; Koole, L.; Jérôme, C.; Lecomte, P. *Macromolecules* **2012**, *45*, 4476.

(7) Iwasaki, Y.; Wachiralarpphaithoon, C.; Akiyoshi, K. *Macromolecules* **2007**, *40*, 8136.

(8) Wang, Y.-C.; Tang, L.-Y.; Li, Y.; Wang, J. *Biomacromolecules* **2009**, *10*, 66.

(9) Steinbach, T.; Ritz, S.; Wurm, F. R. *ACS Macro Letters* **2014**, *3*, 244.

(10) Iwasaki, Y. In *Biomedical Engineering - Frontiers and Challenges*; Fazel-Rezai, R., Ed.; InTech: 2011.

(11) Richards, M.; Dahiyat, B. I.; Arm, D. M.; Lin, S.; Leong, K. W. *Journal of Polymer Science Part A: Polymer Chemistry* **1991**, *29*, 1157.

(12) Pretula, S. K., K.; Szymanski, R.; Penczek, S. *Journal of Polymer Science Part A: Polymer Chemistry* **1999**, *37*, 1365.

(13) Wen, J.; Zhuo, R.-X. *Macromolecular Rapid Communications* **1998**, *19*, 641.

(14) Xiao, C.-S.; Wang, Y.-C.; Du, J.-Z.; Chen, X.-S.; Wang, J. *Macromolecules* **2006**, *39*, 6825.

(15) Dove, A. P.; Pratt, R. C.; Lohmeijer, B. G. G.; Waymouth, R. M.; Hedrick, J. L. *Journal of the American Chemical Society* **2005**, *127*, 13798.

(16) Lohmeijer, B. G. G.; Pratt, R. C.; Leibfarth, F.; Logan, J. W.; Long, D. A.; Dove, A. P.; Nederberg, F.; Choi, J.; Wade, C.; Waymouth, R. M.; Hedrick, J. L. *Macromolecules* **2006**, *39*, 8574.

(17) Pratt, R. C.; Lohmeijer, B. G. G.; Long, D. A.; Waymouth, R. M.; Hedrick, J. L. *Journal of the American Chemical Society* **2006**, *128*, 4556.

(18) Tonhauser, C.; Natalello, A.; Löwe, H.; Frey, H. *Macromolecules* **2012**, *45*, 9551.

(19) Vandenbergh, J.; Junkers, T. *Polymer Chemistry* **2012**, *3*, 2739.

(20) Wiles, C.; Watts, P. *European Journal of Organic Chemistry* **2008**, 1655.

(21) Chatterjee, S. In *IFPAC Annual Meeting* Baltimore, 2012.

(22) Lee, S.; O'Connor, T.; Yang, X.; Cruz, C.; Chatterjee, S.; Madurawe, R.; Moore, C. V.; Yu, L.; Woodcock, J. *Journal of Pharmaceutical Innovation* **2015**, *10*, 191.

(23) Koo, S. P. S.; Stamenović, M. M.; Prasath, R. A.; Inglis, A. J.; Du Prez, F. E.; Barner-Kowollik, C.; Van Camp, W.; Junkers, T. *Journal of Polymer Science Part A: Polymer Chemistry* **2010**, *48*, 1699.

(24) Barner-Kowollik, C.; Du Prez, F. E.; Espeel, P.; Hawker, C. J.; Junkers, T.; Schlaad, H.; Van Camp, W. *Angewandte Chemie International Edition* **2011**, *50*, 60.

(25) Jasinski, F.; Lobry, E.; Tarablsi, B.; Chemtob, A.; Croutxé-Barghorn, C.; Le Nouen, D.; Criqui, A. *ACS Macro Letters* **2014**, *3*, 958.

(26) Lowe, A. B. *Polymer Chemistry* **2010**, *1*, 17.

(27) Lowe, A. B. *Polymer Chemistry* **2014**, *5*, 4820.

(28) Xu, J.; Boyer, C. *Macromolecules* **2015**, *48*, 520.

(29) Junkers, T.; Wenn, B. *Reaction Chemistry & Engineering* **2016**, *1*, 60.

(30) Wojcik, F.; O'Brien, A. G.; Götze, S.; Seeberger, P. H.; Hartmann, L. *Chemistry* **2013**, *19*, 3090.

(31) Prasath, R. A.; Gokmen, M. T.; Espeel, P.; Du Prez, F. E. *Polymer Chemistry* **2010**, *1*, 685.

(32) Goetze, S.; Klein, J. C.; Laurino, P.; O'brien, A.; Raghavendra, K.; Seeberger, P. H. *Patent WO 2012069188* **2012**.

(33) Zaquen, N.; Baeten, E.; Vandenbergh, J.; Lutsen, L.; Vanderzande, D.; Junkers, T. *Chemical Engineering & Technology* **2015**, *38*, 1749.

(34) Yilmaz, Z. E.; Vanslambrouck, S.; Cajot, S.; Thiry, J.; Debuigne, A.; Lecomte, P.; Jérôme, C.; Riva, R. *RSC Advances* **2016**, *6*, 42081.

(35) Zhang, S.; Li, A.; Zou, J.; Lin, L. Y.; Wooley, K. L. *ACS Macro Letters* **2012**, *1*, 328.

CHAPTER 4

RAFT multiblock copolymers via a continuous reactor cascade

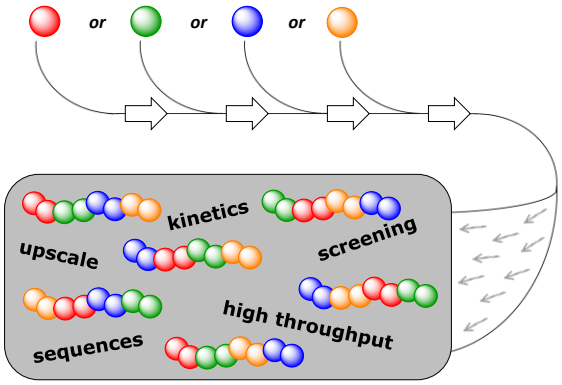

Well-defined multiblock copolymers were synthesized via reversible addition-fragmentation chain transfer (RAFT) polymerization in a fully continuous multireactor cascade. Based on theoretical considerations, reactor volumes and reactant concentrations were optimized. A broad variety of homo-, diblock, triblock and tetrablock copolymers was obtained. The tetrablock copolymer P*n*BuA-*b*-PMA-*b*-PEA-*b*-P*t*BuA was obtained in quantities of 150 g in 26 h, illustrating the high potential of continuous flow processes for polymerizations.

E. Baeten, J. J. Haven, T. Junkers, *Polymer Chemistry* **2017**, *8*, 3815.

4.1 Continuous RAFT polymerizations

Today's polymer manufacturing is under pressure to provide tailor-made polymer materials with specific properties at low production costs.[1] Block copolymers are the most frequently sought-after structures, and synthesis costs are closely related to an in-depth understanding of reaction kinetics, thorough optimization and reaction monitoring, and mostly to manual labor. In this respect, the continuous flow manufacturing of functional block copolymers in microstructured reactors is highly desirable. Continuous flow techniques are not only efficient and inherently green approaches, but also allow for operation of reactors by non-specialists.[2] On industrial scale, block copolymers are often prepared via living anionic batch polymerizations.[3] Yet, the discovery of reversible-deactivation radical polymerization (RDRP)[4] made the synthesis of these complex architectures more accessible due to less stringent reaction conditions, even if only in recent years commercial production became more frequent.[5] Nitroxide mediated polymerization (NMP),[6,7] atom transfer radical polymerization (ATRP)[8,9] and reversible addition-fragmentation chain transfer (RAFT) polymerization[10-16] have already been employed for the synthesis of multiblock copolymers. Among these different methods, RAFT polymerizations give access to the broadest range of functionalities, and is in this context the method of choice for multiblock copolymerizations.[10-16] Multiblock copolymerization via RAFT is very efficient when carried out under correct conditions,[12-15] and based on the fundament of previous RAFT multiblock copolymerization studies,[16] we extended the approach to continuous flow processing, making use of reactor telescoping.[17,18]

The versatile RAFT polymerization is often employed to access multiblock copolymers.[5,10-14,16] In batch, Perrier and coworkers were the first to obtain an icosablock (20 blocks) copolymer with a narrow molecular weight distribution.[12] Later, the same team reduced the polymerization time from 24 h per block to 2 h,[13] and later even to 3 min per block.[14] Yet, the employed system is limited to few acrylamide monomers and is thus not applicable to a broader range of monomers, as we will also discuss below. The batch-wise approach also limits the scale of production, even though impressive amounts of polymer were already made. Moad and coworkers investigated the development of higher order quasi-block copolymer libraries via the use of an automated (batch) synthesizer, to assure a higher throughput.[10,11] Yet, the throughput can be increased even more by employing a flow process – which is not only beneficial for the volume output, but also enhances the polymer end group fidelity due to better isothermicity of flow reactors.[19] A combination of the RAFT polymerization technique and continuous flow processing constitutes an ideal tool for the synthesis of functional multiblock copolymers with low dispersities and high end group fidelities, while suppressing possible side reactions related to backbiting and β-scission.[19,20] Evidently, all characteristics and limitations inherent to the polymerization (e.g. residual dispersity depending on initiator concentrations) itself will not change when transferring to a continuous flow process. The benefits of performing RAFT (homo)polymerizations in flow have been demonstrated by Diehl et al.[21] and Hornung et al.[22] Vandenbergh et al.[16] developed a RAFT pentablock copolymer via subsequent copolymerizations in a microchip reactor. A drawback of this process was, however, its sequential approach: after every polymerization step, the polymer is isolated whereby the solvent and residual monomer are evaporated. On the other hand, Hornung et al.[23] described a two-stage

continuous flow process for the synthesis of diblock copolymers without the purification or isolation of the first block. Yet, the use of a commercially available reactor set-up limits the employed reaction conditions drastically since the reactor volume of the second block cannot be adapted. Hence, the residence time for the second block is corresponding with the residence time for the first polymerization and vice versa, limiting the versatility of the system. More recently, Zhu and coworkers[24] reported a similar two-stage continuous flow process for the synthesis of a double hydrophilic block copolymer in water. Yet, reaction conditions were limited towards the synthesis of one specific hydrophilic diblock copolymer (based on 3-sulfopropyl methacrylate potassium salt (SPMA) and poly(ethylene glycol) methyl ether methacrylate (PEGMA)), rather than developing a standard procedure applicable for various multiblock copolymers.

In this study, a simple and comparatively cheap home-made tubular reactor cascade was employed to produce multiblock copolymers via RAFT polymerization in continuous multistage 'one-flow' process (the flow equivalent to a 'one-pot' batch process) (Figure 4.1). Full monomer conversions are targeted to avoid copolymer formation and purification steps of macroRAFT agents.[10,11] A similar approach was already carried out to develop poly(2-oxazoline) triblock copolymers via the use of coupled glass chip reactors (Chapter 2). However, the use of a home-made tubular reactor cascade is more versatile in this extent, since every reactor volume – and thus the residence time of each separate block – can be adapted at any time. Hence, full monomer conversion and complete initiator consumption (so called dead end polymerization conditions) will be targeted to avoid any isolation or purification step. Furthermore, the aim of this project is not to synthesize one specific multiblock copolymer, but to develop a more uniform

continuous flow procedure towards a large variety of well-defined multiblock copolymers. In this sense, the reactor cannot only be used for facile upscaling and reduction of synthesis costs, but also to screen multiblock copolymer sequences and compositions in a high-throughput approach. In principle, a multistage reactor cascade allows to program the desired sequence at the start of the reaction, and hence to quickly synthesize a broad polymer library for further testing.

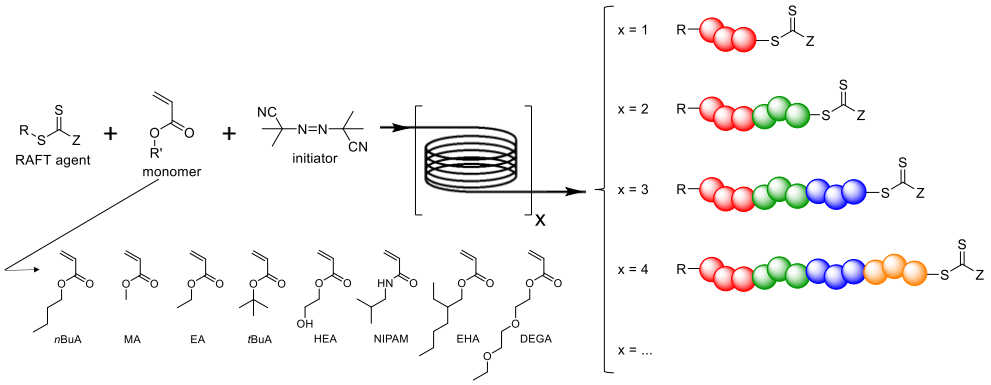

Figure 4.1. Multistage reactor concept for the continuous 'one-flow' synthesis of multiblock copolymers via RAFT polymerization.

For this purpose, a theoretic approach was followed to determine the required reaction conditions. Important for a programmable sequence is that the reactor can be used under a strict set of conditions to fit all different monomers available for synthesis. In other words, a "one size fits all" strategy must be employed, in which all different monomers must be able to reach quasi-full conversion of monomer in the same reaction time. The use of RAFT polymerizations to synthesize different poly(acrylate)s is ideal for such approach. Yet, as we will show below, high propagation rates are required for successful flow polymerizations in

the given setup, thus the methodology cannot be as easily applied to slower propagating monomers such as methacrylates or styrene and further optimization is required before it can be used for these systems. Since an exogenous initiator source is required, residence times can be adjusted to the half-life time of the initiator, assuming that any polymerization will come to an end (full monomer conversion or not) after 4 to 5 half-life times as overall reactor residence times. The reactor sequence and individual stage operation can hence be adjusted to the universal initiator kinetics rather than the varying monomer propagation rates. In this view, the polymerization of eight different acrylates (*n*-butyl acrylate (*n*BuA), methyl acrylate (MA), ethyl acrylate (EA), *t*-butyl acrylate (*t*BuA), 2-hydroxyethyl acrylate (HEA), 2-ethylhexyl acrylate (EHA), 2-(2-ethoxyethoxy)ethyl acrylate (DEGA)) and isobornyl acrylate (iBoA) was investigated and carried out under the exact same conditions. Acrylates offer a large range of functional groups, are easily tailorable via postpolymerization modification reactions[25] and are compatible with most organic solvents. To show the versatility of the system, an acrylamide (*N*-isopropyl acrylamide (NIPAM)) was included in the study as well. Next, systematic studies have been carried out on the di- and triblock copolymers with several well-defined sequences, based on these eight monomeric units. Generally, chain lengths of 10 monomer units were targeted during each chain extension, targeting block copolymers for biomedical and electronical applications.[12-14] Longer segment chain lengths can be achieved, but this must be traded off against an increase in dispersity. Different monomer/monomer ratios were targeted as well. The employed procedure could also be extended to synthesize a P*n*BuA-*b*-PMA-*b*-PEA-*b*-P*t*BuA tetrablock copolymer in large quantities (± 150 g) in 26 h.

4.2 Theoretical considerations

To develop multiblock copolymers via RAFT in one continuous process, reaction conditions must be chosen to assure full monomer conversion and complete initiator consumption. Every chain extension towards a new block – hence every separate polymerization step – must reach full monomer conversion to avoid copolymer formation through residual monomer being present from the previous stage.[10,11] As mentioned above, this can be reached by adjusting the reactor length and volume to the half-life time of the initiator. Assuming that all monomer will have reacted before all initiator is depleted (a non-trivial assumption), will give access to a broadly applicable reactor. Important to note is that should all monomer have been reacted before the initiator is consumed, then radicals are generated on a non-polymerizing system. This can in principle have negative impact on dispersity and chain end fidelity. As Perrier and coworkers had demonstrated before,[12-14] it is hence important to keep overall initiator levels at an absolute minimum. A balance must be found between minimum initiator concentration and at the same time avoidance of so-called premature dead-end polymerizations, where polymerizations end at intermediate monomer conversion due to full depletion of initiator. To solve this riddle, calculations were carried out to find optimal reaction conditions for a general acrylate homopolymerization (where k_p is typically above 10 000 L mol^{-1} s^{-1}) to reach almost full conversion in a reasonable time scale (≤ 40 min). Ideally, RAFT polymerization is identical in kinetics to a free radical polymerization, as rates of initiation, propagation and termination are not affected by the RAFT equilibrium. Hence, rate calculations of RAFT polymerizations (and hence calculations on required initiator concentrations)

can be performed based on free radical polymerization kinetics. Knowledge of RAFT specific rate coefficients is hereby not required. Based on the kinetics of an ideal radical chain polymerization, equation (**1**) can be applied for dead-end polymerizations.[26] Aiming for 99% conversion, $\ln\frac{[M]_t}{[M]_0}$ $[= \ln(1-x)]$ should be –4.6. Five times the initiator half-life time is chosen as t_{end} $\left[=\frac{5\ln 2}{k_{\mathrm{d}}}\right]$ to assure full initiator consumption. Assuming an initiator efficiency f of 0.6 and an overall termination rate k_{t} of 10^8 L mol^{-1} s^{-1} (dilute conditions), equation (**2**) is derived, correlating the rate of propagation (k_{p}) (monomer dependent), the initiator dissociation rate constant and initial initiator concentration (k_{d} and $[I]_0$) for the desired monomer conversion.

$$-\ln\frac{[M]_t}{[M]_0} = 2\,k_{\mathrm{p}}\left(\frac{f\,[I]_0}{k_{\mathrm{d}}k_{\mathrm{t}}}\right)^{\frac{1}{2}}\left(1-\mathrm{e}^{-0.5\,k_{\mathrm{d}}t_{\mathrm{end}}}\right) \quad (\mathbf{1})$$

$$k_{\mathrm{p}} = 2.8\left(\frac{k_{\mathrm{d}}}{1.2\;10^{-8}[I]_0}\right)^{\frac{1}{2}} \quad (\mathbf{2})$$

Via equation (**2**), for any given initiator concentrations ($[I]_0$), the propagation constant (k_{p}) and the dissociation constant (k_{d}) are directly correlated, showing which pair of parameters will yield the desired result (99 % conversion in 5τ). These correlation graphs for various $[I]_0$ are depicted in Figure 4.2a. As an example, fast-propagating monomers (e.g. k_{p} = 25 000 L mol^{-1} s^{-1}) in combination with a slowly decomposing initiator (e.g. k_{d} ~ 0.001 s^{-1}) require a low initiator concentration (e.g. $[I]_0$ ~ 0.001 mol L^{-1}). Slow-propagating monomers on the other hand (e.g. k_{p} = 5 000 L mol^{-1} s^{-1}), combined with a fast-decomposing initiator (e.g. k_{d} ~ 0.004 s^{-1}) require a higher initiator concentration (e.g. $[I]_0$ ~ 0.1 mol L^{-1}) to reach the same high conversion before the dead-end (t_{end}) case is reached (as would be the case of methacrylates). In practice, too

high initiator concentrations are unpractical, as the RAFT agent concentration must be chosen accordingly to the initiator concentration (ensuring good control). High $[I]_0$ would lead to too concentrated polymer solutions, which in turn leads to reactor channel blockages. Aiming for the polymerization of acrylates (k_p typically above 10 000 L mol^{-1} s^{-1} at elevated temperatures) in a reasonable time frame (t_{end} ≤ 40 min and thus k_d ~ 0.0014 s^{-1}), it can be concluded that an optimal $[I]_0$ should be at least 0.01 M.

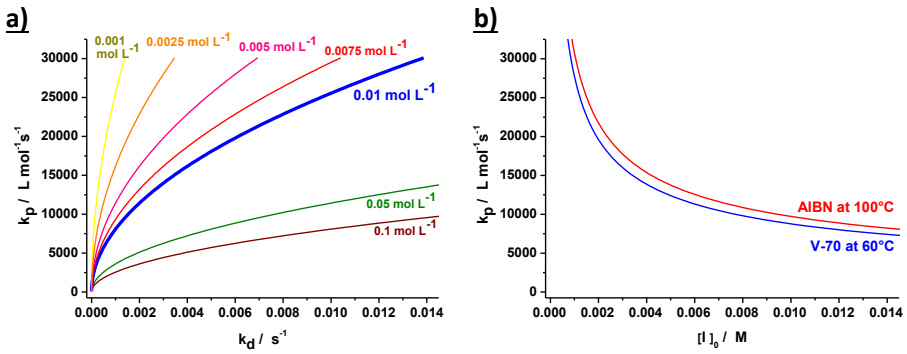

Figure 4.2. a) correlation of k_p in function of k_d at different initiator concentrations. b) correlation of k_p in function of $[I]_0$ for given k_d.

Slowly propagating monomers such as methacrylates or styrenes – as can be seen from Figure 4.2a – would require the use of initiators with very low k_d, which in turn would result in very long reaction times that are unpractical for flow operation. Hence, we limited ourselves in the present study to the acrylate family. For this purpose, a thermal initiator can be chosen based on the desired dissociation constant (k_d ~ 0.0014 s^{-1}) to fulfill the time limitation (t_{end} ≤ 40 min). As long as k_d values match, the choice of the initiator itself does not have a significant influence, as can be seen in Figure 4.2b. For example, 2,2'-azobis(4-

methoxy-2.4-dimethyl valeronitrile) (Wako Chemicals, V-70) would require $[I]_0$ = 0.0077M (with k_d = 0.001178 s^{-1} at 60°C) to reach the set minimum k_p. A slower initiator, such as 1,1'-azobis(isobutyronitrile) (AIBN), would require a higher temperature but also requires $[I]_0$ = 0.0095M (with k_d = 0.001449 s^{-1} at 100°C).[27] Since acrylates are typically associated with activation energies for the rate of propagation in the range of 17-20 kJ mol^{-1}, higher temperatures are favorable, and hence AIBN was chosen for all further experiments at 100 °C. It is thereby pure coincidence that AIBN – the probably most used thermal initiator in the realm of radical polymerization – was found to be the most suitable initiator for the purpose of the RAFT multiblock copolymerizations.

A note must be made on the targeted chain length. The above calculations do not take the RAFT agent concentration into account as they are only concerned with the rate of polymerization. In RAFT, however, the RAFT to initiator concentration is crucial for aiming at low dispersity polymers. Increasing the targeted chain length (be it in homo- or block copolymers) will lead to a lowering of the RAFT concentration compared to monomer concentration, which in turn yields lower RAFT to initiator ratios when the overall polymerization rate is kept constant. RAFT is thus inherently better suited for polymerization of multiblock copolymers with short block lengths.

4.3 Reactor design

To assure a flexible and easily variable reactor set-up, home-made tubular reactors were employed. Therefore, gastight PFA tubing (Advanced Polymer Tubing GmbH, 1/16" OD, 0.75 mm ID) was wrapped around a metal framework and placed in a silicon oil bath for heating purposes (IKA RCT basic hot plate). Reactor volumes could easily be adjusted by varying the length of the reactor tubing. Reaction solutions were pumped into the reactor via Knauer Azura P 2.1S HPLC Pumps.

Initial studies focused on the reaction kinetics of a *n*BuA homopolymerization carried out in a standardized home-made 1 mL reactor. Identical results were obtained for a residence time of 16 min (twice the half-life time of AIBN at 100°C) and a residence time of 40 min (five times the half-life time of AIBN at 100°C). It should be noted that this is no contradiction to the calculations presented above. *N*-butyl acrylate is a relatively "fast" monomer and the propagation rate coefficient is significantly larger than the limiting 10 000 L mol^{-1} s^{-1}. The reactor is though chosen to also accommodate slower monomers. Hence, in a later stage, a dedicated tubular reactor of 0.8 mL (1.81 m length) was built to carry out the polymerization of the first block at a reasonable flow rate of 0.050 mL min^{-1} (well-above the pump limitation). Depending on these choices to carry out the polymerization of the first block, the reactor volumes and flow rates in the following reactors were chosen. To provide a 1:1 ratio between the first and the second block, an equimolar flow rate was chosen between both monomers. Hence, the second stock solution was added with a flow rate of 0.040 mL min^{-1} (5 M

monomer concentration – giving a 0.2 mmol min^{-1} flow rate of monomer 2, equimolar to monomer 1) into a 3.6 mL reactor to provide a residence time of 40 min (0.090 ml min^{-1} in total). Thus, a 0.8 mL tubular reactor (as employed for the homopolymerizations), was coupled to a 3.6 mL tubular reactor to target diblock copolymers, leading to a [0.8 mL + 3.6 mL] tubular reactor cascade. According to this similar strategy, each following reactor was designed to match equimolar flow rates and 40 min residence times. Hence, triblock copolymerizations were carried out in a [0.8 mL + 3.6 mL + 5.2 mL] tubular reactor cascade, which could further be extended with a 6.8 mL tubular reactor when targeting tetrablock copolymers, leading to the [0.8 mL + 3.6 mL + 5.2 mL + 6.8 mL] tubular reactor cascade as depicted in Figure 4.3.

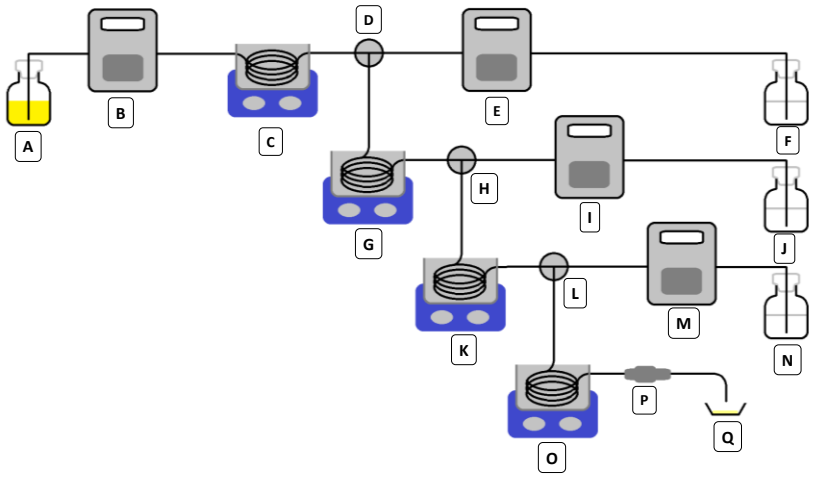

Figure 4.3. Schematic flow chart of the reactor cascade, consisting of 4 reactor units. A. Stock solution of monomer 1, DoPAT (2-(dodecylthiocarbonothioylthio) propionic acid) and AIBN; B, E, I, M. HPLC pumps; C, G, K, O. 0.8 mL / 3.6 mL / 5.2 mL / 6.8 mL tubular reactor in a heated silicon oil bath; D, H, L. T-piece, inlet flows are connected perpendicular to the outlet flow; F, J, N. stock solution of monomer 2 / 3 / 4 and AIBN; P. back pressure regulator and Q. sample collection.

In addition, experimental tests and theoretic simulations via PREDICI® were carried out to investigate the effect of sequential dosing of initiator via additional inlets. Yet, sequential dosing of initiator has no advantageous effect over propagation kinetics. A total amount $[I]_{tot}$, dosed at the beginning of the reactor or divided over multiple inlets, gives the same conversion in all cases, in simulations (Figure 4.4) as well as in experiments.

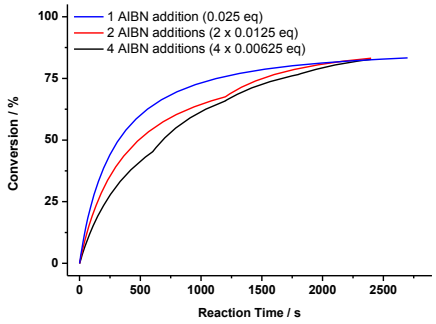

Figure 4.4. Simulating the sequential dosing of a specific amount of initiator.

Also the mixing effect at the (second) reactor inlet was tested during chain extension experiments. An inefficient mixing might lead to broadening of the molecular weight distribution and to uncontrolled polymerization of the added monomer. Therefore the effect of mixing was tested experimentally by linking two reactors to each other via the use of a T-piece (with both inlet flows connected perpendicular to the outlet flow) (Vici, ZT1, 0.75 mm bore) or via the use of a static mixing tee (Upchurch Scientific, U-466, swept volume of 2.2 μL). The static mixer should provide significantly better mixing, especially when dealing with monomer injection into a polymer solution. Yet, no differences were observed in the resulting diblock copolymer, so the cheapest and easiest solution, a T-piece, was employed further in the reactor cascades.

4.4 Homopolymerization

Based on the rational outlined above, AIBN was applied as initiator at 100°C to assure full-conversion dead-end polymerization within 40 min residence time for practically any acrylate monomer. Targeting a DP 10 homopolymer, a monomer/RAFT agent/initiator ratio of 10/1/0.05 was employed to avoid the loss of chain end functionality.[28] To reduce the mid-chain radical formation (and hence to speed up the overall polymerization), *n*-butanol was used as solvent.[29] *N*-butanol is known to cause reduced mid-chain radical formation rates, resulting in a higher actively propagating radical species concentration.[29] Maximum monomer concentrations – taking into account the limited solubility of the RAFT agent to assure homogeneous reaction conditions - turned out to be 4 M for *n*-butyl acrylate (*n*BuA), methyl acrylate (MA), ethyl acrylate (EA), *t*-butyl acrylate (*t*BuA), 2-hydroxyethyl acrylate (HEA) and *N*-isopropyl acrylamide (NIPAM). (Due to the bulkiness of 2-ethylhexyl acrylate (EHA), isobornyl acrylate (iBoA) and 2-(2-ethoxyethoxy)ethyl acrylate (DEGA), lower monomer concentrations had to be employed. In these cases 2.7 M, 2.7 M and 3 M, respectively.) The corresponding initiator concentrations are hence 0.02 M (or 0.0135 M, 0.0135 M and 0.015 M in the EHA, iBoA and DEGA system, respectively). These values are all well above the theoretically calculated lower limit for the initiator concentration (0.0095 M). Despite these highly concentrated solutions, no viscosity problems were encountered. For the homopolymerizations, monomer conversions were screened using on-line FT-IR spectroscopy. Almost full conversions were already obtained after 16 min, where FT-IR showed the absence of the typical acrylate monomer peaks (1650 – 1600 cm^{-1}). More accurate monomer conversions were further

determined via ^{1}H NMR (Table 4.1), confirming the on-line measurements. For practical reasons, 90% conversion was in the framework of the current study set as sufficient experimental limit. This means that the polymer blocks obtained in the following steps are associated with a maximum of 10% contamination. The residual monomers will be implemented along the whole sequential polymer block (random). Yet, since the amount of residual monomer is minimal, the self-assembly behavior of the polymer will not be affected significantly. Most acrylates allow to polymerize significantly above 90%, only EHA and iBoA did not reach this conversion limit, due to the lower monomer (2.7 M instead of 4 M) and initiator concentrations (0.0135 M instead of 0.02 M).

Table 4.1. Continuous homopolymerization of different acrylates and an acrylamide via the use of DoPAT as a RAFT agent. A 0.8 mL tubular reactor was employed to carry out each polymerization at 100°C and 16 min residence time. M_n^{theor} is calculated for full monomer conversion. Determinations of M_n^{app} are based on the Mark-Houwink parameters of P*n*BuA.

Polymer	$[M]_0$ / M	***M / RAFT / I ratio***	***Conversion / %***	***Đ***	M_n^{app} / g · mol^{-1}	M_n^{theor} / g · mol^{-1}
P*n*BuA	4	10 / 1 / 0.05	95	1.11	1630	1630
PMA	4	10 / 1 / 0.05	93	1.15	1110	1210
PEA	4	10 / 1 / 0.05	91	1.14	1240	1350
P*t*BuA	4	10 / 1 / 0.05	97	1.12	1610	1630
PHEA	4	10 / 1 / 0.05	98	1.14	1100	1510
PNIPAM	4	10 / 1 / 0.05	85	1.10	1170	1480
PEHA	2.7	10 / 1 / 0.05	87	1.12	2040	2190
PDEGA	3	10 / 1 / 0.05	95	1.16	2030	2230
PiBoA	2.7	10 / 1 / 0.05	89	1.12	1720	2430

To vary the chain length of the first block, different monomer/RAFT agent ratios were injected into the reactor set-up, employing otherwise identical conditions.

Monomer concentrations were kept constant at 4 M (except for DP 5 where $[M]_0$ = 2 M, corresponding to a maximum DoPAT concentration of 0.4 M given by solubility constrains). Again, no viscosity problems were encountered in the reactor. The corresponding decrease of the RAFT agent and initiator concentration led to lower monomer conversions for longer chains (Figure 4.5) and thus a larger deviation from the theoretic molecular weights (calculated for 100% monomer conversion). The increase of the molecular weight can easily be followed by SEC (Figure 4.5). The homopolymerization procedure is thus highly versatile and shows the complete formation of a first block, allowing for chain extension towards diblock copolymers, but limits must be respected with respect to the desired chain length. As described above, when longer chain segments are targeted, the RAFT to initiator concentration ratio is changed to more unfavorable conditions, leading to a slight detoriation of the RAFT end group fidelity. The increase in dispersity is hence not an effect of the flow conditions, but is inherent to the RAFT mechanism. This effect is more limiting to the present technique than viscosity issues.

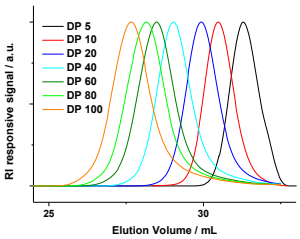

Targeted DP	*$[M]_0$ / M*	*M / RAFT / I ratio*	*Conversion / %*	*Đ*	*M_n^{app} / g · mol^{-1}*	*M_n^{theor} / g · mol^{-1}*
5	2	5 / 1 / 0.05	90	1.12	1180	990
10	4	10 / 1 / 0.05	95	1.11	1630	1630
20	4	20 / 1 / 0.05	93	1.15	2770	2910
40	4	40 / 1 / 0.05	91	1.21	4430	5480
60	4	60 / 1 / 0.05	87	1.25	6060	8040
80	4	80 / 1 / 0.05	85	1.27	7250	10600
100	4	100 / 1 / 0.05	84	1.32	9020	13170

Figure 4.5. Molecular weight distributions of *n*BuA homopolymers with different chain lengths, polymerized in a 0.8 mL tubular reactor, at 100°C and 16 min residence time. M_n^{theor} is calculated for full monomer conversion. Determinations of M_n^{app} are based on the Mark-Houwink parameters of P*n*BuA.

4.5 Diblock copolymerization

To extend the reactor to two stages, the 0.8 mL reactor employed for homopolymerizations was coupled to a second 3.6 mL reactor. Reactor volumes are carefully chosen based on the flow rates and monomer concentrations to provide a 1/1 monomer/monomer ratio. To perform a systematic study, *n*BuA, MA, HEA and DEGA were each polymerized as first block and immediately chain extended with 7 different acrylates (*n*BuA, MA, EA, *t*BuA, HEA, EHA, DEGA) and an acrylamide (*N*-isopropylacrylamide (NIPAM)). Also iBoA was employed during the chain extension of P*n*BuA, yet due to viscosity reasons, iBoA was not employed further. The results of all P*n*BuA-containing diblock copolymers are given in Table 4.2. PMA-containing diblock copolymers can be found in Table 4.3, PHEA-containing diblock copolymers in Table 4.4 and PDEGA-containing diblock copolymers in Table 4.5. High monomer conversions (≥ 90%) were obtained for most diblock copolymers. Molecular weight distributions were determined from SEC using universal calibration, based on P*n*BuA Mark-Houwink parameters. Dispersities between 1.19 and 1.27 were observed, underpinning that control is still good even after renewed injection of initiator. This broadening is related to the α chain end of the polymer, inherent to the RAFT mechanism (Figure 1.2).[28] The slight broadening of the molecular weight distributions causes a small deviation between the apparent and the theoretic average molecular weight, whereby the observed peak molecular weights are corresponding well.

Table 4.2. Diblock copolymers based on P*n*BuA as first block, obtained from a [0.8 mL + 3.6 mL] tubular reactor cascade without intermediate purification or isolation. The first block was obtained at 100°C and 16 min residence time, the second block at 100°C and 40 min residence time. M_n^{theor} is calculated for full monomer conversion. M_n^{app} and M_p^{app} are determined via SEC, based on the Mark-Houwink parameters of P*n*BuA.

Entry	***Polymer***	$[M]_0$ / M	***Conversion*** / %	***Đ***	M_n^{app} / g · mol^{-1}	M_p^{app} / g · mol^{-1}	M_n^{theor} / g · mol^{-1}
1	P*n*BuA	-	95	1.11	1630	1840	1630
2	P*n*BuA-*b*-P*n*BuA	5	92	1.19	2750	3260	2910
3	P*n*BuA-*b*-PMA	5	96	1.21	1950	2450	2490
4	P*n*BuA-*b*-PEA	5	92	1.19	2300	2750	2630
5	P*n*BuA-*b*-P*t*BuA	5	94	1.23	2480	2960	2910
6	P*n*BuA-*b*-PHEA	5	97	1.27	1990	2470	2790
7	P*n*BuA-*b*-PNIPAM	3.3	91	1.27	2210	2510	2760
8	P*n*BuA-*b*-PEHA	3.3	91	1.20	2710	3270	3470
9	P*n*BuA-*b*-PDEGA	3.3	93	1.26	2800	3340	3510
10	P*n*BuA-*b*-PiBoA	2.5	90	1.14	2870	3250	3720

Table 4.3 (right page). Diblock copolymers based on PMA as first block, obtained from a [0.8 mL + 3.6 mL] tubular reactor cascade without intermediate purification or isolation. The first block (homopolymer PMA – entry 1) was carried out in the 0.8 mL reactor, with a monomer concentration of 4 M, at 100°C and 16 min residence time (19.5 min for entries 7-9). The second block was directly polymerized in the 3.6 mL reactor at 100°C and 40 min residence time. M_n^{theor} is calculated for full monomer conversion. M_n^{app} and M_p^{app} are determined via SEC, based on the Mark-Houwink parameters of P*n*BuA.

Entry	*Polymer*	$[M]_0$ / M	*Conversion* / %	*Đ*	M_n^{app} / g · mol^{-1}	M_p^{app} / g · mol^{-1}	M_n^{theor} / g · mol^{-1}
1	PMA	-	93	1.15	1110	1270	1210
2	PMA-*b*-P*n*BuA	5	90	1.23	1940	2390	2490
3	PMA-*b*-PMA	5	91	1.23	1630	2040	2070
4	PMA-*b*-PEA	5	92	1.22	1770	2190	2210
5	PMA-*b*-P*t*BuA	5	95	1.26	2060	2640	2493
6	PMA-*b*-PHEA	5	96	1.27	1510	2040	2370
7	PMA-*b*-PNIPAM	3.3	96	1.25	1560	1910	2340
8	PMA-*b*-PEHA	3.3	85	1.23	1750	2030	3050
9	PMA-*b*-PDEGA	3.3	84	1.29	2050	2470	3090

Table 4.4. Diblock copolymers based on PHEA as first block, obtained from a [0.8 mL + 3.6 mL] tubular reactor cascade without intermediate purification or isolation. The first block (homopolymer PHEA – entry 1) was carried out in the 0.8 mL reactor, with a monomer concentration of 3 M, at 100°C and 16 min residence time (17 min for entries 7-9). The second block was directly polymerized in the 3.6 mL reactor at 100°C and 45 min residence time (40.5 min for entries 7-9). M_n^{theor} is calculated for full monomer conversion. M_n^{app} and M_p^{app} are determined via SEC, based on the Mark-Houwink parameters of P*n*BuA.

Entry	*Polymer*	$[M]_0$ / M	*Conversion* / %	*Đ*	M_n^{app} / g · mol^{-1}	M_p^{app} / g · mol^{-1}	M_n^{theor} / g · mol^{-1}
1	PHEA	-	98	1.14	1100	1340	1510
2	PHEA-*b*-P*n*BuA	5	92	1.45	1560	2520	2790
3	PHEA-*b*-PMA	5	88	1.32	1290	1930	2370
4	PHEA-*b*-PEA	5	94	1.37	1550	2250	2510
5	PHEA-*b*-P*t*BuA	5	91	1.33	1350	2030	2790
6	PHEA-*b*-PHEA	5	96	1.29	1170	1780	2673
7	PHEA-*b*-PNIPAM	3.3	95	1.34	1330	1820	2640
8	PHEA-*b*-PEHA	3.3	89	1.46	1660	2630	3350
9	PHEA-*b*-PDEGA	3.3	96	1.47	1980	2820	3390

Table 4.5 (next page). Diblock copolymers based on PDEGA as first block, obtained from a [0.8 mL + 3.6 mL] tubular reactor cascade without intermediate

purification or isolation. The first block (homopolymer DEGA – entry 1) was carried out in the 0.8 mL reactor, with a monomer concentration of 3 M, at 100°C and 16 min residence time (17 min for entries 7-9). The second block was directly polymerized in the 3.6 mL reactor at 100°C and 45 min residence time (40.5 min for entries 7-9). M_n^{theor} is calculated for full monomer conversion. M_n^{app} and M_p^{app} are determined via SEC, based on the Mark-Houwink parameters of P*n*BuA.

Entry	***Polymer***	$[M]_0$ **/ M**	***Conversion* / %**	***Đ***	M_n^{app} **/ g · mol^{-1}**	M_p^{app} **/ g · mol^{-1}**	M_n^{theor} **/ g · mol^{-1}**
1	PDEGA	-	95	1.16	2031	2378	2230
2	PDEGA-*b*-P*n*BuA	5	85	1.25	2699	3288	3510
3	PDEGA-*b*-PMA	5	89	1.23	2273	2795	3090
4	PDEGA-*b*-PEA	5	83	1.31	2431	3148	3230
5	PDEGA-*b*-P*t*BuA	5	93	1.32	2683	3405	3510
6	PDEGA-*b*-PHEA	5	98	1.22	2296	2250	3390
7	PDEGA-*b*-PNIPAM	3.3	93	1.29	2289	2647	3360
8	PDEGA-*b*-PEHA	3.3	91	1.28	2663	3326	4076
9	PDEGA-*b*-PDEGA	3.3	95	1.37	2837	3594	4110

So far, flow rates were chosen carefully to provide a 1/1 monomer/monomer ratio. Yet, to show the versatility of the system, the flow rate of the second monomer was adapted, allowing the synthesis of a "10/10", a "10/20" and a "10/40" P*n*BuA-*b*-PMA diblock copolymer (on a DP 10 P*n*BuA block). Molecular weight distributions of these diblock copolymers, in comparison to the P*n*BuA homopolymer, are shown in Figure 4.6 and Table 4.6. Of course, this approach is not limited to P*n*BuA-*b*-PMA diblock copolymers. Also a variety of P*n*BuA-*b*-PHEA and P*n*BuA-*b*-PDEGA diblock copolymers was targeted (Table 4.7 and Table 4.8, respectively). The procedure towards diblock copolymers is thus highly versatile, even though the same trend is observed as for the homopolymers; with increasing chain length of the block, a broadening of the distributions is observed.

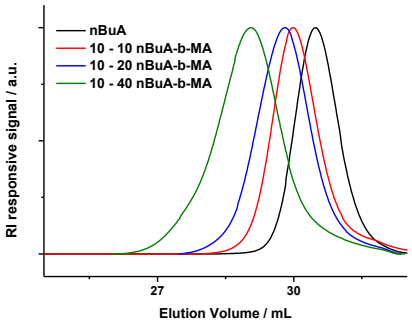

Figure 4.6. Molecular weight distributions of P*n*BuA-*b*-PMA diblock copolymers (monomer ratio 10/10, 10/20, 10/40) in comparison to the initial P*n*BuA homopolymer.

Table 4.6. P*n*BuA-*b*-PMA diblock copolymers with different monomer/monomer ratios. The first block, *n*BuA, was polymerized in the 0.8 mL reactor, with a monomer concentration of 4M, at 100°C and 16 min residence time (26.6 min for 10/40). The second block, MA, was directly polymerized in the 3.6 mL reactor, with a monomer concentration of 5M, at 100°C and 40 min residence time (51.4 min for 10/5). M_n^{theor} is calculated for full monomer conversion. M_n^{app} and M_p^{app} are determined via SEC, based on the Mark-Houwink parameters of P*n*BuA.

Polymer	***monomer/monomer ratios***	***Conversion / %***	***Đ***	M_n^{app} / g · mol^{-1}	M_p^{app} / g · mol^{-1}	M_n^{theor} / g · mol^{-1}
P*n*BuA	10 / 0	95	1.11	1630	1840	1630
P*n*BuA-*b*-PMA	10 / 5	84	1.16	1830	2140	2060
	10 / 10	96	1.21	1950	2450	2490
	10 / 20	95	1.24	2700	3160	3350
	10 /40	96	1.41	3830	4920	5080

Table 4.7. P*n*BuA-*b*-PHEA diblock copolymers with different monomer/monomer ratios. The first block, *n*BuA, was polymerized in the 0.8 mL reactor, with a monomer concentration of 4 M, at 100°C and 16 min residence time (26.6 min for 10/40). The second block, HEA, was directly polymerized in the 3.6 mL reactor, with a monomer concentration of 5 M, at 100°C and 40 min residence time (51.4 min for 10/5). M_n^{theor} is calculated for full monomer conversion. M_n^{app} and M_p^{app} are determined via SEC, based on the Mark-Houwink parameters of P*n*BuA.

Polymer	***monomer/monomer ratios***	***Conversion / %***	***Đ***	M_n^{app} / g · mol^{-1}	M_p^{app} / g · mol^{-1}	M_n^{theor} / g · mol^{-1}
P*n*BuA	10 / 0	95	1.11	1630	1840	1630
P*n*BuA-*b*-PHEA	10 / 5	91	1.20	1920	2150	2210
	10 / 10	97	1.27	1990	2470	2790
	10 / 20	98	1.22	2240	2570	3950
	10 /40	97	1.32	2360	3490	6280

Table 4.8. P*n*BuA-*b*-PDEGA diblock copolymers with different monomer/monomer ratios. The first block, *n*BuA, was polymerized in the 0.8 mL reactor, with a monomer concentration of 4 M, at 100°C, with 16 min; 19.5 min; 21 min and 36.4 min residence times for the 10/5, 10/10, 10/20 and 10/40 diblock copolymers, respectively. The second block, DEGA, was directly polymerized in the 3.6 mL (10/5 and 10/10) or the 5.2 mL reactor (10/20 and 10/40), with a monomer concentration of 3.3 M, at 100°C and 40 min residence time. M_n^{theor} is calculated for full monomer conversion. M_n^{app} and M_p^{app} are determined via SEC, based on the Mark-Houwink parameters of P*n*BuA.

Polymer	***monomer/monomer ratios***	***Conversion / %***	***Đ***	M_n^{app} / g · mol^{-1}	M_p^{app} / g · mol^{-1}	M_n^{theor} / g · mol^{-1}
P*n*BuA	10 / 0	95	1.11	1630	1840	1630
P*n*BuA-*b*-PDEGA	10 / 5	84	1.18	2160	2500	2570
	10 / 10	93	1.26	2800	3310	3510
	10 / 20	95	1.47	3570	4530	5400
	10 /40	98	2.10	5430	6690	9160

4.6 Tri- and tetrablock copolymerization

After the successful implementation of continuous diblock copolymer formation, the cascade was further extended with a 5.2 mL reactor. Reaction conditions were slightly adapted: 0.09 eq and 0.13 eq of AIBN were added in the second and third reactor, respectively, to provide a 0.02 M AIBN concentration throughout the whole reaction. On one hand, these increased AIBN concentrations provide a slight increase of conversion in the second block and a higher conversion in the third reactor, making multiblock copolymer formation more feasible. On the other hand, this also leads to broadening of the molecular weight distribution due to the adapted monomer/macroRAFT/initiator ratio (10/1/0.09 and 10/1/0.13, respectively) (decrease of the α end-group fidelity) (Figure 1.2).[28] Yet, to limit copolymer formation, maximum conversions were preferred over more narrow molecular weight distributions. Again, triblock copolymer formation was studied systematically. Based on P*n*BuA-*b*-PMA block copolymers, triblock copolymers were successfully synthesized, as can be seen in Table 4.9, with the same variety in acrylate monomers as above. Almost complete monomer conversions were observed (via the use of CH_2Br_2 as internal standard in ^{1}H NMR). The molecular weight distributions are broader than for the diblock copolymers ($1.29 \leq Đ \leq 1.35$), which is directly connected to the higher overall initiator concentration. Again, the observed peak molecular weight corresponds well to theoretic molecular weight distribution.

Table 4.9. Results for the synthesis of various triblock copolymers based on P*n*BuA-*b*-PMA macroRAFT agents. The third block was directly polymerized in a 5.2 mL reactor at 100°C and 40 min residence time. M_n^{theor} is calculated for full monomer conversion. M_n^{app} and M_p^{app} are determined via SEC, based on the Mark-Houwink parameters of P*n*BuA.

Entry	***Polymer***	$[M]_0$ / M	***Conversion*** / %	***Đ***	M_n^{app} / g · mol^{-1}	M_p^{app} / g · mol^{-1}	M_n^{theor} / g · mol^{-1}
1	P*n*BuA	-	95	1.11	1630	1840	1630
2	P*n*BuA-*b*-PMA	-	95	1.23	1960	2490	2490
3	P*n*BuA-*b*-PMA-*b*-P*n*BuA	5	91	1.35	2730	4000	3770
4	P*n*BuA-*b*-PMA-*b*-PMA	5	91	1.35	2260	3200	3350
5	P*n*BuA-*b*-PMA-*b*-PEA	5	92	1.34	2380	3330	3490
6	P*n*BuA-*b*-PMA-*b*-P*t*BuA	5	94	1.29	2820	3800	3770
7	P*n*BuA-*b*-PMA-*b*-PHEA	5	96	1.30	3470	3350	3650
8	P*n*BuA-*b*-PMA-*b*-PNIPAM	3.3	92	1.34	2150	2930	3620
9	P*n*BuA-*b*-PMA-*b*-PEHA	3.3	91	1.29	3200	4290	4330
10	P*n*BuA-*b*-PMA-*b*-PDEGA	3.3	93	1.35	2790	4020	4370

The complete formation of the third block allows for chain extension towards tetrablock copolymers via the use of a [0.8 mL + 3.6 mL + 5.2 mL + 6.8 mL] reactor cascade. Stock solutions were prepared in a similar way to the triblock copolymers. Again a higher amount of AIBN (0.17 eq) was added into the fourth reactor to provide an initiator concentration of 0.02 M. As an example, a P*n*BuA-*b*-PMA-*b*-PEA-*b*-P*t*BuA tetrablock copolymer was targeted. The employed reactor set-up, the molecular weight distributions and the results of the synthesis of the tetrablock copolymer are depicted in Figure 4.7. The copolymer was obtained with a dispersity of 1.47, at almost complete *t*BuA conversion. In contrast to batch procedures, this reactor set-up and experimental procedure could be used to synthesize a significant amount of the tetrablock copolymer by just extending the reactor run time and thus avoiding batch-to-batch variations. By collecting for

26 h, ± 150 g of the P*n*BuA-*b*-PMA-*b*-PEA-*b*-P*t*BuA tetrablock copolymer could be obtained, which is very close to the theoretically expected amount of polymer under such runtime.

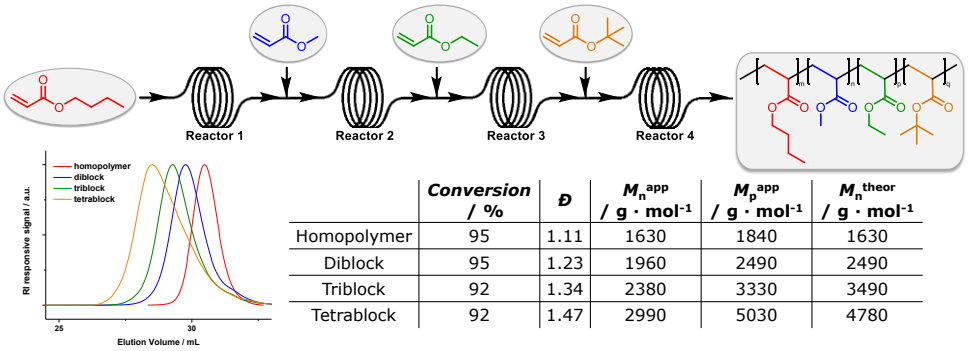

	***Conversion* / %**	***Đ***	M_n^{app} / g · mol^{-1}	M_p^{app} / g · mol^{-1}	M_n^{theor} / g · mol^{-1}
Homopolymer	95	1.11	1630	1840	1630
Diblock	95	1.23	1960	2490	2490
Triblock	92	1.34	2380	3330	3490
Tetrablock	92	1.47	2990	5030	4780

Figure 4.7. Schematic representation of the synthesis of a P*n*BuA-*b*-PMA-*b*-PEA-*b*-P*t*BuA tetrablock copolymer via the use of a [0.8 mL + 3.6 mL + 5.2 mL + 6.8 mL] reactor cascade. M_n^{theor} is calculated for full monomer conversion. M_n^{app} and M_p^{app} are determined via SEC, based on the Mark-Houwink parameters of P*n*BuA.

With the described setup, practically any tetrablock copolymer can be obtained. To show the versability of the system, also a second tetrablock copolymer was targeted, as can be seen in Figure 4.8. In principle, further extension of the cascade towards pentablock or higher block copolymers is possible, yet such set-up would require an even larger amount of pumps and mixer units. Further, the obtained tetrablock copolymers can be reinjected in the first stage in an iterative manner. First results for such approach have been encouraging, yet a further broadening of molecular weight distributions (Figure 1.2)[28] and increasing issues with maximal polymer concentration and viscosity can be expected.

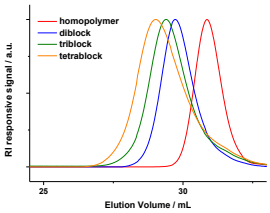

	***Conversion* / %**	***Đ***	M_n^{app} / g · mol^{-1}	M_p^{app} / g · mol^{-1}	M_n^{theor} / g · mol^{-1}
Homopolymer	91	1.14	1240	1430	1350
Diblock	96	1.23	1980	2560	2630
Triblock	97	1.37	2220	3080	3790
Tetrablock	87	1.51	2400	3850	4650

Figure 4.8. Results of the PEA-*b*-P*t*BuA-*b*-PHEA-*b*-PMA tetrablock copolymerization via the use of a [0.8 mL + 3.6 mL + 5.2 mL + 6.8 mL] reactor cascade. M_n^{theor} is calculated for full monomer conversion. M_n^{app} and M_p^{app} are determined via SEC, based on the Mark-Houwink parameters of P*n*BuA.

4.7 Conclusions

In a self-made tubular reactor cascade, multiblock copolymers were synthesized via RAFT polymerization in a single setup without the requirement of intermediate polymer isolation or purification. Theoretic calculations were carried out to target full monomer conversion in order to avoid copolymer formation (while a few percent of statistical copolymer cannot be fully avoided). The use of AIBN as initiator at 100°C, with an initiator concentration of at least 0.0095 M, provides full monomer conversion within residence times of 40 min. The (homo)polymerizations of nine different monomers (*n*BuA, MA, EA, *t*BuA, HEA, NIPAM, EHA, DEGA and *i*BoA) were carried out successfully, under the exact same reaction conditions, showing that the reactor design is very versatile and does not require reoptimization towards different acrylates. The chain length of these polymers could easily be varied. Practically full monomer conversions allowed for chain extension towards diblock copolymers, which were based on the same

monomers. Continuation of the concept allows to obtain up to tetrablock copolymers whereby the position of the different acrylates in the block structure and the length of the blocks (with a upper limit of ~40 units per block) can be chosen freely. Generally, an increase in chain (or block) length results in slight broadening of the distributions, which is inherent to the process in circumstances where the dispersity is limited by the extent of termination, if polymerization rates are meant to be kept constant as is here the case. The reactor can hence be used for high-throughput screening as it allows to synthesize a large number of different block copolymers in short time, under very reproducible reaction conditions. In total, for this study a number of 55 diblock, triblock and tetrablock copolymers (based on 8 different acrylates and an acrylamide) were obtained. Further, the reactor also allows for facile upscaling of the reactions, making the desired block copolymers also available to extensive mechanical testing. P*n*BuA-*b*-PMA-*b*-PEA-*b*-P*t*BuA tetrablocks were obtained as proof of principle in very significant amount (± 150 g in 26 h). The developed procedure is thus highly versatile, allows for a stable production over extended period of time and can in principle easily be employed for even further chain extensions. As a final note, in view of literature describing block copolymers with ten or more segments, a tetrablock copolymer might appear to be small in size. It should, however, be noted that our method is wide in scope and not limited to certain very fast monomers or very few monomer unit insertions, and due to its automated nature is available to scientists outside the field of synthetic macromolecular chemistry. Furthermore, theoretical understanding of self-assembly effects of multiblock copolymers is highly complex, and 4 consecutive blocks with variable chain length is more than sufficient to advance the field of research in this area.

4.8 Outlook

A tubular reactor cascade was developed in order to produce multiblock copolymers via RAFT polymerization. Flow chemistry was hereby used as an efficient toolbox, providing the possibility of reactor telescoping and an easy upscaling procedure. This, in combination with the continuous nature of the protocol, makes this study interesting for further research applications. Various multiblock copolymers can be synthesized with ease and can be used for further chain extension experiments,[30] surface grafting, micellization studies, etc.

Still, to fulfill some industrial requirements, further investigations can be carried out based on a different type of polymers. On one hand, polymethacrylates are very popular as polymeric additives such as dispersants.[31] Polyacrylamides on the other hand are often used for the paper industry, for water treatment, mining and oil explorations.[32] Hence, continuous polymerization of such polymer classes would be interesting as well from an industrial point of view. Next to these polymer classes, it might also be interesting to investigate a fundamentally different approach. The use of photo-initiation instead of thermal initiation should be beneficial for the procedure as well, since less molecular weight broadening is expected. Simultaneously, this approach might also be cost-reducing and more energy-sufficient. Still, this study towards the continuous RAFT polymerization of multiblock copolymers via the use of a single reactor cascade can definitely be considered as a first step towards the production, and thus also towards the industrialization of this type of polymer materials.

4.9 References

(1) Ruzette, A.-V.; Leibler, L. *Nature Materials* **2005**, *4*, 19.

(2) Junkers, T. *Macromolecular Chemistry and Physics* **2017**, *218*, 1600421.

(3) Szwarc, M. *Journal of Polymer Science Part A: Polymer Chemistry* **1998**, *36*, IX.

(4) Jenkins, A. D.; Jones, R. G.; Moad, G. In *Pure And Applied Chemistry* 2009; Vol. 82, p 483.

(5) Keddie, D. J. *Chemical Society Reviews* **2014**, *43*, 496.

(6) Hawker, C. J.; Bosman, A. W.; Harth, E. *Chemical Reviews* **2001**, *101*, 3661.

(7) Nicolas, J.; Guillaneuf, Y.; Lefay, C.; Bertin, D.; Gigmes, D.; Charleux, B. *Progress in Polymer Science* **2013**, *38*, 63.

(8) Matyjaszewski, K. *Macromolecules* **2012**, *45*, 4015.

(9) Noda, T.; Grice, A. J.; Levere, M. E.; Haddleton, D. M. *European Polymer Journal* **2007**, *43*, 2321.

(10) Haven, J. J.; Guerrero-Sanchez, C.; Keddie, D. J.; Moad, G. *Macromolecular Rapid Communications* **2013**, *33*, 492.

(11) Haven, J. J.; Guerrero-Sanchez, C.; Keddie, D. J.; Moad, G.; Thang, S. H.; Schubert, U. S. *Polymer Chemistry* **2014**, *5*, 5236.

(12) Gody, G.; Maschmeyer, T.; Zetterlund, P. B.; Perrier, S. *Nature Communications* **2013**, *4*, 2505.

(13) Gody, G.; Maschmeyer, T.; Zetterlund, P. B.; Perrier, S. *Macromolecules* **2014**, *47*, 3451.

(14) Gody, G.; Barbey, R.; Danial, M.; Perrier, S. *Polymer Chemistry* **2015**, *6*, 1502.

(15) Gemici, H.; Legge, T. M.; Whittaker, M.; Monteiro, M. J.; Perrier, S. *Journal of Polymer Science Part A: Polymer Chemistry* **2007**, *45*, 2334.

(16) Vandenbergh, J.; de Moraes Ogawa, T.; Junkers, T. *Journal of Polymer Science Part A: Polymer Chemistry* **2013**, *51*, 2366.

(17) Webb, D.; Jamison, T. F. *Chemical Science* **2010**, *1*, 675.

(18) Monbaliu, J.-C. M.; Emmanuel, N.; Gérardy, R. *Chimie Nouvelle* **2016**, *122*.

(19) Derboven, P.; Van Steenberge, P. H. M.; Vandenbergh, J.; Reyniers, M.-F.; Junkers, T.; D'Hooge, D. R.; Marin, G. B. *Macromolecular Rapid Communications* **2015**, *36*, 2149.

(20) Haven, J. J.; Zaquen, N.; Rubens, M.; Junkers, T. *Macromolecular Reaction Engineering*, 1700016.

(21) Diehl, C.; Laurino, P.; Azzouz, N.; Seeberger, P. H. *Macromolecules* **2010**, *43*, 10311.

(22) Hornung, C. H.; Guerrero-Sanchez, C.; Brasholz, M.; Saubern, S.; Chiefari, J.; Moad, G.; Rizzardo, E.; Thang, S. H. *Organic Process Research & Development* **2011**, *15*, 593.

(23) Hornung, C. H.; Nguyen, X.; Kyi, S.; Chiefari, J.; Saubern, S. *Australian Journal of Chemistry* **2013**, *66*, 192.

(24) Li, Z.; Chen, W.; Zhang, L.; Cheng, Z.; Zhu, X. *Polymer Chemistry* **2015**, *6*, 5030.

(25) Gauthier, M. A.; Gibson, M. I.; Klok, H.-A. *Angewandte Chemie International Edition* **2009**, *48*, 48.

(26) Odian, G. *Principles of polymerization*; fourth edition ed.; John Wiley & Sons, 2004.

(27) Van Hook, J. P.; Tobolsky, A. V. *Journal of the American Chemical Society* **1958**, *80*, 779.

(28) Vandenbergh, J.; Junkers, T. *Macromolecules* **2014**, *47*, 5051.

(29) Liang, K.; Hutchinson, R. A.; Barth, J.; Samrock, S.; Buback, M. *Macromolecules* **2011**, *44*, 5843.

(30) Haven, J. J.; Baeten, E.; Claes, J.; Vandenbergh, J.; Junkers, T. *Polymer Chemistry* **2017**, *8*, 2972.

(31) Evonik *http://methyl-methacrylate-monomers.evonik.com/product/visiomer/en/application-areas/specialty-applications/dispersants/pages/default.aspx*, *2017-06-11*.

(32) BASF *http://www.performancechemicals.basf.com/ev/internet/performance-chemicals/en/content/Performance_Chemicals/news/2013_07_25_BASF_further_strengthening_Water-Oilfield-Mining-Solutions_businesses*, *2017-06-11*.

CHAPTER 5

Enzymatic controlled radical polymerizations via microfluidics

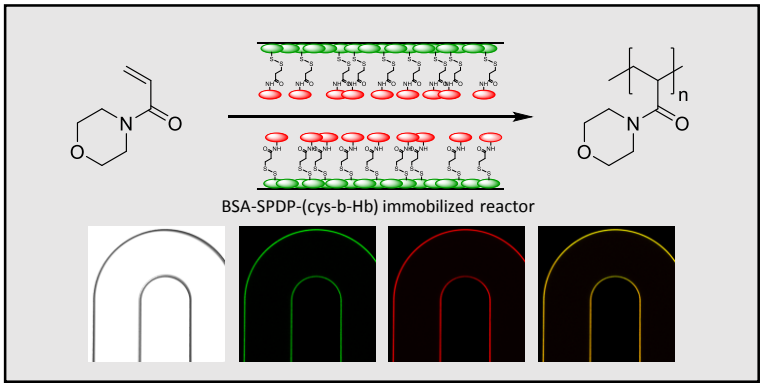

Enzymatic controlled radical polymerizations were investigated under continuous flow conditions. Therefore, a reversible immobilization route of hemoglobin (Hb) towards an enzyme-immobilized microreactor was developed, in order to perform enzyme-catalyzed controlled radical polymerizations. Secondly, the continuous homogeneous polymerization of 4-acryloylmorpholine (AcMo) – via the use of Hb as catalyst – was investigated. In a later stage, the Hb-immobilized reactor chips were tested to carry out the enzyme-catalyzed radical polymerization of AcMo.

(collaboration with B. Gajewska, J. Pollard, N. Bruns; Macromolecular Chemistry Research Group, Adolphe Merckle Institute, University of Fribourg, Switzerland)

5.1 Enzymatic controlled polymerizations

One of the foundations of polymer synthesis has always been catalysis, for which transition metal complexes are used most frequently.[1] Such catalysts are often difficult to remove from the polymer product and hamper the application of the resulting polymer. Enzymes – nature's sustainable catalysts – have been proposed as an environmentally friendly and non-toxic alternative.[2] The use of enzymes avoids the need for scarce precious-metal catalysts, which is not only economically favorable but also environmentally benign.[2] Derived from renewable resources (such as animals, plants and minerals), enzymes are biocompatible, biodegradable, nonhazardous and non-toxic.[3]

Intrinsically, enzymatic reactions are best performed in water, under mild reaction conditions with regards to temperature, pressure and pH.[4,5] Next to the acceleration of the reaction rate, enzymes are very selective due to the molecular recognition of the substrate by the enzyme.[4] This selectivity can be explained by the so-called 'Key and Lock' theory, as represented in Figure 5.1.[5] Still, it should be noted that the substrate-enzyme relationship is not always as strict as represented by the 'Key and Lock' principle. Enzymes are dynamic and sometimes very generous towards their substrates, allowing the synthesis of not only natural polymers but also a variety of unnatural polymers.[5]

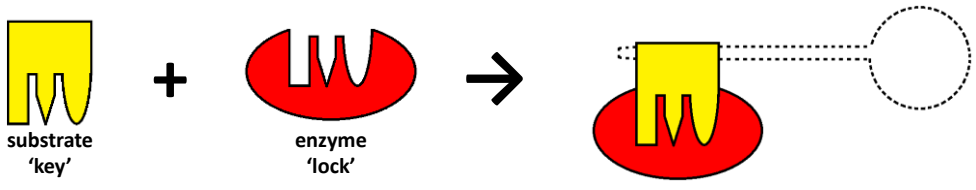

Figure 5.1. Enzyme-substrate relationship – the 'Key and Lock' principle.

Table 5.1. Typical polymers synthesized by the different classes of enzymes.[5-7]

Enzymes	Typical Polymers
oxidoreductases	polyphenols, polyanilines, vinyl polymers
transferases	polysaccharides, polyesters
hydrolases	polysaccharides, polyesters, polycarbonates, polyamides, polyphosphates, polythioesters
lyases	/
isomerases	/
ligases	/

Different macromolecules have already been targeted via enzymatic polymerizations. Depending on the nature of the enzyme (and the substrate), different types of polymerizations can occur. Generally, enzymes are classified into six groups, of which three classes have been reported to be used for enzymatic polymerizations (Table 5.1).[5-7] An excellent overview on those has been described by Kobayashi et al.[5-7]

Some of these enzymatic polymerizations exhibit living characteristics. Enzymatic controlled radical polymerizations have independently been described by two research groups.[8-13] On one hand, Bruns and coworkers investigated the use of the hemoprotein horseradish peroxidase (HRP) as catalyst for the polymerization of *N*-isopropylacrylamide under the conditions of an atom transfer radical polymerization (ATRP).[8] Hereby, the name 'ATRPase' was proposed to describe the ability of an enzyme to perform catalytic activity under ATRP conditions.[8] Later, they also investigated the use of bovine hemoglobin (Hb) as ATRPase (see also further).[9] On the other hand, di Lena and coworkers investigated the use of catalase and laccase to catalyze similar polymerizations.[10,11]

Besides radical polymerizations, enzymes can also catalyze ring-opening polymerizations, as has been demonstrated by Gross et al.[14] They also reported the first continuous enzyme-catalyzed polymerization. Therefore, they carried out the ring-opening polymerization of ε-caprolactone to polycaprolactone via the use of a packed bed reactor, where *Candida Antartica* Lipase B (Novozyme 435) was immobilized on solid beads.[15,16] So far, to the best of our knowledge, this is however the only example of a continuous enzyme-catalyzed polymerization.

Yet, enzymes (immobilized and non-immobilized) have been used previously in microreactors for organic synthesis reactions.[17,18] Different methodologies exist to carry out enzyme-catalyzed reactions via the use of a microreactor. The simplest methodology is the homogeneous approach: injecting substrate and enzyme into the reactor via separate inlets in order to carry out the reaction in solution phase.[17,18] The use of immobilized enzymes is however preferable due to the possibility to reuse the biocatalyst without any complicated isolation or purification protocol. This minimalizes the loss of the enzymatic reagent and leads to higher product yields per utilized enzymes. In addition, the stability of the enzyme increases due to their immobilization. Immobilized enzymes have a higher resistance to denaturation as well as an increased tolerance toward elevated temperature, which directly relates to a prolonged lifetime of the enzyme.[18] Two types of enzyme-immobilized (micro)reactors exist: packed enzymatic reactors – loaded with enzyme-immobilized bead or monoliths – and open-tubular enzymatic reactors where the enzymes are immobilized on the microchannel surface.[17] Compared to packed reactors, open tubular reactors provide a lower enzyme density – and thus a decreased surface-to-volume ratio. Related to this, open tubular reactors are characterized by a longer diffusion length between the

substrate and the immobilized enzyme, which has a negative impact on the reaction efficiency and might lead simultaneously to a decreased control over the reaction.[18] Despite the shorter (and thus beneficial) diffusion lengths, packed reactors are characterized by a pressure drop (high flow resistance) and are highly unfavorable in large-scale processing due to their susceptibility to increasing pressures.[17] Open-tubular reactors on the other hand have a lower flow resistance, leading to more stable reaction conditions and a better flow profile.[18,19] For this reason, an enzyme immobilization strategy was developed in this thesis towards an open-tubular reactor whereby the enzyme was immobilized on the microchannel surface.

Here, a reversible immobilization route of hemoglobin (Hb) is developed toward an enzyme-immobilized microreactor in order to perform an enzyme-catalyzed radical polymerization. In a first step (Figure 5.2), an immobilization strategy was established to immobilize Hb on the inner wall of a glass microchip reactor and to cleave it off again to be able to recover and reuse the glass microchip reactor. Secondly, the homogeneous enzyme-catalyzed polymerization of 4-acryloylmorpholine (AcMo) was carried out in a microreactor to investigate the required reaction conditions. In a later stage, the Hb-immobilized reactor chips were tested for the enzymatic controlled radical polymerization of AcMo.

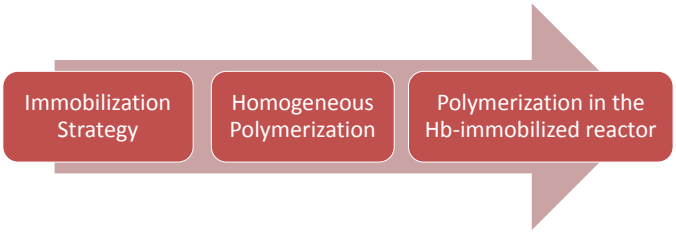

Figure 5.2. Enzyme-catalyzed radical polymerization in an immobilized reactor.

5.2 Enzyme immobilization strategy

Aiming for an enzyme-immobilized microreactor, we strived to develop a reversible immobilization route in order to recover and reuse the microreactor chip in a later stage. Previous studies already showed the possibility to immobilize an enzyme on the inner wall of a PTFE microtube with an inner diameter of 500 μm, by forming a cross-linked polymerization network on the reactor wall.[20] Yet, since this route is rather invasive for the reactor and cannot be undone afterwards, a different strategy was targeted here. Hence, in order to develop a reversible route, the adsorption of the enzyme on the surface (the reactor wall) had to be reversible as well. The strength of the adsorption should thus be fine-tuned: strong enough to hold the enzyme and at the same time weak enough to cleave it afterwards in order to recover the reactor. Therefore, the physisorption of bovine serum albumin (BSA) was chosen as adsorption method on the reactor wall to immobilize the enzyme (since BSA has the tendency to readily stick to any surface).[21] Afterwards, the cysteine groups of BSA can directly be linked to the lysines of the catalytically active enzyme by employing the commercially available linker SPDP (*N*-succimidyl 3-(2-pyridyldithio)propionate)) (Figure 5.3).[22,23]

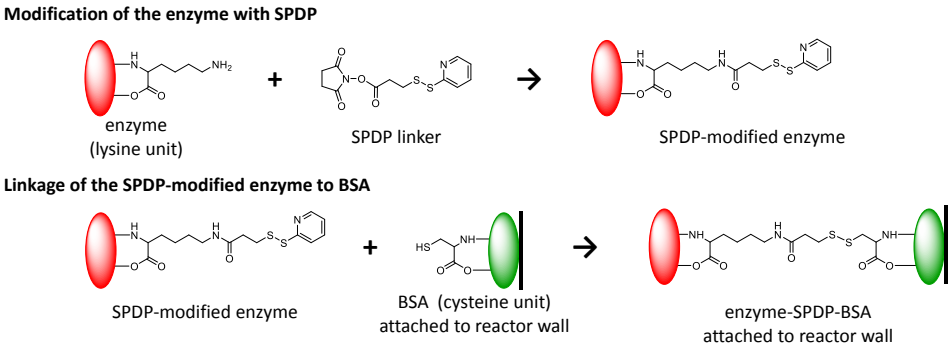

Figure 5.3. Protein-to-protein conjugation strategy involving SPDP.[22]

In practice, a clean glass microchip reactor (oven 400°C, step 0 in Figure 5.5) was loaded with BSA by flushing a 1 mg mL^{-1} BSA stock solution through the reactor (5 min residence time, 1 h incubation time, step 1 in Figure 5.5). Afterwards, the reactor was rinsed with a 1 mg mL^{-1} solution of dithiothreitol (DTT) to reduce the disulfide bonds and activate the BSA-cysteines in the reactor (5 min residence time, 1 h incubation time, step 2 in Figure 5.5). By flushing a 1 mg mL^{-1} solution of SPDP-modified enzyme, chemisorption of the catalytically active enzyme occurs on the BSA to form an enzyme-SPDP-BSA complex, which is physically adsorbed on the reactor wall.

To evaluate the success of the immobilization strategy, confocal fluorescence microscopy might be one of the most suited visualization techniques.[24] Therefore, amine-reactive ATTO-Tec dyes (based on *N*-hydroxysuccimidyl-esters (NHS-esters))[25] were used, of which the NHS-ester interacts with the lysine-sidechain of the enzyme to form an amide bond (Figure 5.4).[26] Hence, BSA was labeled with ATTO 488, a fluorescent dye with an absorption maximum around 500 nm. As catalytic active enzyme (ATRPase), two different types of enzymes were employed, horseradish peroxidase (HRP) and hemoglobin (Hb), to test the immobilization strategy. HPR was labeled with ATTO 647, while ATTO 550 was employed for the labeling of Hb.[26] Those labeled enzymes were then attached to the reactor wall as discussed above.

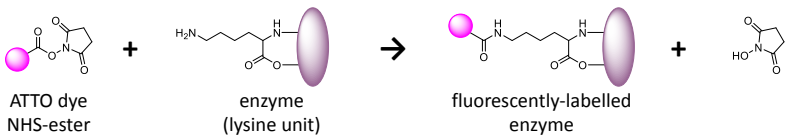

Figure 5.4. Fluorescent labeling of an enzyme via the NHS-ester.[25]

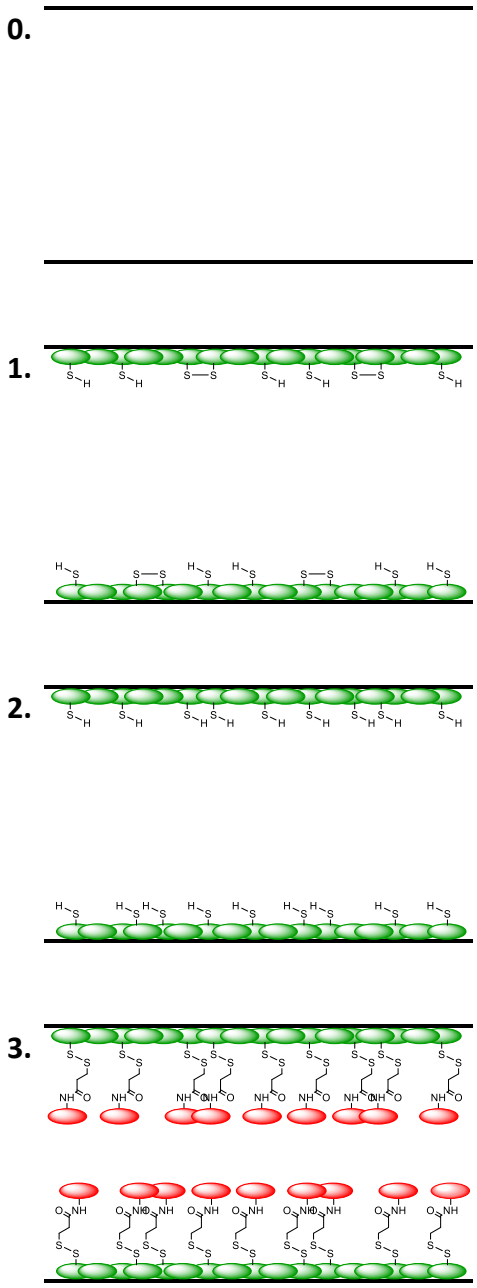

Figure 5.5. Enzyme-immobilization strategy: 0 – clean reactor channel, 1 – physisorption of BSA, 2 – activation BSA-cysteines via DTT and 3 – chemisorption of the SPDP-modified enzyme to BSA-cysteines.

Hence, a clean glass microchip reactor (step 0 in Figure 5.5) was loaded with fluorescently-labeled BSA (step 1 in Figure 5.5) in order to evaluate the physisorption of BSA to the reactor wall. The reactor was flushed extensively afterwards with the labeling buffer (Chapter 7) in order to remove residual (non-attached) fluorescent BSA. Confocal fluorescence microscopy was used to visualize the presence of fluorescently-labeled BSA. Though no quantitative analysis was carried out, the BSA-immobilization is clearly visible. As can be seen in Figure 5.6, the fluorescently-labeled BSA sticks clearly to the reactor wall. The reactor walls are completely covered with BSA, while no fluorescently-labeled BSA is found at the inner part of the reactor channel.

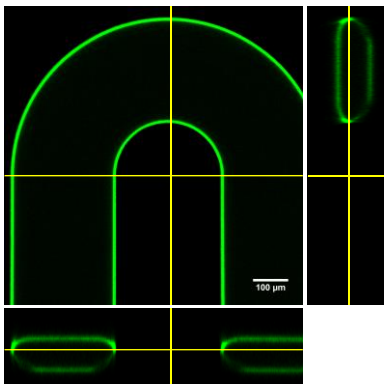

Figure 5.6. Confocal fluorescence microscopy image of a BSA-immobilized reactor wall, including the orthogonal XZ and YZ views.

Next, the reactor was flushed with DTT in order to activate the BSA cysteines (step 2 in Figure 5.5). No differences in fluorescence were observed, re-illustrating the success of the BSA-immobilization. Afterwards, the fluorescently-labeled SPDP-modified enzyme was directly linked to the BSA, immobilized on the reactor wall. Two different types of SPDP-modified enzymes were tested in different reactors. In a first reactor chip (which had the same BSA treatment as described

above, but which is not shown in Figure 5.6.), SPDP-modified HRP was employed. Again, it can clearly be seen via confocal fluorescence microscopy that the fluorescently-labeled HRP (right) is present at the same places as the fluorescently-labeled BSA (left) (Figure 5.7). Hence, the reactor walls are completely covered with BSA-SPDP-HRP, while no fluorescent species (neither BSA nor HRP) are present at the inner part of the reactor channel.

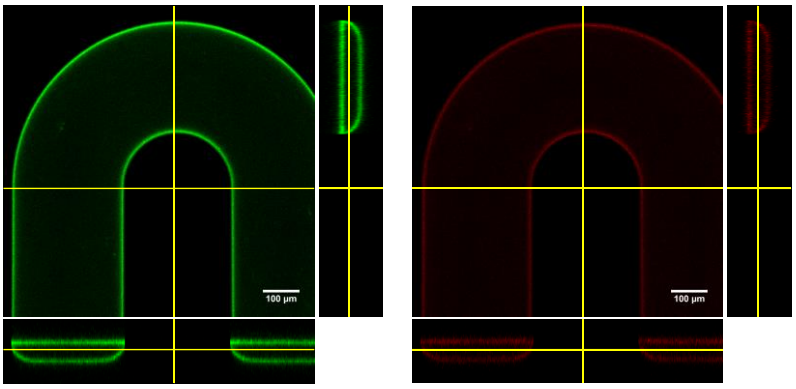

Figure 5.7. Confocal fluorescence microscopy images of immobilized reactor wall. Left: BSA-immobilization, right: HRP-immobilization. The orthogonal XZ and YZ views for both BSA and HRP are shown as well.

Next to HRP, also Hb was tested during this immobilization strategy. Therefore, a second reactor chip (the same one as employed in Figure 5.6) was flushed with SPDP-modified Hb and rinsed with the linkage buffer (Chapter 7) afterwards. Confocal fluorescence microscopy images were taken Z-stack-wise, of which a few selected slides are shown in Figure 5.8. The fluorescently-labeled Hb (middle) is present at the same places as the fluorescently-labeled BSA (left), as can also be seen in the overlay (right). Hence, the immobilization of the catalytically active enzyme via the use of a SPDP linker on the BSA-immobilized reactor wall can definitely be considered successful.

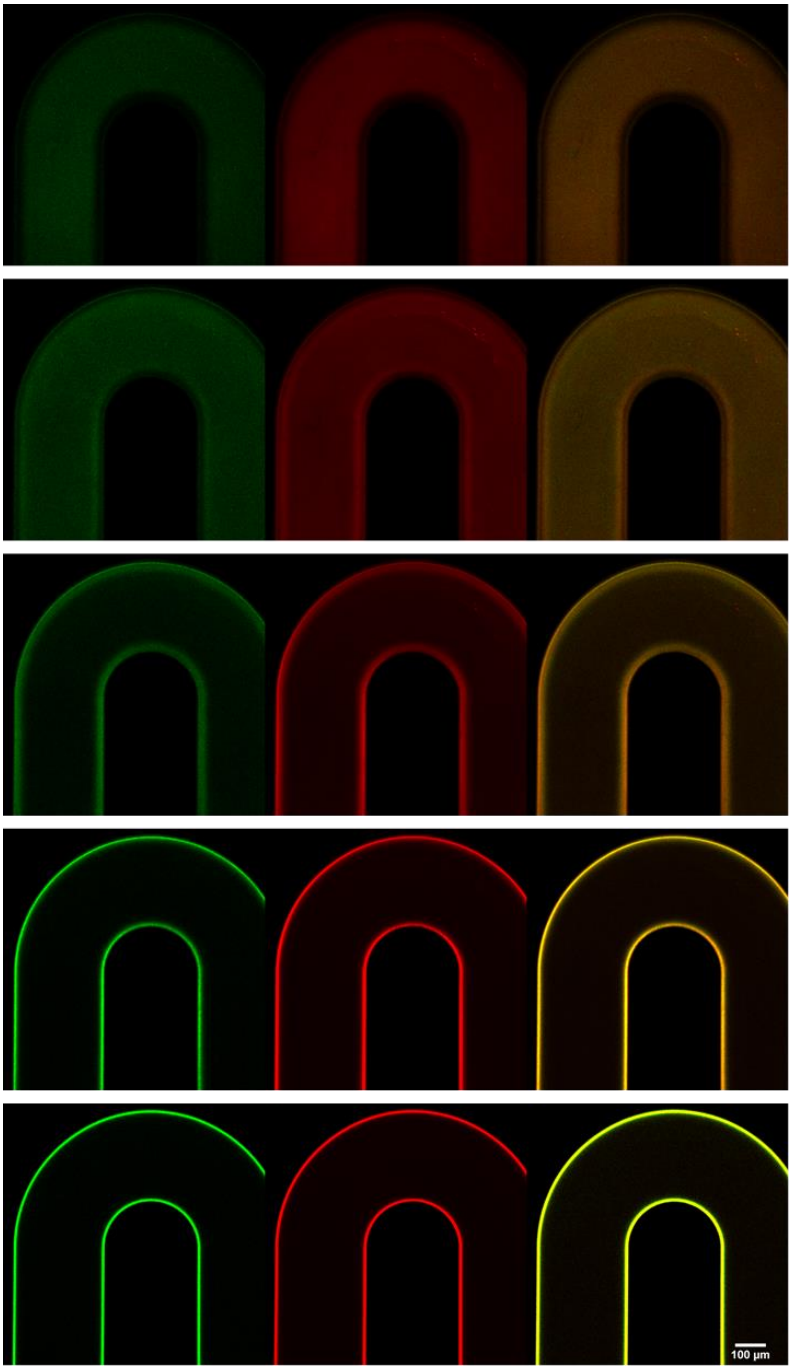

Figure 5.8. Z-stack of fluorescence microscopy images of the immobilized reactor wall. Left: BSA-immobilization, middle: Hb-immobilization, right: overlay.

Next to the success of the immobilization, also the removal of the proteins is important when aiming for a reversible immobilization route. Different protein removal strategies have already been described in literature, where it was concluded that not all strategies work equally well on every type of material.[27] Yet, a much more straightforward method was targeted here. Basically, it is rather simple to remove proteins from a glass surface. A solution of 10 mg mL^{-1} dishwasher detergent in water was flushed through the reactor for several hours. After a rinsing step with water, confocal fluorescence microscopy (left, Figure 5.9) confirmed the absence of any fluorescent species, proving the success of the protein removal.

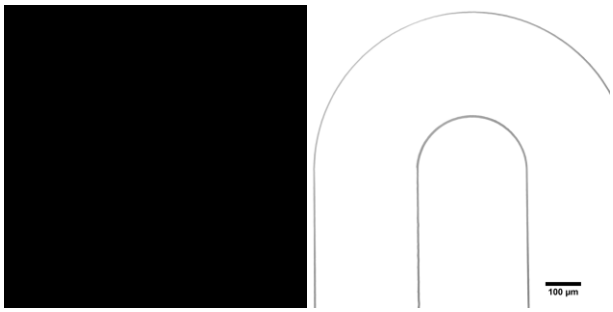

Figure 5.9. Confocal microscopy of the reactor channel after protein removal.

The reactor wall inside a glass microchip reactor has thus successfully been covered by BSA via physisorption. Next, a catalytically active enzyme such as HRP or Hb was successfully linked to the cysteines of BSA via the use of a SPDP-linker. Afterwards, the proteins can completely be removed via the use of ordinary dishwasher detergent in order to recover and reuse the reactor chip in a later stage.

5.3 Homogeneous enzyme-catalyzed polymerization

To investigate the required reaction conditions, the homogeneous enzyme-catalyzed polymerization of 4-acryloylmorpholine (AcMo) was carried out. The polymerization occurs via an activators regenerated by electron transfer atom transfer radical polymerization (ARGET ATRP), whereby sodium ascorbate (NaAsc) is employed as reducing agent. As catalyst, HRP as well as Hb should be suitable to carry out the polymerization under ARGET ATRP conditions.[8,13] Here, cys-blocked hemoglobin (cys-b-Hb) was employed to catalyze the polymerization, with the free cysteine groups of Hb blocked to inhibit chain transfer/initiation via the thiol groups. Promising results could be obtained via this polymerization in batch: high conversions in short time periods, monomodal molecular weight distributions and polydispersities < 1.50 (Table 5.2). Extended reaction times showed indications of side reactions occurring since a decrease of molecular weights was observed. Yet, such problems can often be overcome by transferring the batch procedure to flow due to an improved heat transfer.

Table 5.2. Results of the (cys-b-Hb)-catalyzed polymerization of AcMo in batch.

Reaction Temperature	***Reaction Time***	***Conversion / %***	M_n^{app} **/ g · mol^{-1}**	***Đ***
RT	1h	50	980	1.02
	1h30	85	7180	1.20
	2h	77	5840	1.24
40°C	0h30	76	7020	1.29
	1h	94	6750	1.36
	1h30	96	4660	1.44

The polymerization in batch was completely homogeneous and no precipitates were observed. Hence, the same parameters were taken as initial conditions for the continuous flow polymerization. Though such an approach is usually a good starting point to optimize the flow procedure, problems occurred here due to the presence of the enzyme. When employing the glass microchip reactor, hemoglobin sticks partially to the reactor wall (Figure 5.10). Hence, reaction conditions cannot be compared to the original batch experiment and are not reproducible. Even after longer reaction run times, no stable conditions were achieved. The enzyme seems to bind and to detach randomly, as could be observed visually. Such behavior might eventually lead to reactor clogging after longer reaction run times.

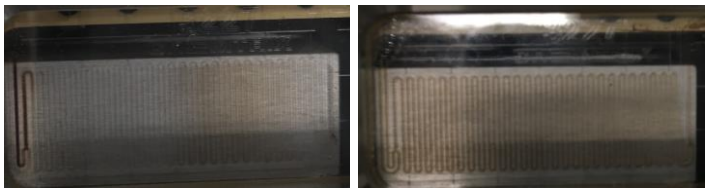

Figure 5.10. Hemoglobin sticks to the reactor walls of a glass microchip reactor.

Hence, to carry out the homogeneous polymerization in flow, a different type of reactor had to be employed. To keep the reactor volume comparable to the glass microchip reactor (19.5 μL), a tubular reactor was made of 5 ft long PEEK tubing with an internal diameter of 125 μm (reactor volume 19.3 μL) (Figure 5.11).

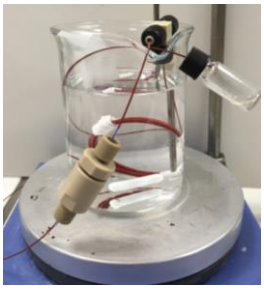

Figure 5.11. A 19.3 μL tubular reactor, made of PEEK tubing.

The 19.3 μL tubular reactor was employed to carry out the homogeneous polymerization of AcMo, employing the same parameters as described above. The reaction was carried out at 40°C, to target high monomer conversions. Results of the polymerization after 30 min and after 1 h are shown in Table 5.3. Less variation in product outcome was observed. Yet, a broader molecular weight distribution and lower monomer conversions were obtained compared to the batch procedures. The absence of thermal hot spots in a flow reactor might explain the lower monomer conversion, though this not explains the broad molecular weight distributions.

Table 5.3. Results of the homogeneous (cys-b-Hb)-catalyzed polymerization of AcMo in the 19.3 μL tubular microreactor at 40°C.

Reaction Temperature	***Residence Time***	***Conversion / %***	***M_n^{app} / g · mol^{-1}***	***Đ***
40°C	30 min	24	5130	2.19
	1 h	16	4140	1.75

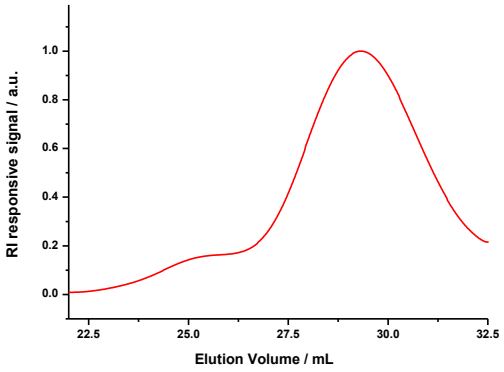

Figure 5.12. SEC results of the homogeneous (cys-b-Hb)-catalyzed polymerization of AcMo in the 19.3 μL tubular microreactor at 60°C.

To increase the monomer conversion, a higher temperature was targeted. As a first trial, the reaction was carried out at 60°C for 30 min. However, clogging of the reactor was observed. A second trial, with the same conditions, did not result in higher yields, neither a smaller molecular weight distribution was observed. Moreover, degradation of the hemoglobin solution in the syringe was observed (formation of aggregates) during the reaction run time (± 20 h, syringe is kept at RT) – which might explain the broad molecular weight distributions and even the low monomer conversions. Thus, to carry out the homogeneous polymerization in flow, a different approach must be found. Perhaps a bigger reactor set-up (and thus shorter reaction run times) or cooling the syringe solution might be a viable alternative.

5.4 Polymerization in the (cys-b-Hb)-immobilized reactor

An enzyme-catalyzed polymerization of AcMo has also been carried out in the reactor immobilized with cys-b-Hb (as described in 5.2). At first, similar conditions to the batch polymerization were applied by injecting a stock solution of AcMo, 2-hydroxyethyl 2-bromoisobutyrate (HEBIB) and NaAsc in an acetate buffer/DMF mixture, into the (cys-b-Hb)-immobilized reactor. Yet, even after 30 min residence times at 40°C, only a few percentages monomer conversion (5%) were observed leading to an overlap of molecular weight distributions of the formed polymer and the monomer (red curve, Figure 5.13). A possible explanation might come from the amount of immobilized cys-b-Hb on the reactor wall – this amount might be too small to catalyze or to control the polymerization. To overcome this problem, a stronger reducing agent, namely sodium dithionite (sodium hydrosulfite, $Na_2S_2O_4$), was employed. A higher monomer conversion (91%) and improved molecular weight distribution were obtained (blue curve, Figure 5.13), though further optimization was required to improve the control over the polymerization.

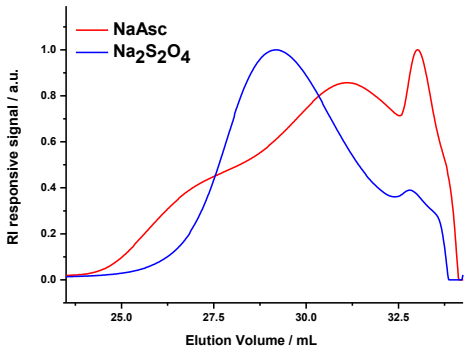

Figure 5.13. Preliminary results for the polymerization in the immobilized reactor, via the use of NaAsc (red) or $Na_2S_2O_4$ (blue) as reducing agent.

Table 5.4. Results of the enzyme-catalyzed polymerization via $Na_2S_2O_4$ as reducing agent, in the (cys-b-Hb)-immobilized reactor.

AcMO/HEBIB/$Na_2S_2O_4$ equivalents	***Conversion / %***	***M_n^{app} / g · mol^{-1}***	***Đ***
70 / 1 / 1	82	7470	3.81
70 / 1 / 2.5	91	1660	2.84
140 / 1 / 1	52	2630	3.75
200 / 1 / 2.5	71	2050	3.07
200 / 1 / 5	48	4780	3.75

Hence, to further optimize the polymerization, various experiments were carried out with different AcMo and $Na_2S_2O_4$ concentrations. Generally, a controlled polymerization should follow some trends: higher AcMo/HEBIB ratios should normally lead to higher molecular weights while higher $Na_2S_2O_4$ concentrations should give a faster catalytic activity and thus higher monomer conversions. Yet, none of these were observed (Table 5.4). The polymerization seemed to occur randomly and was thus not reproducible. A possible explanation could be the limited accessibility of the enzyme embedded on the reactor wall. Perhaps the propagating chain is not able to interact with the enzyme, limited by the diffusion length between the propagating species and the immobilized reactor wall. The lack of control by the enzyme might lead to the (uncontrolled) free radical polymerization and could thus explain the broad molecular weight distributions. On the other hand, a second possible explanation would be the degradation of the immobilized reactor during the polymerization reaction: either the enzyme degrades (which is rather unlikely due to successful batch experiments) or the immobilization is damaged during polymerization conditions. To test this last hypothesis, we used fluorescence spectroscopy in order to test the stability of the immobilization itself. Therefore, fluorescently-labeled Hb-SPDP was linked to the

BSA cysteines of a BSA-immobilized reactor, activated with DTT (Figure 5.5). Afterwards, the reactor was continuously rinsed with a 10 mg mL^{-1} solution of $Na_2S_2O_4$ in a buffer (acetate buffer, pH 3). The reactor outcome was collected during the first 10 min (when still non-attached fluorescent dye was rinsing out) (entry 3), during the next hour (entry 4), and during the next 4 hours (entry 5, Table 5.5). Yet, even in the last sample, an increase of fluorescence in comparison to the buffer (blank) was observed. Hence, it can be concluded that the immobilized reactor is indeed not stable against the employed polymerization conditions. A possible explanation might be the interaction of $Na_2S_2O_4$ as strong reducing agent with the SPDP-linker between BSA and the cys-b-Hb, interrupting the disulfide bonds. Different polymerization conditions are thus required to carry out the (cys-b-Hb)-catalyzed polymerization of AcMo in this (cys-b-Hb)-immobilized reactor. Alternatively, a different immobilization strategy has to be followed to develop an immobilized reactor, stable under these polymerization conditions. Yet, the limited approachability of the enzyme might still lead to a loss of control in both cases.

Table 5.5. Fluorescence spectroscopy results, testing the stability of the immobilized reactor against $Na_2S_2O_4$.

Entry	***Sample***	***Fluorescence Intensity***
1	Blank (acetate buffer)	20
2	Fluorescently labelled Hb-SPDP	7140
3	10 min flushing of $Na_2S_2O_4$ / acetate buffer	2540
4	1 h flushing of $Na_2S_2O_4$ / acetate buffer	470
5	4 h flushing of $Na_2S_2O_4$ / acetate buffer	100

5.5 Conclusions and outlook

In this project, a reversible immobilization route of hemoglobin (Hb) towards an enzyme-immobilized microreactor was targeted, in order to perform a continuous enzyme-catalyzed controlled radical polymerization. In a first step, a reversible immobilization strategy was tested in order to immobilize Hb as enzyme on the inner wall of a glass microchip reactor. To immobilize the enzyme on the reactor wall, a clean glass microchip reactor was covered with BSA via physisorption, after which the BSA-cysteines were activated by a rinsing step with DTT. The catalytically active enzyme was modified via an SPDP linker and directly coupled to the BSA attached to the reactor wall. This way, two different types of immobilized reactors were developed (HRP and Hb). The success of this immobilization step was confirmed by confocal fluorescence microscopy. Afterwards, the removal of the proteins has been investigated as well. By flushing dishwasher detergent through the reactor, all fluorescently-labeled proteins were removed. Hence, a reversible immobilization route of hemoglobin towards an enzyme-immobilized reactor was successfully developed.

In a second step, the homogeneous polymerization of AcMo was investigated in order to determine the required reaction conditions. At first, a glass microchip reactor was employed. However the employed enzyme, cys-b-Hb, tends to stick to the glass chip reactor leading to irreproducible and unstable conditions. An alternative microreactor set-up was made out of PEEK tubing to avoid the sticking of the enzyme. Yet, broad molecular weight distributions and low monomer conversions (~ 20%) were obtained. Degradation of the cys-b-Hb solution was

observed which might explain these results. To carry out the homogeneous polymerization in flow, a bigger reactor set-up (and thus shorter reaction run times) or cooling the syringe solution might be viable alternatives. More research is thus needed.

In addition, the immobilized reactor was employed to carry out the homopolymerization. At first, NaAsc was used as reducing agent, while employing the same reaction conditions from the batch procedure. However only low monomer conversions were obtained, probably due to the low amount of immobilized enzyme. Therefore, a stronger reducing agent, $Na_2S_2O_4$ was employed to carry out the polymerization. The use of this reducing agent led to higher monomer conversions, but also to a decreased control over the polymerization. Further investigations revealed the instability of the immobilized reactor during these polymerization conditions. Hence, different polymerization conditions, not affecting the immobilized reactor, are required to carry out the polymerization. Alternatively, a different immobilization strategy has to be followed to develop an immobilized reactor stable under these polymerization conditions.

5.6 References

(1) Wong, C.-H.; Whitesides, G. M. *Enzymes in synthetic organic chemistry*; Elsevier, 1994.

(2) Ritter, S. K. *C&EN Washington* **2017**, *95*, 26.

(3) Sheldon, R. A. *Green Chemistry* **2017**, *19*, 18.

(4) Whitesides, G. M.; Wong, C.-H. *Angewandte Chemie International Edition in English* **1985**, *24*, 617.

(5) Kobayashi, S.; Uyama, H.; Kimura, S. *Chemical Reviews* **2001**, *101*, 3793.

(6) Kobayashi, S.; Makino, A. *Chemical Reviews* **2009**, *109*, 5288.

(7) Kobayashi, S. In *Encyclopedia of Polymer Science and Technology*; John Wiley & Sons, Inc.: 2011.

(8) Sigg, S. J.; Seidi, F.; Renggli, K.; Silva, T. B.; Kali, G.; Bruns, N. *Macromolecular Rapid Communications* **2011**, *32*, 1710.

(9) Silva, T. B.; Spulber, M.; Kocik, M. K.; Seidi, F.; Charan, H.; Rother, M.; Sigg, S. J.; Renggli, K.; Kali, G.; Bruns, N. *Biomacromolecules* **2013**, *14*, 2703.

(10) Ng, Y.-H.; di Lena, F.; Chai, C. L. L. *Polymer Chemistry* **2011**, *2*, 589.

(11) Ng, Y.-H.; di Lena, F.; Chai, C. L. L. *Chemical Communications* **2011**, *47*, 6464.

(12) Fodor, C.; Gajewska, B.; Rifaie-Graham, O.; Apebende, E. A.; Pollard, J.; Bruns, N. *Polymer Chemistry* **2016**, *7*, 6617.

(13) Renggli, K.; Sauter, N.; Rother, M.; Nussbaumer, M. G.; Urbani, R.; Pfohl, T.; Bruns, N. *Polymer Chemistry* **2017**, *8*, 2133.

(14) Gross, R. A.; Kumar, A.; Kalra, B. *Chemical Reviews* **2001**, *101*, 2097.

(15) Kundu, S.; Bhangale, A. S.; Wallace, W. E.; Flynn, K. M.; Guttman, C. M.; Gross, R. A.; Beers, K. L. *Journal of the American Chemical Society* **2011**, *133*, 6006.

(16) Bhangale, A. S.; Beers, K. L.; Gross, R. A. *Macromolecules* **2012**, *45*, 7000.

(17) Miyazaki, M.; Maeda, H. *Trends in Biotechnology* **2006**, *24*, 463.

(18) Meller, K.; Szumski, M.; Buszewski, B. *Sensors and Actuators B: Chemical* **2017**, *244*, 84.

(19) Chaplin, M. *http://www1.lsbu.ac.uk/water/enztech/pbr.html, retrieved on 28-06-2017.* **2014**.

(20) Lloret, L.; Eibes, G.; Moreira, M. T.; Feijoo, G.; Lema, J. M.; Miyazaki, M. *Chemical Engineering Journal* **2013**, *223*, 497.

(21) Folch, A. *Introduction to BioMEMS*; CRC Press, 2013.

(22) ThermoScientific *Instructions - PG82087 and PG82088 - Pierce Premium Grade SPDP*.

(23) Cumber, A. J.; Forrester, J. A.; Foxwell, B. M. J.; Ross, W. C. J.; Thorpe, P. E. *Methods in Enzymology* **1985**, *112*, 207.

(24) Togashi, D. M.; Ryder, A. G.; Heiss, G. *Colloids and Surfaces B: Biointerfaces* **2009**, *72*, 219.

(25) Kalkhof, S.; Sinz, A. *Analytical and Bioanalytical Chemistry* **2008**, *392*, 305.

(26) *ATTO-Tec: General Coupling Procedures - Recommended Procedures for Labeling* **2016**.

(27) Kratz, F.; Grass, S.; Umanskaya, N.; Scheibe, C.; Müller-Renno, C.; Davoudi, N.; Hannig, M.; Ziegler, C. *Colloids and Surfaces B: Biointerfaces* **2015**, *128*, 28.

CHAPTER 6

Cyclic polymer preparation via a looped flow reactor

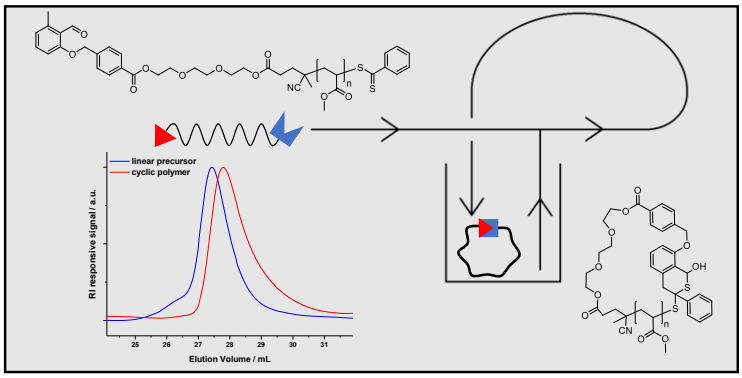

Cyclic polymers possess unique physical properties compared to linear analogues, though their preparation procedure is limited. To efficiently synthesize these cyclic polymers in high purity, the ring-closure has to be carried out in a highly diluted reaction solution (< 0.1 g L^{-1}). A first flow process towards cyclic polymer synthesis was already described, but required 17.3 L solvent per gram produced polymer product. Here, a looped-flow reactor has been designed in order to prepare cyclic polymers in a more efficient manner.

(collaboration with K. N. R. Wuest, E. Biasco, C. Barner-Kowollik, Macromolecular Architectures, Karlsruhe Institute of Technology, Germany and Queensland University of Technology, Australia)

6.1 Cyclic polymers

Cyclic polymers, also termed as polymer rings or macrocycles, possess unique physical properties compared to linear analogues.[1] Due to their endless molecular topology, and thus the absence of polymer end groups, cyclic polymers have a smaller hydrodynamic volume than their linear counterparts with the same molecular weight. Cyclic polymers also exhibit higher glass transition temperatures, lower intrinsic viscosities, higher critical solution temperatures, increased crystallization rates and so on. Thereby, cyclic polymers are also interesting for potential applications in the biomedical field due to their self-assembly behavior, reduced cell toxicity and enhanced thermostability.[1-7]

Various preparation methods toward cyclic polymers have been developed during the last decades.[1] Generally, two synthetic strategies can be distinguished: the ring-expansion and the ring-closure pathway.[1,4,6-8] The ring-expansion method involves the successive insertion of a monomer into a growing ring, via a labile bond (such as a metal-carbon, commonly Sn-O bond) (Figure 6.1).[1,3,4] This technique allows the production of cyclic polymers with high purity and large molecular weights at concentrated solutions.[9] Yet, most ring-expansion methods cannot be employed to control molecular weight and dispersity of the polymers.[9]

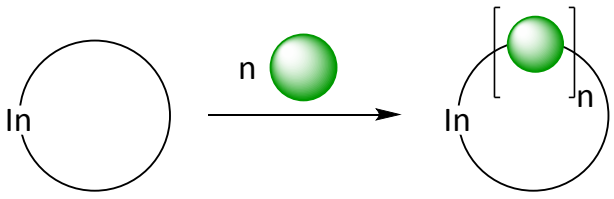

Figure 6.1. General ring-expansion route toward cyclic polymers.

The ring-closure pathway on the other hand requires an α,ω-functionalized linear precursor, whereby the α-end group can directly be linked to the ω-chain end (Figure 6.2). A two-step approach is thus followed here: first an α,ω-functionalized linear precursor has to be synthesized, after which the α,ω-coupling can take place. The α,ω-functionalized linear precursors are often synthesized via the use of reversible deactivation radical polymerizations (RDRP).[4,7,9,10] Hence, well-defined α,ω-functionalized linear precursors can be obtained and can later be employed to produce well-defined cyclic polymers (with good control over the molecular weight and polydispersity).[9] This approach thus also allows a large variety of molecular structures and functionalities.[2] The well-defined α,ω-functionalized linear precursor can undergo an intramolecular coupling reaction via coupling the α- and ω-chain ends.[4,10] This α,ω-coupling reaction must be very efficient to generate high purity cyclic polymers. Some well-known examples are copper-catalyzed azide-alkyne cycloadditions (CuAAC) and Diels-Alder cycloadditions.[4,11] Yet, highly diluted reaction solutions (< 0.1 g L^{-1}) are required to selectively achieve intramolecular cyclization and to avoid intermolecular oligomerization.[2,4] The use of these highly diluted conditions severely limits the preparation of well-defined cyclic polymers since a large volume has be handled (> 10 L to produce 1 g of cyclic polymer). Especially via classical batch synthesis, it is difficult to handle such huge volumes under oxygen free conditions and stimulate them via heat/light to carry out the coupling reaction. Hence, to date, the access to the upscaled synthesis of cyclic polymers is severely limited.[2]

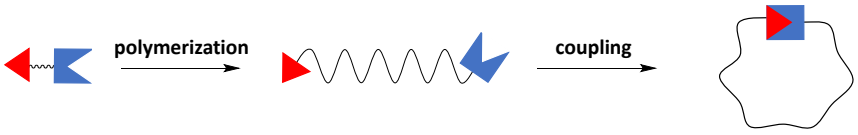

Figure 6.2. General ring-closure pathway toward cyclic polymers.

A first attempt to overcome this limitation – via the use of a continuous flow process – has been made by Zhang and coworkers.[2] They carried out a reversible addition-fragmentation chain transfer (RAFT) polymerization via the use of a functional RAFT agent, to later couple the polymeric chain ends via a light-induced Diels-Alder click reaction between an *o*-methyl-substituted aromatic aldehyde and a dithioester. The use of a flow reactor is beneficial for the light-induced coupling reaction due to the enhanced irradiation, related to the shorter optical path length in a flow reactor. In addition, the continuous nature of the process simplified the handling of a huge volume of reaction solution: 17.3 L reaction volume was flushed through the flow reactor during 3 h, at a flow rate of 100 mL min^{-1}, in order to prepare 1 g of cyclic polystyrene. Zhang and coworkers propose this technique as a universal solution to overcome the low production efficiency and to prepare cyclic polymers on large scale. Yet, their procedure still makes use of the same volume of solvent – only the handling is improved. Cumbersome evaporation work-up is thus also still required. Practically, handling 17.3 L reaction solution in order to obtain 1 g of cyclic polymer is still not very efficient.

Hence, our aim is to develop a looped flow procedure, whereby the polymer precursor is gradually added, in order to overcome the limitations of ring-closure coupling reactions. First, the looped flow reactor was designed by taking several reactor requirements into account. Next, an α,ω-functionalized linear precursor was prepared via the use of a functional RAFT agent, after which the intramolecular coupling of the linear precursor was investigated under continuous conditions in order to synthesize cyclic polymers. In a later stage, the cyclic polymers were prepared via the use of the looped flow reactor.

6.2 Reactor requirements and design

In order to develop a recycle flow procedure, a looped flow reactor is designed. So far, looped processes have only rarely been employed for the production of polymers. In 1990, liquid phase (free radical) polymerizations of olefins were carried out in a 'loop reactor' on industrial scale.[12-14] Later, also emulsion polymerizations were carried out in a continuous 'loop reactor'.[15,16] Only recently, the first 'looped flow process' for controlled radical polymerizations has been reported.[17]

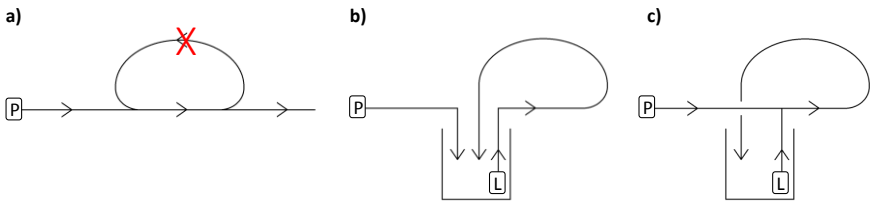

Figure 6.3. Reactor design of a looped flow reactor for cyclic polymer synthesis. a) one pump system, b) use of a loop pump, c) direct injection into the loop.

Hence, the looped flow reactor is based on the use of a recycle loop, whereby the solution keeps running in a closed reactor loop and whereby the polymer precursor is gradually added. Such system can be considered as equivalent to the batch-wise 'slow-addition' method via the use of a drop funnel (or via the use of a syringe pump). The injection pump ('P') takes care of injecting the α,ω-functionalized linear precursor gradually into the reactor system, where it will immediately be diluted in the reaction mixture. Yet, the main feature of the system is the loop pump ('L'), which provides the flow of the recycle stream. Without this pump, no recycling flow can be observed (Figure 6.3a). In addition, also the point of

injection, and thus the position of the injection pump ('P') is important. The injected α,ω-functionalized linear precursor should be diluted and undergo the ring-closure reaction immediately. If not, the amount of α,ω-functionalized linear precursor piles up leading to a concentration increase (Figure 6.3b). Hence, the α,ω-functionalized linear precursor should be directly added in the reactor, where it is diluted with the solvent/cyclic polymer mixture. The formed product (the cyclic polymer) is collected and recirculated into the reactor loop, as depicted in Figure 6.3c.

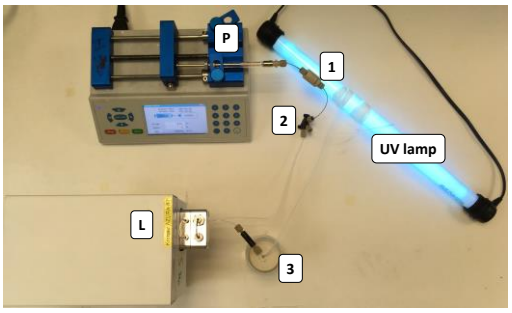

Figure 6.4. Home-made looped reactor, normally protected from daylight.

A home-made looped reactor system, based on Figure 6.3c, was created (Figure 6.4). Here, a syringe pump was employed as injection pump ('P'). A check valve ('1') has been placed after the injection pump in order to prevent backflow. An HPLC pump was employed as loop pump ('L') to recirculate the solvent/cyclic polymer mixture. This mixture and the injected precursor are mixed via the use of U-466 static mixing tee ('2') and flushed through a 1 mL reactor, wrapped around a UV lamp of 312 nm. The volume contained in the reactor coil is kept rather low compared to the total reaction mixture (≥ 50 mL). Additionally, the solvent/cyclic polymer mixture ('3') as well as the precursor solution are kept in the dark, so no reaction can occur outside the reactor coil.

6.3 Synthesis of an α,ω-functionalized linear precursor

In order to synthesize a cyclic polymer via the ring-closure strategy, an α,ω-functionalized linear precursor is synthesized. A dithioester functionality and an *o*-methyl-substituted aromatic aldehyde were chosen as functional end groups, so they could later undergo a Diels-Alder click reaction via the light-induced formation of *o*-quinomethane (see further). These type of reactions are highly efficient and occur within seconds.[18] Hence, an α,ω-functionalized linear precursor was prepared via a controlled radical polymerization employing a functional RAFT agent, carrying a dithioester functionality and an *o*-methyl-substituted aromatic aldehyde as R-group (Figure 6.5). In order to obtain the highest end group fidelity possible, a temperature of 70°C and a low AIBN equivalence (0.05 eq compared to the RAFT agent) were employed. For the same reason, conversions less than 100% were targeted. Therefore, a RAFT polymerization of methyl acrylate (MA) was carried out, with a 100/1/0.05 monomer/RAFT agent/AIBN ratio. After 19 h reaction time, 68% monomer conversion was observed, and an α,ω-functionalized MA polymer was collected with a molecular weight of 6890 g mol^{-1} and a dispersity of 1.27 (Figure 6.6). The slight broadening can be explained by the not ideal match between the acrylate monomer and the dithio-RAFT agent. Yet, also the presence of light cannot completely be avoided, leading to the presence of high molecular weights related to the intermolecular coupling of several polymer chains.

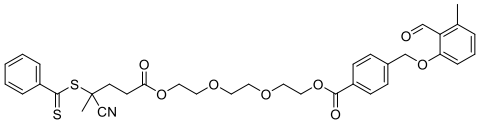

Figure 6.5. Structure of the employed RAFT agent.

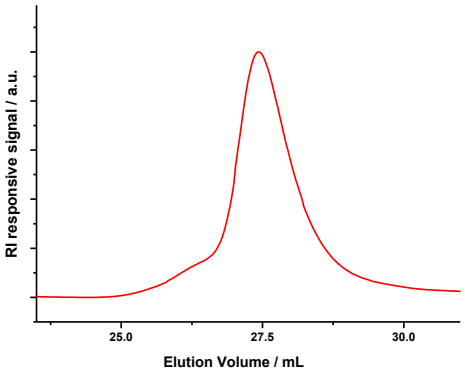

Figure 6.6. SEC result of the α,ω-functionalized linear polymer precursor.

6.4 Intramolecular coupling toward cyclic polymers

A light-induced Diels-Alder reaction was employed for the intramolecular coupling of the chain ends of the α,ω-functionalized linear precursor. Such Diels-Alder reactions exhibit a rapid reactivity and lead to high yields, even when the precursor compounds are present in equimolar amounts. The reaction is rather robust and tolerates a large variety of chemical solvents. In addition, no byproducts are formed during the reaction, simplifying the work-up of these reactions. The light-induced Diels-Alder click reactions are thus an efficient conjugation tool for polymer reactions.[10,18-20]

Here, the light-induced Diels-Alder reaction between a dithioester (as dienophile) and an *o*-methyl-substituted aromatic aldehyde was investigated. The *o*-methyl-substituted aromatic aldehyde is excited by absorption of a photon when

illuminated with a wavelength around the absorption maximum (λ_{max} = 306 nm, a UV lamp of 312 nm will be employed here). The excitation of the *o*-methyl-substituted aromatic aldehyde leads to the formation of an highly reactive diene (triplet state), called *o*-quinomethane (sometimes referred to as 'photoenol'), as represented in Figure 6.7.[18,19] The light-induced formation of this *o*-quinomethane is thus the trigger for the Diels-Alder reaction between the *o*-quinomethane and the dithioester (Figure 6.8). A similar Diels-Alder reaction has already been studied in a continuous flow set-up before[21] to overcome the upscaling limitations of the batch procedure. Based on these experimental details (2 min reaction time, acetonitrile (ACN) as solvent system), the same starting conditions were chosen for the intramolecular coupling.

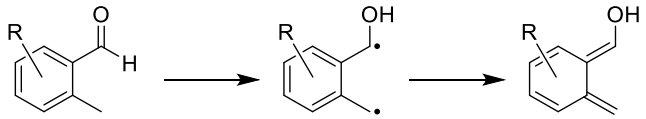

Figure 6.7. Light-induced equilibrium between an *o*-methyl-substituted aromatic aldehyde and its photo-enol product: an *o*-quinomethane.[19]

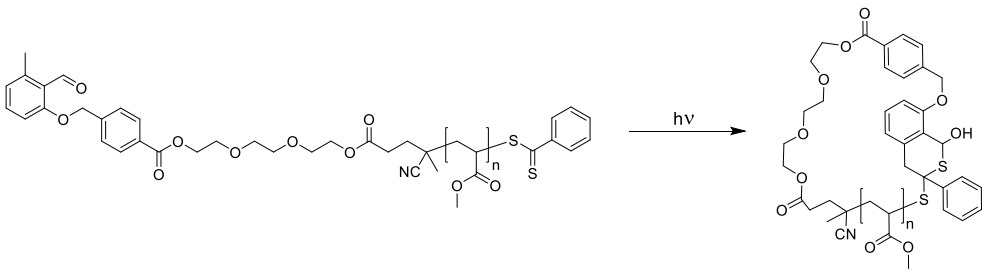

Figure 6.8. Intramolecular coupling reaction of the dithioester and the *o*-methyl-substituted aromatic aldehyde end groups of the linear polymer precursor.

The light-induced Diels-Alder reaction between a dithioester (as dienophile) and an *o*-methyl-substituted aromatic aldehyde was investigated via the use of the synthesized precursor polymer (Figure 6.8). As reactor set-up, the looped flow reactor was employed, yet the reaction mixture was not recirculated back into the system but it was collected instead. Hereby, a solution of 5 g L^{-1} precursor in ACN was injected via the syringe pump and diluted with pure ACN by a factor 50 via the HPLC pump (the 'loop' pump). Two different residence times were tested: 30 s and 15 s. Due to the limited amount of obtained product, ^{1}H NMR results were inconclusive to determine exact conversion. Still, from the SEC results (Figure 6.9), a shift of the main distribution to lower apparent molecular weights is observed, due to the small hydrodynamic volume of the cyclic polymer, indicating quantitative conversion even for 15 s reaction time.

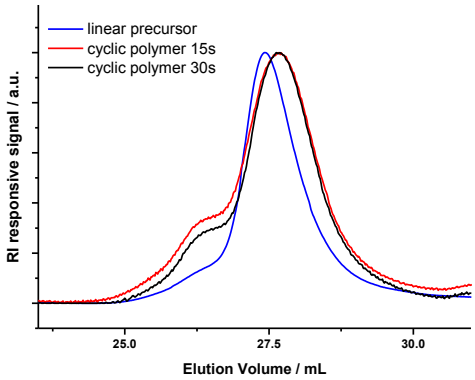

Figure 6.9. SEC results of the intramolecular coupling after 30 s and 15 s versus the linear precursor polymer.

A shoulder in the SEC results indicates the presence of the by-product due to intermolecular coupling (higher molecular weight), which was also present during the synthesis of the precursor polymer but increased here during the preparation of the cyclic polymer. Such formation of by-product is also reported for the continuous flow procedure reported by Zhang and coworkers.[2] To stay on the side of caution, 30 s was employed as residence time for further testing. To reduce this intermolecular coupling, different concentrations of linear precursor polymer were tested by varying the flowrate of the injection pump. Three different concentrations were employed: 0.1 g L^{-1}, 0.05 g L^{-1} and 0.025 g L^{-1}, of which the results are shown in Table 6.1.

Table 6.1. Results of the intramolecular coupling with different concentrations.

Type of polymer	***Concentration* / g · L^{-1}**	M_n^{app} **/ g · mol^{-1}**	**Đ**	M_p^{app} **/ g · mol^{-1}**
Linear polymer	/	7070	1.25	8840
Cyclic polymer	0.1	7200	1.26	7890
Cyclic polymer	0.05	6500	1.29	8040
Cyclic polymer	0.025	6380	1.26	8170

Yet, the success of the intramolecular coupling is clearly indicated by the shift to lower apparent molecular weights (Figure 6.10). Moreover, a clear decrease of intermolecular coupling is observed when decreasing the concentration of the linear precursor from 0.1 g L^{-1} to 0.05 g L^{-1}. Less effect can be seen between the experiments with a concentration of 0.05 g L^{-1} and 0.025 g L^{-1}. Though the differences between those concentrations are low, 0.025 g L^{-1} was employed for further experiments to assure minimal formation of intermolecular coupling products and to assure maximum purity of the produced cyclic polymer.

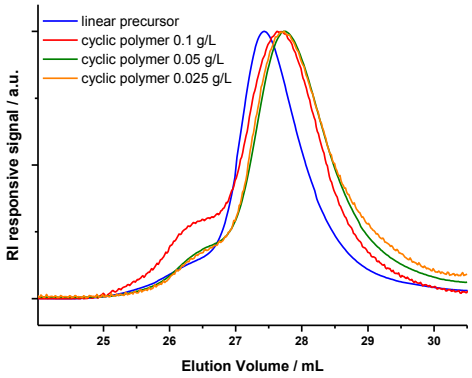

Figure 6.10. SEC results of the intramolecular coupling with a concentration of 0.01 g L^{-1}, 0.05 g L^{-1} and 0.025 g L^{-1} versus the linear precursor polymer.

6.5 Cyclic polymer preparation via a looped flow reactor

Next, the cyclic polymers were prepared via the use of the looped flow reactor by employing the conditions derived above. Hence, a concentration of 0.025 g L^{-1} α,ω-functionalized linear precursor polymer was provided by injecting the precursor polymer directly into the loop reactor. Therefore, a 5 mg mL^{-1} precursor polymer solution was injected into the loop reactor, where it is directly diluted to 0.025 g L^{-1}. The light-induced Diels-Alder reaction takes place in the reactor loop with residence time of 30 s by injecting the precursor polymer with a flow rate of 10 μL min^{-1}. Simultaneously, the looped pump was used to dilute the precursor polymer with the solvent/product mixture (initial solvent volume 10 mL) at a flow rate of 2 mL min^{-1}. The reaction was allowed to run for 16 h 40 min, till 50 mg

precursor polymer was injected into the reactor loop – to produce 50 mg of cyclic polymer in a total volume of 20 mL. The cyclic polymer could be collected in a quantitative manner, by evaporating the solvent/polymer mixture. Compared to the previously reported required volumes (Zhang and coworkers produced 1 g cyclic PS in 17.3 L),[2] we were thus able to diminish the required solution volumes with a factor 43 (50 mg in 20 mL ~ 1 g in 400 mL). It should be noted that our production rate seems rather low: a minimal amount of product has been obtained during an extended reaction time (50 mg in 16 h 40), especially when compared to previously reported production rates (Zhang and coworkers produced 1 g cyclic PS in 3 h).[2] Yet, this is rather related to the employed reactor with a loop volume of 1 mL, schematically represented in Figure 2.11, than to the technology. Employing the same principle, a reactor with a bigger loop volume (Zhang and coworkers used a reactor volume of 200 mL)[2] would thus lead to the upscaled synthesis of the cyclic polymer. Most likely, the amount of required solution volume could be decreased even more when employing a bigger loop volume, though this was not further tested due to a limited amount of RAFT agent and thus a limited amount of α,ω-functionalized linear precursor.

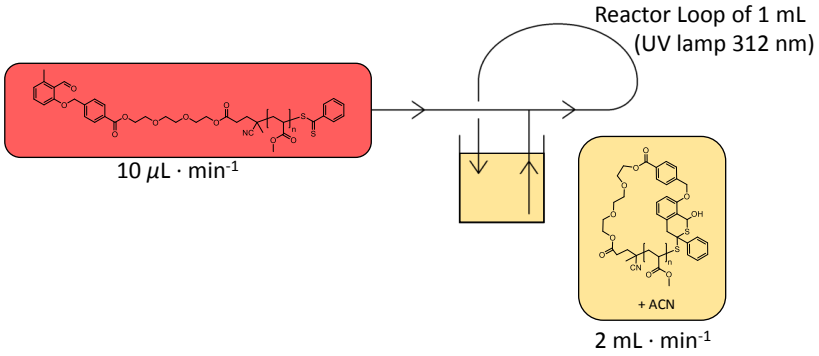

Figure 6.11. Schematic representation of the looped flow reactor set-up.

The success of the intramolecular coupling via the looped flow reactor is clearly indicated by the shift to lower apparent molecular weights in the SEC results (Figure 6.12 and Table 6.2). The intermolecular coupling product seems less present in the cyclic polymer than in the original precursor polymer, for which no plausible explanation can be given so far. Also a larger amount of small molecular weight products seems to be present in the cyclic polymer product, which relates to the drastic decrease of the number average molecular weight value. A possible explanation would be the degradation of the cyclic polymer under the influence of light or heat (the UV-lamp heats up to ± 60°C), yet such degradation is rather unlikely for cyclic polymers. In addition to the SEC results, the disappearance of the UV-VIS absorption peak (306 nm) of the dithioester also indicates the success of the cyclic polymer preparation (Figure 6.13).

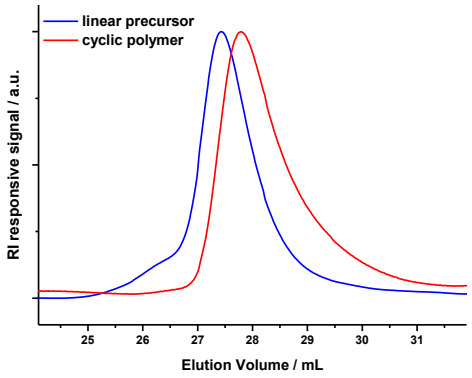

Figure 6.12. SEC results of the intramolecular coupling in a looped flow reactor.

Table 6.2. Results of the intramolecular coupling in a looped flow reactor

Type of polymer	M_n^{app} / g · mol^{-1}	*Đ*	M_p^{app} / g · mol^{-1}
Linear polymer	7070	1.25	8840
Cyclic polymer	5170	1.27	7850

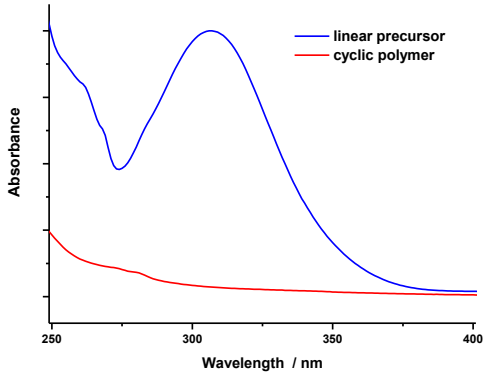

Figure 6.13. UV-Vis spectra of the linear vs the cyclic polymer.

6.6 Conclusions and outlook

Cyclic polymers possess unique physical properties compared to their linear analogues and have a great potential for future applications. They can be prepared via a ring-closure strategy, whereby the end groups of an α,ω-functionalized linear precursor are intramolecularly coupled to each other. Yet, highly diluted reaction solutions (< 0.1 g L^{-1}) are required to avoid intermolecular side reactions. To overcome this limitation, a continuous flow procedure has been proposed by Zhang and coworkers whereby 17.3 L reaction solution had to be processed in order to produce 1 g of cyclic polymer.[2] Here, a looped flow procedure is developed in order to increase the reaction efficiency and reduce the amount of solvent. First, a looped flow reactor was designed, whereby the polymer precursor is gradually added via an injection pump. The polymer precursor is directly diluted by the solvent/cyclic polymer mixture, which recirculates through the recycle loop

via the use of a loop pump. Next to the reactor design, an α,ω-functionalized linear precursor was successfully prepared via RAFT polymerization, employing a functional RAFT agent carrying a dithioester functionality and an *o*-methyl-substituted aromatic aldehyde. Afterwards, the intramolecular coupling of the chain ends of the linear precursor was investigated under continuous flow conditions. The reaction turned out to be working efficiently within 30 s and low precursor concentrations (0.025 g L^{-1}) are needed to avoid intermolecular coupling. In a later stage, the cyclic polymers were successfully prepared via the use of the looped flow reactor, whereby 50 mg cyclic polymer was prepared in a total volume of 20 mL reaction solution. Compared to the previously required volumes (Zhang and coworkers produced 1 g cyclic PS in 17.3 L),[2] we were thus able to diminish the required solution volumes with a factor 43 (50 mg in 20 mL ~ 1 g in 400 mL).

Further research is however required to show the real potential of this technique. The concentration limit should be tested in order to establish the technique and to prove its reproducibility. In addition, the stability of the cyclic polymer has to be tested as well – no degradation may occur during the recirculation. Yet, the true potential of this technique lies in the production of cyclic polymers, even though a looped flow reactor is generally not considered as a continuous production process ('semi-batch'). At this point, only a low production rate could be reported due to the limited volume of the reactor and the limited amount of available RAFT agent. Yet, a looped flow reactor with a larger loop volume could be designed to boost the production of cyclic polymers enhancing the research on possible applications of the cyclic polymers and thus their industrial applicability.

6.7 References

(1) Tu, X.-Y.; Liu, M.-Z.; Wei, H. *Journal of Polymer Science Part A: Polymer Chemistry* **2016**, *54*, 1447.

(2) Sun, P.; Liu, J.; Zhang, Z.; Zhang, K. *Polymer Chemistry* **2016**, *7*, 2239.

(3) Roland, C. D.; Li, H.; Abboud, K. A.; Wagener, K. B.; Veige, A. S. *Nature Chemistry* **2016**, *8*, 791.

(4) Hoskins, J. N.; Grayson, S. M. *Polymer Chemistry* **2011**, *2*, 289.

(5) Tezuka, Y.; Oike, H. *Progress in Polymer Science* **2002**, *27*, 1069.

(6) Zhu, Y.; Hosmane, N. S. *Chemistry Open* **2015**, *4*, 408.

(7) Josse, T.; De Winter, J.; Gerbaux, P.; Coulembier, O. *Angewandte Chemie International Edition* **2016**, *55*, 13944.

(8) Laurent, B. A.; Grayson, S. M. *Chemical Society Reviews* **2009**, *38*, 2202.

(9) Tang, Q.; Wu, Y.; Sun, P.; Chen, Y.; Zhang, K. *Macromolecules* **2014**, *47*, 3775.

(10) Glassner, M.; Blinco, J. P.; Barner-Kowollik, C. *Macromolecular Rapid Communications* **2011**, *32*, 724.

(11) Oehlenschlaeger, K. K.; Mueller, J. O.; Heine, N. B.; Glassner, M.; Guimard, N. K.; Delaittre, G.; Schmidt, F. G.; Barner-Kowollik, C. *Angewandte Chemie International Edition* **2013**, *52*, 762.

(12) Ferrero, M. A.; Chiovetta, M. G. *Polymer-Plastics Technology and Engineering* **1990**, *29*, 263.

(13) Hottovy, J. D.; Lawrence, F. C.; Lowe, B. W.; Fangmeier, J. S. *Phillips Petroleum Company, Patent CA 2044782 A1* **1990**.

(14) Zacca, J. J.; Ray, W. H. *Chemical Engineering Science* **1993**, *48*, 3743.

(15) Abad, C.; De La Cal, J. C.; Asua, J. M. *Chemical Engineering Science* **1994**, *49*, 5025.

(16) Lee, D.-Y.; Wang, J.-H.; Kuo, J.-F. *Polymer Engineering & Science* **1992**, *32*, 198.

(17) Kuroki, A.; Martinez-Botella, I.; Hornung, C. H.; Martin, L.; Williams, E. G. L.; Locock, K. E. S.; Hartlieb, M.; Perrier, S. *Polymer Chemistry* **2017**, *8*, 3249.

(18) Gruendling, T.; Oehlenschlaeger, K. K.; Frick, E.; Glassner, M.; Schmid, C.; Barner-Kowollik, C. *Macromolecular Rapid Communications* **2011**, *32*, 807.

(19) Hiltebrandt, K.; Elies, K.; D'hooge, D. R.; Blinco, J. P.; Barner-Kowollik, C. *Journal of the American Chemical Society* **2016**, *138*, 7048.

(20) Barner-Kowollik, C.; Du Prez, F. E.; Espeel, P.; Hawker, C. J.; Junkers, T.; Schlaad, H.; Van Camp, W. *Angewandte Chemie International Edition* **2011**, *50*, 60.

(21) Zaquen, N.; Haven, J. J. ; Rubens, M.; Altinas, O.; Bohländer, P.; Offenloch, J. T.; Barner-Kowollik, C.; Junkers, T. *in preparation*.

CHAPTER 7

Experimental details

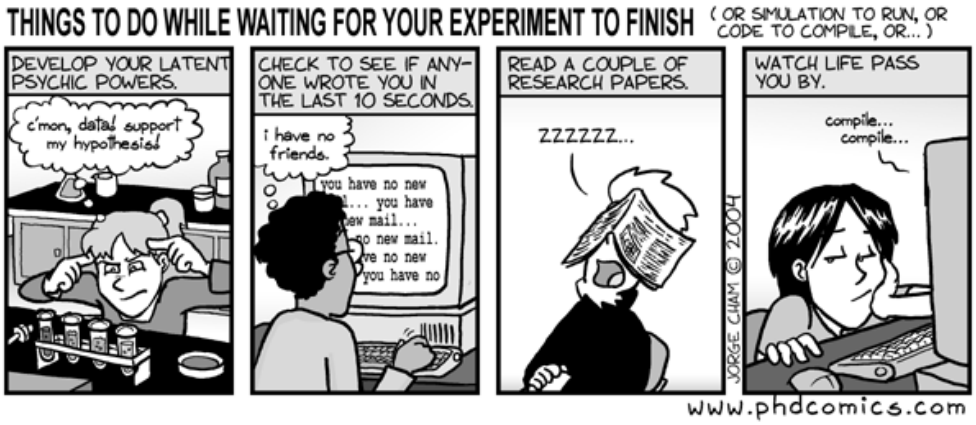

7.1 Characterization

Generally, characterizations were carried out in-house, by employing equipment of Hasselt University (or one of its research groups). This equipment, employed in most research projects, is listed here below. Some research parts were carried out as collaboration projects, whereby equipment of those collaboration partners was employed. Characteristics on this equipment can additionally be found in the related project section in this chapter.

7.1.1 Nuclear Magnetic Resonance (NMR)

Monomer conversions and monomer to monomer ratios were determined by Nuclear Magnetic Resonance (NMR) spectra, which were generally recorded in $CDCl_3$ at room temperature on a 400 Megahertz (MHz; 9.4 Tesla) Varian Inova spectrometer at 400 MHz for ^1H NMR using a 5 mm OneNMR PFG probe (Agilent Technologies Inc, Santa Clara, CA, USA). The chemical shift scale (δ) in ppm was calibrated relative to TMS (0 ppm). Free induction decays were collected with a 90° pulse of 6.9 μs, a spectral width of 6400 Hz, an acquisition time of 3 s, a preparation delay of 12 s and 64 accumulations. A line-broadening factor of 0.2 Hz was applied before Fourier transformation to the frequency domain.

7.1.2 Size-exclusion chromatography (SEC)

Size-exclusion chromatography (SEC) was generally performed on a Tosoh EcoSEC operated by PSS WinGPC software, equipped with a PLgel 5.0 μm guard column (50 x 8 mm), followed by three PLgel 5 μm mixed-C columns (300 x 8 mm) and a differential refractive index detector using THF as eluent at 40°C with a flow rate of 1 mL min^{-1}. The SEC system was calibrated using linear narrow PS standards ranging from 474 to 7.5 x 10^6 g mol^{-1} (K = 14.1 x 10^{-5} dLg^{-1} and α = 0.70), and toluene as a flow marker.

7.1.3 Electrospray Ionisation Mass Spectrometry (ESI-MS)

Electrospray Ionisation Mass Spectrometry (ESI-MS) was performed using an LTQ Orbitrap Velos Pro mass spectrometer (ThermoFisher Scientific) equipped with an atmospheric pressure ionization source operating in the nebulizer assisted electro spray mode. The instrument was calibrated in the m/z range 220-2000 using a standard solution containing caffeine, MRFA and Ultramark 1621. A constant spray voltage of 5 kV was used and nitrogen at a dimensionless sheath gas flow-rate of 7 was applied. Capillary temperature was set to 275°C. A mixture of THF and methanol (THF:MeOH = 3:2), all HPLC grade, was used as solvent. Spectra were analyzed via Thermo Xcalibur Qual Browser software.

7.2 Flow Equipment

7.2.1 Microfluidic reactor set-up

The microfluidic reactor set-up – employed in Chapter 2, 3 and 5 – is a Labtrix® Start R2.2 system (Chemtrix BV, NL) (Figure 1.4 and 7.1). This commercially available microreactor system can be fitted with different glass chip reactors. The most frequently used microchip reactor has a reactor volume of 19.5 μL (Chemtrix 3227 reactor, 3 inlets). Yet, microchip reactors with smaller reactor volumes were employed as well, such as a 10 μL microreactor (Chemtrix 3223 reactor, 3 inlets), a 5 μL microreactor (Chemtrix 3222 reactor, 3 inlets) and a 1 μL microreactor (Chemtrix 3221, 3 inlets). In addition, a microreactor with an additional inlet in the reactor was employed: a 15 μL microreactor (Chemtrix 3224 reactor, 4 inlets, 5 + 10 μL). All employed reactor chips employ staggered oriented ridge (SOR-2) static micromixers to assure fast mixing. Reaction temperatures are controlled via a MTTC1410 temperature controller (Melcor Thermal Solutions, temperature range –20 to 195°C), while the reactor pressure could be maintained at 20 bar back pressure via a preset back pressure regulator (Upchurch Scientific). Reactant solutions are injected into the reactor via 1 mL gastight syringes (SGE or ILS). Flow rates vary between 0.1 and 40 μL min^{-1}, and are controlled via syringe pumps (Chemyx).

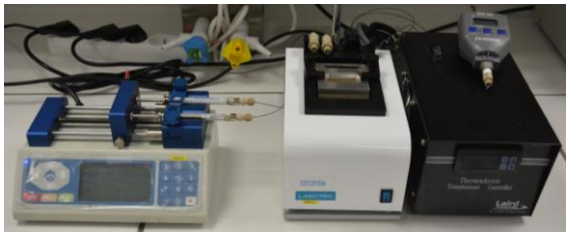

Figure 7.1. The employed microfluidic reactor set-up.

7.2.2 Mesofluidic reactor set-up

The reactor system employed in Chapter 4 and 6, was a home-made tubular reactor, made of gastight perfluoroalkoxy polymer (PFA) tubing (Advanced Polymer Tubing GmbH, 1/16" OD) with an internal diameter of 0.75 mm. Hence, this reactor system is considered as mesofluidic. The use of tubular reactors allows for a very simple building-block or modular approach, whereby every part of the set-up (micromixers, fittings, back pressure regulators, etc.) can be exchanged or modified. Most of these parts were designed by Upchurch Scientific (Idex Health and Science) and are distributed by Achrom, VWR and Inacom. Generally, 10-32 coned fingertight fittings (F-120) and 1/4-28 flat-bottom flangeless fittings (XP-230) with a flangeless ferrule (P-200) were employed to connect two or more tubings. As connector pieces, a 10-32 coned polyether ether ketone (PEEK) union (P-704), a 1/4-28 flat-bottom PEEK union (P-702) and a 10-32 coned to 1/4-28 flat-bottom PEEK adapter (P-627) were used with 0.020" thru-holes. The employed micromixer was a PEEK static mixing tee, fitted with a 10 μm ultrahigh molecular weight polyethylene (UHMWPE) frit and with 0.020" thru-hole (U-466). A biocompatible back pressure regulator made of PEEK with a 100 psi/7 bar cartridge (P-787) was employed to retain the pressure and to ensure stable flow conditions. Reaction solutions were pumped into the reactor via Knauer Azura P 2.1S HPLC Pumps. For thermal reactions (Chapter 4), the tubular reactor was placed in a silicon oil bath on an IKA RCT basic hot plate (Figure 1.6, 1.7, 4.3 and 7.4). On the other hand, the tubing could also be wrapped around a UV lamp when targeting light-induced reactions (Chapter 6) (Figure 6.4).

7.3 Experimental Chapter 2 – Poly(2-oxazoline)s

7.3.1 Materials

Methyl tosylate (MeOTs) was purchased from Sigma-Aldrich and was distilled over barium oxide under reduced pressure. Acetonitrile (ACN) was purchased from VWR and was distilled over barium oxide under inert atmosphere. 2-Ethyl-2-oxazoline (EtOx) was kindly provided by Polymer Chemistry Innovations Inc, and has been distilled over barium oxide under inert atmosphere. The synthesis of 2-*n*-propyl-2-oxazoline (*n*PropOx) was described previously.[2,3] Prior to use, *n*PropOx was distilled over barium oxide under reduced pressure. Potassium hydroxide (KOH) and methanol (MeOH) for the quench solution were purchased from VWR and Acros, respectively.

7.3.2 Characterization

Monomer conversions and monomer to monomer ratios were determined via the use of ^{1}H NMR, described in 7.1.1.

Molecular weight distributions were determined by employing the equipment of our collaboration partner: the Supramolecular Chemistry Group, Department of Organic and Macromolecular Chemistry, Ghent University. There, analytical SEC was performed on an Agilent 1260-series HPLC system equipped with a 1260 online degasser, a 1260 ISO-pump, a 1260 automatic liquid sampler (ALS), a thermostated column compartment (TCC) at 50°C equipped with a PLgel 5 μm mixed-D guard column and two PLgel 5 μm mixed-D columns in series, a 1260 diode array detector (DAD) and a 1260 refractive index detector (RID). The used eluent was dimethylacetamide (DMA), containing 50 mM of lithium chloride, at an optimized flow rate of 0.593 mL min^{-1}. The spectra were analyzed using the Agilent Chemstation software with the GPC add on. Molar mass and dispersity values were calculated against polymethylmethacrylate (PMMA) standards from PSS.

7.3.3 Microreactor set-up

Poly(2-oxazoline)s were synthesized by employing a Labtrix® Start R2.2 system (7.2.1), equipped with a 19.5 μL microchip reactor for homopolymerizations and a 15 μL (5 + 10 μL) microchip reactor for diblock (co)polymerizations. Reactor pressure was maintained at 20 bar back pressure.

Triblock copolymerizations were carried out in a microreactor cascade, consisting of two coupled Labtrix® Start R2.2 systems (Figure 7.2). The first system was fitted with a 15 μL microreactor (Chemtrix 3224 reactor, 5 + 10 μL). The outlet of the first reactor chip was connected directly to the inlet of a second microreactor system, via a short piece of unheated PEEK 1/32" tubing and an in-line manometer to monitor and detect possible blockages at a premature stage. No additional check valves were placed in order to avoid temperature decreases between both reactors. The second microreactor system was fitted with a 19.5 μL microreactor (Chemtrix 3227 reactor). At the end of the reactor cascade, a pre-set back pressure regulator (Upchurch Scientific) was placed to maintain the system at 20 bar of back pressure.

Figure 7.2. Microreactor cascade as used for the triblock copolymerizations.

7.3.4 Homopolymerization of 2-ethyl-2-oxazoline (EtOx)

Stock solutions composed of 4M EtOx in acetonitrile, with a [EtOx]/[MeOTs] ratio of 60 were used in the homopolymerization reactions. Accordingly, typical stock solutions were prepared of 2 mL EtOx, 0.05 mL MeOTs and 3 mL acetonitrile and were injected into a 19.5 μL microreactor by employing two syringes filled under nitrogen atmosphere. A third injecting syringe was used for acetonitrile at the last inlet of the reactor, to avoid blockages at the outlet. In addition, salt precipitation was avoided in the reactor by quenching the reaction mixture with KOH/MeOH (1 M) in the collection vial. Reaction temperatures were screened between 120°C and 180°C, while the pressure was kept constant at 20 bar.

To assure full conversions for EtOx as first block, the same conditions were also tested in the first reactor part (5 μL) of a 15 μL microreactor by employing the third inlet as an outlet. Same conversions were observed for all chosen residence times at 140°C, 160°C and 180°C.

Molecular weights of the poly(2-ethyl-2-oxazoline) homopolymers were varied by changing the monomer/initiator ratio. Hereby, the monomer concentration was kept constant while initiator concentrations were varied.

7.3.5 Homopolymerization of *n*-propyl-2-oxazoline (*n*PropOx)

A similar straightforward optimization strategy was carried out for *n*PropOx, where stock solutions of 2.35 mL *n*PropOx (4M), 0.05 mL MeOTs and 3 mL acetonitrile were employed.

7.3.6 Diblock Copolymerizations of EtOx and *n*PropOx

The synthesis of diblock copolymers was carried out in a 15 μL reactor (5 + 10 μL) (Figure 2.7) at 160°C. To assure full monomer conversions for the first block, optimized conditions of the homopolymerization were applied for the first reactor part (5 μL). Employed stock solutions were thus identical to the ones of the homopolymerization (2 mL EtOx or 2.35 mL *n*PropOx (4M), 0.05 mL MeOTs in 3 mL acetonitrile). Due to the intrinsic volume of the first reactor part, the stock solution was injected via two inlets at a total flow rate of 1 μL min^{-1} leading to 5 min residence time. The second monomer was injected via the third inlet in bulk into the second reactor part (10 μL) – no additional dilution was required since the polymer solution does not cause viscosity problems at high temperatures. Hence, the injection rate of the 'pure' monomer directly correlates to the density and thus to the amount of injected monomer. This way, a flexible set-up is obtained where changing the flow rate leads to a change in monomer 1/monomer 2 ratios. For EtOx-*b*-*n*PropOx diblock copolymers, a 0.47 μL min^{-1} *n*PropOx injection leads to a 1/1 EtOx/*n*PropOx ratio. On the other hand, *n*PropOx-*b*-EtOx diblock copolymers in a 1/1 ratio require an EtOx injection at a 0.4 μL min^{-1} flow rate. Doubling the injection rate of the second monomer leads to a 1/2 ratio, etc. Again acetonitrile was injected at the last inlet of the reactor to avoid blockages at the outlet. Salt precipitation was avoided in the reactor by quenching with KOH/MeOH (1 M) in the collection vial.

7.3.7 Triblock Copolymerizations of EtOx and nPropOx

The synthesis of triblock copolymers was carried out in a microreactor cascade of two coupled microreactors. A 15 μL reactor (5 + 10 μL), was used to make the first two blocks in a similar way as for the diblock copolymers. The first reactor part with an intrinsic volume of 5 μL was used to make the first block. Therefore, the stock solution (identical to the homopolymerization: 2 mL EtOx or 2.35 mL *n*PropOx (4M), 0.05 mL MeOTs in 3 mL acetonitrile) was injected via two inlets at a total flow rate of 1 μL min^{-1} leading to 5 min residence time. The second block was polymerized in the second reactor part (10 μL) by injecting the second monomer via the third inlet in bulk. Employed flow rates directly correlate to the monomer density, and were calculated to give a 1/1 ratio with the first block to assure full monomer conversions for the second block as well. As second reactor, a 19.5 μL reactor was coupled directly to the outlet of the first reactor to assure fully inert conditions. By injecting the third monomer in bulk, its injecting rate correlates to its density and determines the residence time of the last block. Since the targeted triblock copolymers are mirror images, the residence time of the last block is identical.

The temperature of the whole microreactor cascade was kept constant at 160°C, while the back pressure was maintained at 20 bar. Acetonitrile was injected at the last inlet of each reactor, to avoid blockages between both reactors or after the outlet of the second reactor. In this case, acetonitrile was thus also injected at the last inlet of the first reactor, leading to an additional dilution factor for the third block. To avoid salt precipitation in the reactor, quenching of the reaction mixture with KOH/MeOH (1 M) occurred in the collection vial.

7.4 Experimental Chapter 3 – Poly(phosphoester)s

7.4.1 Materials

1,8-Diazobicyclo[5.4.0]undec-7-ene (DBU) (TCI Europe) was dried over CaH_2 at room temperature. 1,5,7-Triazobicyclo[4.4.0]dec-5-ene (TBD) (Aldrich) was dried overnight under vacuum at room temperature. The functionalized thiourea (TU) was synthesized according to the method described previously.[4] The monomers 2-isobutoxy-2-oxo-1,3,2-dioxaphospholane (iBP) and 2-butenoxy-1,3,2-dioxaphospholane (BP) were synthesized according to the method described previously. 2-Mercaptoethanol (Acros), 1-dodecanethiol (Acros), benzyl alcohol (BzOH) (Aldrich), 2,2-dimethoxy-2-phenylacetophenone (DMPA) and acetic acid (VWR) were used as received. Toluene and dichloromethane (Aldrich) were dried via the use of a MB-SPS 800 system.

7.4.2 Characterization

Monomer conversions and monomer to monomer ratios were determined via the use of ^{1}H NMR, as described in 7.1.1.

Molecular weight distributions were determined by employing two SEC systems. A description of the employed THF-SEC system can be found in 7.1.2. The employed DMF-SEC elugrams were measured by our collaboration partner: the Center for Education and Research on Macromolecules, Chemistry Department, University of Liège. There, SEC was carried out in DMF/LiBr (2.17 g L^{-1}) (flow rate 1 mL min^{-1}) at 40°C using a Waters 717 autosampler liquid chromatograph equipped with a differential refractometer index detector when polymers became insoluble in THF. Waters gel 5 μm (10^5, 10^4, 500, and 100 Å) columns were calibrated with polystyrene standards.

The THF-SEC has been employed during the optimization of the iBP polymerization, while a DMF-SEC was used for the samples of the BP polymerization due to the better solubility of the BP polymer in DMF. The data as given in reference to the thiol–ene modified polymers were measured in THF. It should be noted that analysis with DMF-SEC leads to slightly larger molecular weights with respect to measurements performed in THF-SEC. Due to calibration with PS standards, however, both systems systematically underestimate M_n.

7.4.3 Microreactor set-up

The polymerizations of iBP and BP were performed in a Labtrix® Start R2.2 system (7.2.1), equipped with a microchip reactor of which a 19.5 μL microreactor (Chemtrix 3227 reactor) and a 5 μL microreactor (Chemtrix 3222 reactor) were employed.

The UV-mediated thiol-ene reactions were also carried out in a Labtrix® Start R2.2 system. The microreactor system was illuminated with UV light via an OmniCure Series 1000 system equipped with a 100 W high pressure mercury vapor short arc lamp (spectral emission: 320–500 nm, maximum 365 nm).

In order to perform a reaction coupling of both the polymerization as well as the post-modification in one step, a microreactor cascade was employed, consisting of two coupled Labtrix® Start R2.2 systems (Figure 3.3). The outlet of the first reactor chip ('polymerization', 19.5 μL reactor) was connected directly to the inlet of a second microreactor system ('thiol-ene', 5 μL reactor) via a short piece of unheated PEEK 1/32" tubing and an in-line manometer to monitor and detect possible blockages at a premature stage. An additional check valve (Upchurch scientific) was placed at the entrance of the second reactor to prevent solvent or product backflow from the second to the first reactor. At the end of the reactor cascade, a pre-set back pressure regulator (Upchurch Scientific) was placed to maintain the system at 20 bar of back pressure.

7.4.4 Polymerizations of iBP

For the anionic ring-opening polymerization of 2-isobutoxy-2-oxo-1,3,2-dioxaphospholane (iBP), two catalytic systems were tested: either the DBU system with TU as cocatalyst was employed with $[iBP]_0/[BzOH]_0/[DBU]_0/[TU]_0$ = 30 / 1 / 1.5 / 1.5, or TBD as catalyst with $[iBP]_0/[BzOH]_0/[TBD]_0$ = 30 / 1 / 0.15. In both cases, a stock solution was prepared of the catalyst (60 μL DBU and 148 mg TU or 4.7 mg TBD) and the initiator (28 μL BzOH) was prepared in toluene (2 mL). Two gastight 1 mL syringes were filled under nitrogen atmosphere with the stock solution and iBP, respectively, and applied to the microreactor set-up. The relative ratios of the flow rates of the stock solution and iBP were kept constant at 1 / 0.58 providing a polymer with a degree of polymerization (DP) of 30 and a total monomer concentration of 2.53 M. A quench syringe with a 1 M solution of acetic acid in toluene was applied to the third inlet to prevent further polymerization.

7.4.5 Polymerizations of BP

The anionic ring-opening polymerization of 2-butenoxy-1,3,2-dioxaphospholane (BP) was carried out in a similar way as the polymerization of iBP. Here, the relative ratios of the flow rates of the stock solution and BP were kept constant at 1 / 0.60 providing a DP 30 polymer and a total monomer concentration of 2.50 M.

7.4.6 Post-functionalization via UV-mediated thiol-ene

In order to post-functionalize the BP polymer, the obtained BP polymer was dissolved in toluene to mimic the outcome of the BP polymerization (2.5 M BP, 1 eq corresponding to one BP unit). A second stock solution was prepared of the photoinitiator DMPA (32 mg, 0.05 eq) and 1-dodecanethiol (890 μL, 1.5 eq) in DCM (110 μL). Two 1 mL syringes were filled with the polymer solution and the stock solution, respectively. Reaction temperature was kept constant at 25°C. Residence times were varied by adjusting the flow rates, keeping the flow rates of both solutions identical to obtain $[BP]_0/[DMPA]_0/[thiol]_0$ = 1 / 0.05 / 1.5.

7.4.7 Microreactor coupling: polymerization of BP and post-functionalization via one microreactor cascade

In a first microreactor (19.5 μL), the anionic ring-opening polymerization of 2-butenoxy-1,3,2-dioxaphospholane (BP) was carried out in toluene at 40°C with DBU/TU as catalytic system, as described above. The outcome of this reactor was directly coupled to the entrance of the second reactor set-up, (5 μL), where the stock solution of DMPA (32 mg, 0.05 eq) and dodecanethiol (890 μL, 1.5 eq) in DCM (110 μL) was injected via the second inlet. Similarly to the thiol-ene reactons, DCM was continuously injected via the third inlet of the second reactor in order to prevent blockages at this stage. A scheme of the set-up is shown in Figure 7.3.

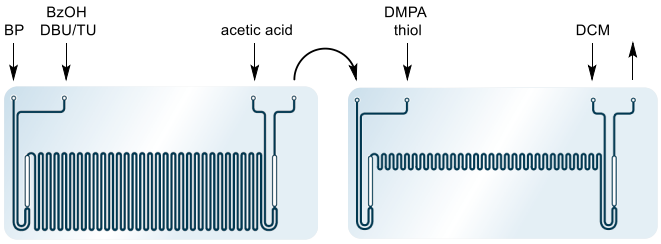

Figure 7.3. Scheme of the microreactor cascade with indicated injection points.

Due to the direct coupling, the flow rates of both systems should correspond to each other. The residence time in the second reactor is therefore completely dependent of the residence time in the first reactor (and the reactor volume of the second reactor). A 19.5 μL reactor was employed for the polymerization and a 5 μL reactor for the thiol-ene reaction. Flow rates were preset at 0.73 μL min^{-1}, 1.22 μL min^{-1}, 0.73 μL min^{-1}, 1.95 μL min^{-1} and 0.73 μL min^{-1} for the injection of BP, the polymerization stock, acetic acid quench, thiol-ene stock and DCM, respectively. Hereby, the molar equivalences of $[BP]_0/[BzOH]_0/[DBU]_0/[TU]_0/[DMPA]_0/[thiol]$ were kept constant at 30 / 1 / 1.5 / 1.5 / 1.5 / 45.

7.5 Experimental Chapter 4 – RAFT multiblock copolymers

7.5.1 Materials

n-Butyl acrylate (*n*BuA) (Acros, 99%), methyl acrylate (MA) (Acros, 99%), ethyl acrylate (EA) (Acros, 99.5%), *t*-butyl acrylate (*t*BuA) (J&K, 98.5%), 2-hydroxyethyl acrylate (HEA) (TCI, 95%), *N*-isopropylacrylamide (NIPAM) (Acros, 99%), 2-ethylhexyl acrylate (EHA) (TCI, 99%) and 2-(2-ethoxyethoxy)ethyl acrylate (DEGA) (TCI, 98%) were deinhibited over a column of activated basic alumina, prior to use. 1,1'-Azobis(isobutyronitrile) (AIBN) (Sigma-Aldrich, 98%) was recrystallized twice from methanol prior to use. The RAFT agent 2-(dodecylthiocarbonothioylthio)propionic acid (DoPAT) was synthesized according to a literature procedure.[5] *n*-Butanol (Fisher, 99%) was used as received.

7.5.2 Characterization

Monomer conversions and monomer to monomer ratios were determined via the use of ^{1}H NMR, as described in 7.1.1. In order to determine monomer conversion of the last block in tri- and tetrablock copolymerizations, dibromomethane was added to the stock solution and employed as internal standard.

Molecular weight distributions were determined via the use of SEC employing THF as eluent, as described in 7.1.2. Molar masses and dispersity values were calculated against the Mark-Houwink parameters of PnBuA ($K = 12.2 \times 10^{-5}$ dL g^{1} and $\alpha = 0.70$).

In-situ FT-IR spectroscopy was employed to monitor monomer conversions by measuring the area of the acrylate peaks (1650 – 1605 cm^{-1}). Therefore, a ReactIR 15 (Mettler Toledo) spectrometer, equipped with a DS Micro Flow Cell with an optical range 4000 – 650 cm^{-1} was connected to the employed reactor set-up.

The fidelity of the polymer end group was observed via the use of ESI-MS, as described in 7.1.3.

7.5.3 Reactor set-up

A home-made tubular reactor cascade was built, consisting of gastight PFA tubing (Advanced Polymer Tubing GmbH, 1/16" OD, 0.75 mm ID), wrapped around a metal framework and placed in a silicon oil bath heated to 100°C on an IKA RCT basic hot plate. Reactor volumes could easily be adapted by varying the length of the reactor tubing. Reaction solutions were pumped into the reactor via Knauer Azura P 2.1S HPLC Pumps. Different reactor cascades were built by coupling several tubular reactors in a row via the use of a T-piece (Vici, ZT1, 0.75 mm bore, whereby both inlet flows were connected perpendicular to the outlet flow for mixing purposes). At the end of the reactor cascade, a back pressure regulator of 100 psi was placed to ensure stable flow conditions. Here, a single 0.8 mL tubular reactor was employed for homopolymerizations. A 0.8 mL tubular reactor was coupled to a 3.6 mL tubular reactor to target diblock copolymers. Triblock copolymerizations were carried out in a [0.8 mL + 3.6 mL + 5.2 mL] tubular reactor cascade (Figure 7.4), which could further be extended with a 6.8 mL tubular reactor when targeting tetrablock copolymers (Figure 4.3). The reasoning behind these specific reactor volumes is explained in Chapter 4.

Figure 7.4. Representation of the [0.8 mL + 3.6 mL + 5.2 mL] tubular reactor cascade, employed for triblock copolymerizations.

7.5.4 Continuous RAFT homopolymerization

In a typical procedure, 40 mmol (5.127 g, 10 eq, 4 M) of the monomer *n*BuA, 4 mmol (1.402 g, 1 eq) of the RAFT agent DoPAT and 0.2 mmol (33 mg, 0.05 eq) of the initiator AIBN were dissolved in *n*-butanol. The solution was kept in a sealed Duran® flask, connected to the reactor set-up via a HPLC pump and purged with argon prior to use. A 0.8 mL tubular reactor was employed for the polymerization at a temperature of 100°C with a residence time of 16 min (0.050 mL min^{-1} flow rate). Monomer conversions were determined via ^{1}H NMR (95%). Molecular weight distributions were analyzed via SEC (1630 g mol^{-1}, $Đ$ = 1.11).

Identical procedures were also followed for the polymerization of MA, EA, *t*BuA and HEA, by employing a monomer concentration of 4 M, while lower monomer concentrations were employed for EHA (2.7 M) and DEGA (3 M).

Long chain lengths could also be targeted by varying the *n*BuA/DoPAT ratio, keeping the monomer concentration constant at 4 M (except of the DP 5 polymer where a 2 M *n*BuA concentration was employed).

7.5.5 Continuous diblock copolymerization

The first stock solution was prepared similar to the homopolymerizations. In a second stock solution, 50 mmol (4.305 g, 10 eq, 5 M) MA and 0.25 mmol (41 mg, 0.05 eq) AIBN were dissolved in *n*-butanol. The solution was kept in a sealed Duran® flask at 0°C and protected from light. The solution was connected to the reactor set-up via a second HPLC pump and purged with Ar prior to use. A [0.8 mL + 3.6 mL] tubular reactor cascade was employed for the polymerizations. The residence time for the first block was kept constant at 16 min (0.050 mL min^{-1} flow rate 1), while 40 min residence time was employed for the second block (0.040 mL min^{-1} flow rate 2). Monomer conversions of the second block were determined via ^{1}H NMR (96%) and molecular weight distributions were analyzed via SEC (1950 g mol^{-1}, $Đ$ = 1.21).

Similar strategies were followed to develop a large variety of diblock copolymers based on 7 different acrylates and an acrylamide. Depending on the monomer concentrations, flow rates could be adjusted to assure a 1/1 monomer/monomer ratio. (For example: a residence time of 19.5 min was employed for the first block (0.041 mL min^{-1} flow rate 1) and 40 min for the second block (0.049 mL min^{-1} flow rate 2) to develop a P*n*BuA-*b*-PDEGA diblock copolymer.)

Diblock copolymers with different monomer/monomer ratios were also targeted by varying flow rate 2 (and adapting the required reactors). For example: a P*n*BuA-*b*-PMA diblock with a "10/20" *n*BuA/MA ratio (DP 10 P*n*BuA block *vs* DP 20 MA block) could be obtained by employing 0.050 mL min^{-1} flow rate of the *n*BuA solution (16 min residence time) and 0.08 mL min^{-1} flow rate of the MA solution (40 min residence time) in a [0.8 mL + 5.2 mL] tubular reactor cascade. Here, 3

types of diblock copolymers were targeted with different monomer/monomer ratios and thus different chain lengths: P*n*BuA-*b*-PMA, P*n*BuA-*b*-PHEA and P*n*BuA-*b*-PDEGA.

7.5.6 Continuous triblock copolymerizations

The first stock solution was prepared similar to the homopolymerizations. The second stock solution was prepared similar to the diblock copolymerizations, though more AIBN was added (0.45 mmol, 74 mg, 0.09 eq). In a third stock solution, 50 mmol (5.006 g, 10 eq, 5 M) of the monomer EA and 0.65 mmol (107 mg, 0.13 eq) of the initiator AIBN were dissolved in *n*-butanol. The solution was kept in a sealed Duran® flask at 0°C and protected from light. The solution was connected to the reactor set-up via a third HPLC pump and purged with Ar prior to use. A [0.8 mL + 3.6 mL + 5.2 mL] tubular reactor cascade was employed for the polymerizations. By carefully choosing the reactor volume of the third block, and its corresponding flow rate, a 1:1:1 ratio between monomer 1, 2 and 3 could be achieved. Hence, residence times of 16 min, 40 min and 40 min were employed for the first, second and third block, respectively (0.050 mL min^{-1} flow rate 1, 0.040 mL min^{-1} flow rate 2 and 0.040mL min^{-1} flow rate 3). Monomer conversions of the third block were determined via ^{1}H NMR (92%) and molecular weight distributions were analyzed via SEC (2260 g mol^{-1}, $Đ$ = 1.35).

Other triblock copolymers could be obtained via a similar procedure as described above. Depending on the monomer concentrations, flow rates could be adjusted to assure 1/1/1 monomer/monomer/monomer ratios.

7.5.7 Continuous tetrablock copolymerizations

The first stock solution was prepared by dissolving 40 mmol (5.127 g, 10 eq, 4 M) *n*BuA, 4 mmol (1.402 g, 1 eq) DoPAT and 0.2 mmol (33 mg, 0.05 eq) AIBN in *n*-butanol. The solution was kept in a sealed Duran® flask, connected to the reactor set-up via the first HPLC pump and purged with Ar prior to use. In a second stock solution, 50 mmol (4.305 g, 10 eq, 5 M) MA and 0.45 mmol (74 mg, 0.09 eq) AIBN were dissolved in *n*-butanol. The solution was kept in a sealed Duran® flask at 0°C and protected from light. The solution was connected to the reactor set-up via a second HPLC pump and purged with Ar prior to use. A third stock solution was prepared by dissolving 50 mmol (5.006 g, 10 eq, 5 M) EA and 0.65 mmol (107 mg, 0.13 eq) AIBN in *n*-butanol. The solution was kept in a sealed Duran® flask at 0°C and protected from light. The solution was connected to the reactor set-up via a third HPLC pump and purged with Ar prior to use. In a fourth stock solution, 50 mmol (6.409 g, 10 eq, 5 M) *t*BuA and 0.85 mmol (140 mg, 0.17 eq) AIBN were dissolved in *n*-butanol. The solution was kept in a sealed Duran® flask at 0°C and protected from light. The solution was connected to the reactor set-up via a fourth HPLC pump and purged with argon prior to use. A schematic overview is shown in Figure 7.4. A [0.8 mL + 3.6 mL + 5.2 mL + 6.4 mL] tubular reactor cascade was employed for the polymerizations (Figure 4.3 and 7.5). By carefully choosing the reactor volume of the third block, and its corresponding flow rate, a 1:1:1:1 ratio between monomer 1, 2, 3 and 4 could be achieved. Hence, residence times of 16 min, 40 min, 40 min and 40 min were employed for the first, second, third and fourth block, respectively (0.050 mL min^{-1} flow rate 1, 0.040 mL min^{-1} flow rate 2, 0.040 mL min^{-1} flow rate 3 and 0.040 mL min^{-1} flow rate 4). Monomer conversions of the fourth block were determined via ^{1}H NMR (92%) and molecular weight distributions were analyzed via SEC

(2990 g mol^{-1}, $Đ$ = 1.47) (calibrated using PS standards, calculations based on the Mark-Houwink parameters of P*n*BuA). By employing the described reactor-set-up and collecting for 26 h 05 min, 152.4 g product could be obtained (after solvent removal).

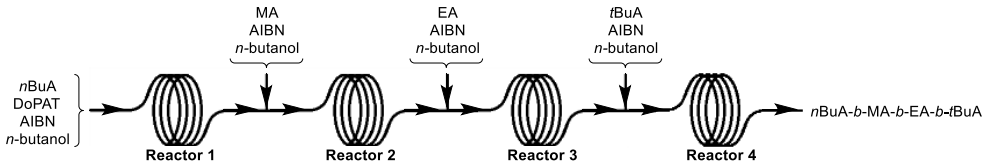

Figure 7.5. Schematic overview of the continuous synthesis of the P*n*BuA-*b*-PMA-*b*-PEA-*b*-P*t*BuA tetrablock copolymer.

Other tetrablock copolymers could be targeted as well. As example, also an EA-*b*-*t*BuA-*b*-HEA-*b*-MA tetrablock copolymer was synthesized by employing the same reactor cascade (Figure 7.6 and Figure 4.3). Yet, depending on the employed monomer concentrations, flow rates must be adjusted to assure a 1:1:1:1 ratio between monomer 1, 2, 3 and 4.

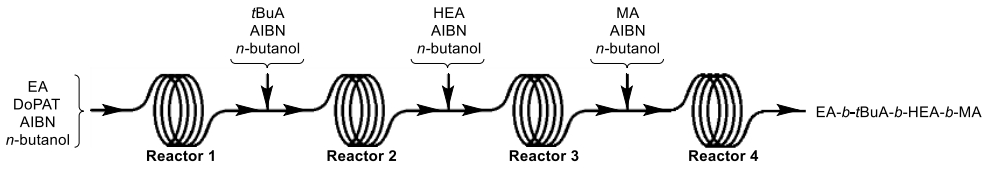

Figure 7.6. Schematic overview of the continuous synthesis of the PEA-*b*-P*t*BuA-*b*-PHEA-*b*-PMA tetrablock copolymer.

7.6 Experimental Chapter 5 – Enzymatic polymerizations

7.6.1 Materials

Bovine serum albumin (BSA), peroxidase from horseradish (HRP), hemoglobin from bovine blood (Hb), DL-dithiothreitol (DTT), (+)-sodium L-ascorbate (NaAsc), 2-hydroxyethyl 2-bromoisobutyrate (HEBIB) and *N,N*-dimethylformamide (DMF) (Chromasolv plus) were purchased from Sigma-Aldrich and were used as received. The fluorescent dyes ATTO 488, ATTO 647 and ATTO 550 based on NHS-esters were directly purchased from ATTO-Tec (Germany) and were used as received. 4-Acryloylmorpholine (AcMo) (Aldrich) was deinhibited over a column of activated basic alumina prior to use. Cys-blocked hemoglobin (cys-b-Hb) was kindly provided by the collaboration partner (Adolphe Merkle Institute). The employed dishwasher detergent was neodisher® LaboClean A8 (Chemische Fabrik Dr. Weigert), distributed by VWR.

7.6.2 Characterization

UV-Vis spectroscopy measurements were conducted using an Analytic Jena Specord 50 PLUS spectrometer from 190 nm to 700 nm, using quartz cuvettes with a path length of 10 mm.

Monomer conversions and the presence/absence of polymer end groups were determined via the use of ^{1}H NMR, employing D_2O as solvent (described in 7.1.1).

Molecular weight distributions were determined via the use of SEC employing THF as eluent. The polymers made via flow experiments were measured in-house (7.1.2). For the polymers produced in batch, the SEC system of our collaboration partner was employed. There, SEC measurements were carried out on an Agilent Technologies 1200 system equipped with a Wyatt Optilab rEX differential refractive index (dRI) detector and a Wyatt miniDAWN TREOS multiangle laser light scattering (MALLS) detector. The column system was composed of an Agilent 5 μm MIXED-C guard column and a PLgel 5 μm MIXED-D (200−400 000 g mol^{-1}) column. THF was employed as solvent/eluent and the measurements were carried out at a flow rate of 1 mL min^{-1}. The mass average molecular weight (M_w) and M_n values were determined in comparison with poly(styrene) standards.

Fluoresence intensities were measured to test the stability of the enzymes by employing a micro plate reader from FLUOstar Omega-BMG Labtech, equipped with a Xenon lamp and measuring from 240 to 750 nm.

7.6.3 Reactor set-up

Several microchip reactors of the Labtrix® Start R2.2 system (7.2.1) were employed during the enzyme immobilization strategy in order to obtain an enzyme-immobilized reactor (7.6.6). Here, a 19.5 μL (3227), a 11.5 μL (3023) and a 10 μL (3223) microreactor were employed. The Labtrix® Start R2.2 system itself (7.2.1) was employed to carry out the homogeneous polymerization of AcMo under flow conditions and to test the enzyme-immobilized reactor chips. A home-made tubular microreactor was made employing 5 ft red PEEK tubing (ID 125 μm) (Figure 5.11). Connection parts and check valves of a Labtrix® Start R2.2 system were employed.

7.6.4 Fluorescent labeling

A labeling buffer solution was prepared in order to perform the fluorescent labeling of the enzymes. First, a phosphate-buffered saline (PBS) buffer with a pH of 7.4 was prepared by dissolving 8 g NaCl, 0.2 g KCl, 1.44 g Na_2HPO_4 . 2 H_2O and 0.24 g KH_2PO_4 in 1 L distilled water. To 20 parts of this PBS buffer (100 mL), 1 part of a 0.2 M $NaHCO_3$ solution (5 mL) (adjusted to pH 9.0 with a 2 M NaOH solution) was added to obtain the labeling buffer (pH 8.3).

Next to a labelling buffer solution, also a dye solution was prepared. The Atto dye (1 mg) was dissolved in 100 μL DMSO. This stock solution was diluted to obtain a 1 mg mL^{-1} dye solution.

To fluorescently label the enzyme, 1 mg of enzyme was dissolved in 1 mL labelling buffer, after which 50 μL of the 1 mg mL^{-1} dye solution (10 eq) was added to the protein solution. After gentle shaking, the resulting solution was placed in the dark to incubate for 1 h. The unbound dye was removed afterwards by employing a Vivaspin®500 centrifugal concentrator (3 kDa MWCO). The obtained protein solution was diluted with the labelling buffer, resulting in a 1 mg mL^{-1} labelled protein solution. UV-Vis was employed to determine the degree of labeling.

BSA was labeled with ATTO 488. An absorption maximum was observed at 500 nm and a degree of labeling of 1.57 was determined. Horseradish peroxidase (HPR) was labeled with ATTO 647. An absorption maximum was observed at 647 nm and a degree of labeling of 1.70 was determined. Hemoglobin (Hb) was labeled with ATTO 550. An absorption maximum was observed at 561 nm and a degree of labeling of 1.98 was determined.

7.6.5 Conjugation of the active enzyme to SPDP

A linkage buffer solution was prepared in order to couple to active enzyme to the SPDP linker. Therefore, 29.3 mg ethylenediaminetetraacetic acid (EDTA) was dissolved in a 10 mL concentrated PBS solution, and diluted to 100 mL. The pH was adjusted to 7.6 via a 4 M NaOH solution.

Next to a linkage buffer solution, also a linker solution was prepared by dissolving 2.5 mg SPDP linker in 320 μL DMSO.

To link the active enzyme to an SPDP linker, 1 mg enzyme was dissolved in 1 mL linkage buffer solution, after which 5 μL linker solution was added. After gentle shaking, the resulting solution was placed in the dark to incubate for 30 min. The unbound SPDP linker was removed afterwards by employing a Vivaspin®500 centrifugal concentrator (3 kDa MWCO). The obtained protein solution was diluted with the linkage buffer, resulting in a 1 mg mL^{-1} SPDP-protein solution.

A fluorescently labeled SPDP-HRP solution was obtained by adding the 5 μL linker solution directly to the 1 mg mL^{-1} fluorescently labeled HRP solution (labeling buffer). By removing the unbound SPDP linker, the protein was transferred to a 1 mg mL^{-1} solution based on the linkage buffer. A similar strategy was employed to obtain a fluorescently labeled SPDP-Hb solution.

7.6.6 Enzyme-immobilized microreactor

A glass chip reactor (7.2.1 and 7.6.3) was cleaned thoroughly. Therefore, the glass chip reactor was placed in the oven and slowly heated (max 4°C min^{-1}) to 400°C. The reactor was manually flushed with the labelling buffer in order to remove all residual particles. A 1 mg mL^{-1} BSA solution (labeling buffer) was continuously injected into the glass reactor with a residence time of 5 min. The reactor was allowed to incubate by continuously injecting of protein solution for 1 h ('incubation time'). Next, the reactor was flushed with a 1 mg mL^{-1} dithiothreitol (DTT) solution (labeling buffer) to activate the BSA cysteines. Afterwards, the SPDP-enzyme was directly linked to the activated BSA on the reactor wall. Therefore, a 1 mg mL^{-1} SPDP-enzyme solution (either SPDP-HRP or SPDP-Hb) (linkage buffer) was flushed through the microreactor with a residence time of 5 min and an incubation time of 1 h. Afterwards, the reactor was extensively rinsed with the linkage buffer to remove residual proteins.

To visualize the success of the immobilization strategy, fluorescently labeled proteins were employed (fluorescently labeled BSA, SPDP-HRP and SPDP-Hb). After each step, an extra rinsing step with the corresponding buffer was carried out to remove all unreacted fluorescently labeled proteins.

7.6.7 Removal of the proteins

In order to reverse the immobilization step and detach the enzymes, a 1 mg mL^{-1} dishwasher detergent solution in water was rinsed through the reactor chip overnight. After rinsing the reactor chip with buffer, the reactors could in principle be reused again. Yet, in order to avoid all interference, the reactor was cleaned thoroughly by repeating the heating step in the oven as well.

7.6.8 (Cys-b-Hb)-catalyzed batch polymerization of AcMo

Two solutions were prepared to carry out the (cys-b-Hb)-catalyzed batch polymerization of AcMo. An enzyme solution was prepared by diluting 0.491 mL cys-b-Hb with 1.510 mL acetate buffer (0.1 M, pH 3.0). Several freeze-pump-thaw cycles were applied to remove all residual oxygen in the solution. A second solution was prepared by dissolving 117.3 mg NaAsc, 34.3 μL HEBIB and 2.09 mL AcMo in 6.15 mL acetate buffer and 1.00 mL DMF. This second solution was purged with argon for 40 min. To carry out the polymerization, 4.64 mL of the second solution were added to the enzyme solution. The resulting solution was allowed to react under argon atmosphere. Aliquots of 1 mL were taken at specific times: 0.5 mL was diluted with D_2O and employed to determine monomer conversions via ^1H NMR. The other 0.5 mL was centrifuged to precipitate the hemoglobin. The residual solution was diluted with THF and dried with $MgSO_4$ to remove all water before SEC measurements were performed.

7.6.9 Homogeneous (cys-b-Hb)-catalyzed flow polymerization of AcMo

Based on the batch procedure described above (7.6.8), a flow procedure was developed. The same stock solutions were prepared (in smaller quantities). Two gastight syringes were filled: one with the enzyme solution and one with the second solution. The syringes were connected to the employed microreactor system and were injected at a 1/2.32 flow rate ratio (0.196 and 0.454 μL min^{-1}, respectively). Two different reactor systems were employed: the Labtrix® Start R2.2 system (7.2.1) and a home-made tubular microreactor with 5 ft long PEEK tubing (ID 125 μm) (Figure 5.11). Despite longer residence times (30 min – 1 h) and despite higher temperatures (60°C), only low monomer conversions were observed.

7.6.10 Continuous polymerization in the (cys-b-Hb) immobilized reactor

A stock solution was prepared by dissolving 39.1 mg NaAsc, 11.4 μL HEBIB and 697 μL AcMo in 2.05 mL acetate buffer and 666 μL DMF. The solution was purged with argon, before filling two gastight syringes. The solution was then injected in a 19.5 μL enzyme-immobilized chip reactor, with a flow rate of 0.325 μL min^{-1} (30 min residence time). Different monomer/initiator/reducing agent ratios were employed. Also different solvent compositions were tested. Yet, no polymer distributions could be observed via SEC. For reactions with a stronger reducing agent, 34.4 mg $Na_2S_2O_4$ was employed instead of 39.1 mg NaAsc, and injected into the enzyme-immobilized reactor. Here, polymer distributions were observed, as depicted in Table 5.4.

7.6.11 Stability tests of the enzyme-immobilized reactor against $Na_2S_2O_4$

An enzyme-immobilized reactor was prepared, with (non-fluorescent) BSA, DTT and fluorescently labeled Hb-SPDP. After the immobilization, the reactor was manually rinsed with water to remove all residual fluorescently labeled proteins. To test the stability of the enzyme-immobilized reactor, a solution of 10 mg mL^{-1} $Na_2S_2O_4$ in the employed acetate buffer (0.1 M, pH 3) was flushed through the reactor. Aliquots were taken at the outlet of the reaction: during the first 10 min, during the first hour and during the next 4 hours. The fluorescence intensity of those aliquots was measured, showing the release of the fluorescently labeled enzyme from the reactor.

7.7 Experimental Chapter 6 – Cyclic polymer preparation

7.7.1 Materials

Methyl acrylate (MA) (Acros, 99%) was deinhibited over a column of activated basic alumina prior to use. 1,1'-Azobis(isobutyronitrile) (AIBN) (Sigma-Aldrich, 98%) was recrystallized twice from methanol prior to use. The RAFT agent (Figure 6.5) was kindly provided by our collaboration partner (Karlsruhe Institute of Technology / Queensland University of Technology). Toluene (Aldrich) was dried via the use of a MB-SPS 800 system. Acetonitrile (ACN) was purchased from VWR and was used as received.

7.7.2 Characterization

Monomer conversions and the presence/absence of polymer end groups were determined via the use of ^{1}H NMR (7.1.1).

Molecular weight distributions were determined via the use of SEC employing THF as eluent (7.1.2).

UV-Vis measurements were recorded on a Varian Cary 500 UV-Vis-NIR spectrometer (scan rate 600 nm min^{-1}, continuous run from 200 to 800 nm).

Preparative (recycling) SEC was performed on a JAI LC-9110 NEXT system equipped with a JAIGEL 2*H* and 3*H* column ($CHCl_3$ as eluent, 3.5 mL min^{-1} as flow rate).

7.7.3 Synthesis of the α,ω-functionalized linear precursor

A solution of 0.6 mg AIBN (0.05 eq), 50 mg RAFT agent (1 eq) (Figure 6.5) and 0.648 g MA (100 eq) in 0.648 g toluene was prepared and purged with argon prior to use. The reaction solution was heated to 70°C. After 19 h reaction time, 68% monomer conversion was observed, and an α,ω-functionalized MA polymer was collected with a molecular weight of 6890 g mol^{-1} and a dispersity of 1.27.

7.7.4 Intramolecular coupling toward cyclic polymers

A stock solution of 19 mg α,ω-functionalized MA polymer in 3.8 mL acetonitrile (5 mg mL^{-1}) was prepared and purged with argon. A gastight syringe was filled and placed on a syringe pump as 'injection pump'. Pure acetonitrile was injected via an HPLC pump ('loop pump') into the system to dilute the precursor polymer before entering the reactor (Figure 6.4). Different times were tested by changing the flow rates of the injection and the loop pump, respectively. The concentration of the precursor polymer could easily be adjusted via varying the ratio between the injection and the loop pump. The reaction mixture was collected at the outlet of the reactor tube (as a non-looped system) and was evaporated under nitrogen flow before analysis.

7.7.5 Cyclic polymer preparation in a looped flow reactor

The intramolecular coupling of the α,ω-functionalized precursor polymer was carried out as described above (7.7.4). Here, the outlet van de reactor was collected in the 'solvent' stock ('3' in Figure 6.4) where the loop flow was generated via the HPLC pump ('loop pump'). A residence time of 30 seconds was applied to every cycle and a total run time of 16.7 h was foreseen.

7.8 References

(1) *http://phdcomics.com/comics/archive.php?comicid=413*, Piled Higher and Deeper, by Jorge Cham, retrieved on 18-06-2017.

(2) Bloksma, M. M.; Weber, C.; Perevyazko, I. Y.; Kuse, A.; Baumgärtel, A.; Vollrath, A.; Hoogenboom, R.; Schubert, U. S. Macromolecules **2011**, 44, 4057.

(3) Goossens, H.; Catak, S.; Glassner, M.; de la Rosa, V. R.; Monnery, B. D.; De Proft, F.; Van Speybroeck, V.; Hoogenboom, R. ACS Macro Letters **2013**, 2, 651.

(4) Pratt, R. C.; Lohmeijer, B. G. G.; Long, D. A.; Lundberg, P. N. P.; Dove, A. P.; Li, H.; Wade, C. G.; Waymouth, R. M.; Hedrick, J. L. Macromolecules **2006**, 39, 7863.

(5) Ferguson, C. J.; Hughes, R. J.; Nguyen, D.; Pham, B. T. T.; Gilbert, R. G.; Serelis, A. K.; Such, C. H.; Hawkett, B. S. Macromolecules **2005**, 38, 2191.

CHAPTER 8

Summary and outlook

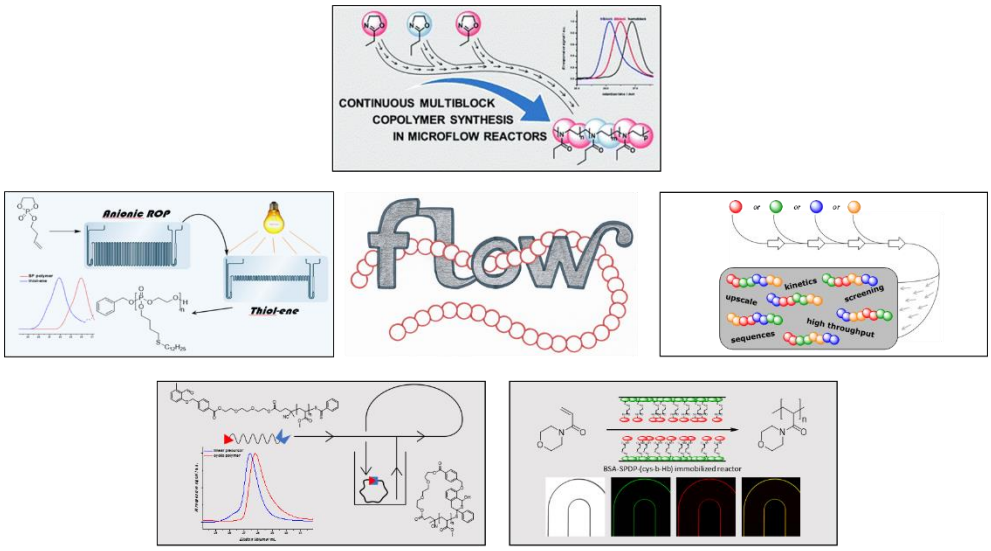

8.1 Summary

Continuous flow processes – an innovative alternative for conventional batch operations – are associated with high control over the reaction parameters, fast heat exchange, high reaction efficiencies and easy scalability. In combination with controlled/"living" polymerization techniques, the polymer field can benefit significantly from microreactor technology. Different polymerization techniques (anionic, cationic, free radical, ATRP, NMP, RAFT, …) were already investigated under continuous conditions. The research in this thesis focused on the development of continuous reactor cascades as an efficient toolbox towards tailor-made polymer materials. Hence, based on the beneficial features of microreactor technology (MRT), different polymerization techniques were employed to synthesize complex polymer materials for future biomedical applications. Divided into five separate research projects, five different reactor set-ups were designed and developed depending on the goal of the project.

Complex macromolecular structures based on poly(2-oxazoline)s have been targeted on a small scale by investigating the cationic ring-opening polymerization of 2-oxazolines in a continuous microflow reactor. The homopolymerizations of 2-ethyl-2-oxazoline and 2-*n*-propyl-2-oxazoline were investigated, aiming for full monomer conversions. Also well-defined diblock and triblock copolymers were produced in a microfluidic reactor cascade (Figure 8.1), demonstrating the high potential of continuous flow chemistry for precision synthesis of complex macromolecules such as block copolymers. (Chapter 2)

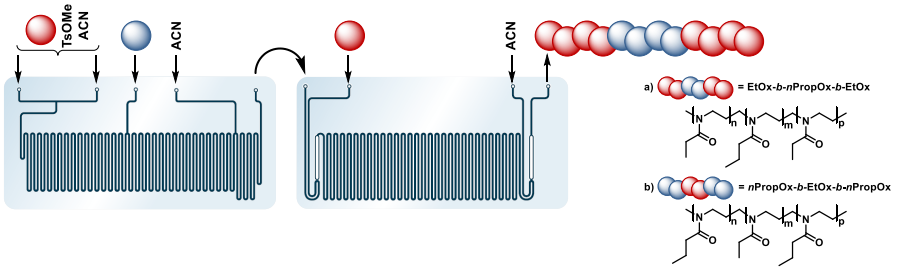

Figure 8.1. Schematic representation of the microfluidic cascade employed for the triblock copolymer synthesis of poly(2-oxazoline)s.

In a second project, the anionic ring-opening polymerization of cyclic phosphates and a direct postmodification step have been investigated towards the synthesis of functional poly(phosphoester)s. Therefore, the homopolymerization of 2-isobutoxy-2-oxo-1,3,2-dioxaphospholane (iBP) has been optimized. After optimization, 2-butenoxy-2-oxo-1,3,2-dioxaphospholane (BP) with an alkene functionality in the side chain was polymerized and directly post modified via a UV-induced radical thiol-ene reaction in a two-stage microfluidic cascade (Figure 8.2) with a high efficiency. (Chapter 3)

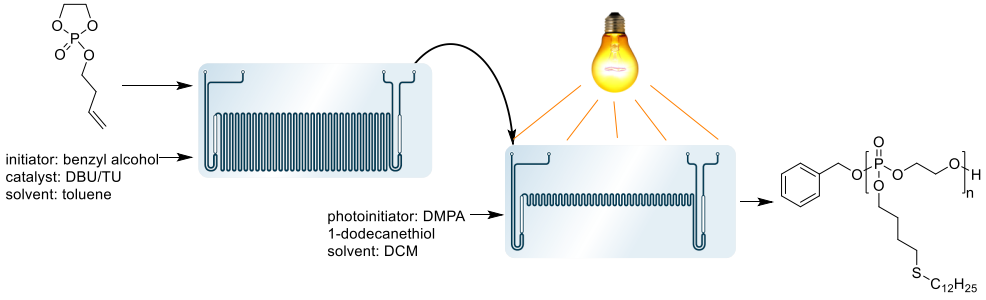

Figure 8.2. Schematic representation of the microfluidic cascade employed for the polymerization and post-functionalization toward functional PPEs.

An upscalable method was investigated for the multiblock copolymer production via reversible addition-fragmentation chain transfer (RAFT) polymerization in a fully continuous multireactor cascade. Theoretic calculations were carried out to target full monomer conversion in order to avoid copolymer formation. A broad variety of homo-, diblock, triblock and tetrablock copolymers was obtained. This procedure is thus extremely useful for high-throughput experimentation. Moreover, the reactor allows for facile upscaling of the reactions: the tetrablock copolymer P*n*BuA-*b*-PMA-*b*-PEA-*b*-P*t*BuA was obtained in quantities of 150 g in 26 h, illustrating the high potential of continuous flow processes for the production of high-value polymer materials (Figure 8.3). (Chapter 4)

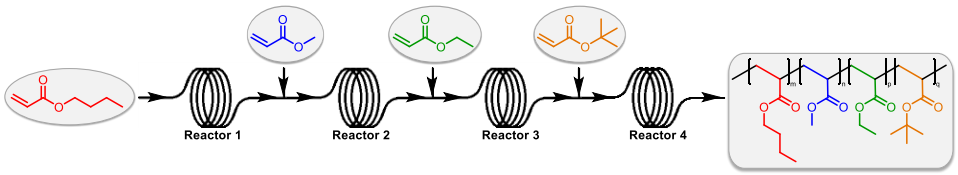

Figure 8.3. Schematic representation of the synthesis of a P*n*BuA-*b*-PMA-*b*-PEA-*b*-P*t*BuA tetrablock copolymer.

Next, an enzyme-immobilized reactor has been developed to carry out continuous enzyme-catalyzed radical polymerizations. A reversible immobilization strategy had been developed to immobilize the enzyme on the reactor wall via physisorption of bovine serum albumin (BSA), which was directly linked to the catalytically active enzyme hemoglobin (Hb) via a *N*-succimidyl 3-(2-pyridyldithio) propionate (SPDP) linker. In a later stage, the Hb-immobilized reactor chips were tested to carry out the enzyme-catalyzed radical polymerization of 4-acryloylmorpholine (AcMo). More research is however needed to establish a polymerization procedure in an immobilized reactor (Figure 8.4). (Chapter 5)

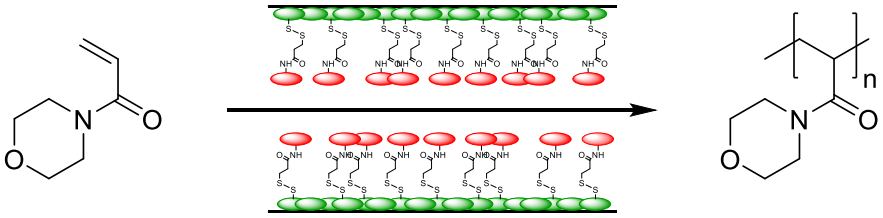

Figure 8.4. Scheme of the enzyme controlled radical polymerization of AcMo in a BSA-SPDP-(cys-b-Hb) immobilized reactor

Finally, cyclic polymers were prepared via a ring-closure strategy in a looped flow reactor. The preparation of cyclic polymers via the ring-closure strategy requires highly diluted reaction solutions (< 0.1 g L^{-1}) to avoid intermolecular side reactions. To overcome this limitation, a looped flow reactor was developed whereby the polymer precursor was gradually added via an injection pump. The polymer precursor was directly diluted by the solvent/cyclic polymer mixture, which recirculates through the recycle loop via the use of a loop pump. This looped flow reactor was then employed to carry out the intramolecular coupling of a synthesized α,ω-functionalized linear polymer precursor, yielding the targeted cyclic polymer (Figure 8.5). (Chapter 6)

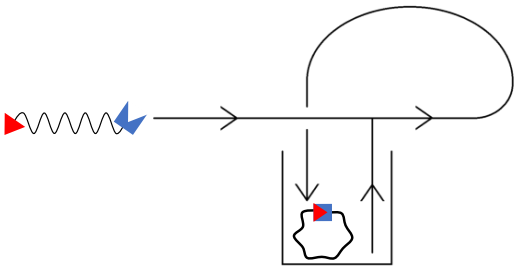

Figure 8.5. Schematic representation of the looped flow reactor as employed for the preparation of cyclic polymers via the ring-closure strategy.

8.2 Samenvatting

Continue flow-processen vormen een innovatief alternatief voor conventionele batch-procedures. Continue flow-processen hebben dan ook heel wat voordelen, zoals een goede controle over de reactieparameters, een efficiënte warmteoverdracht en een eenvoudige (op)schaalbaarheid. In combinatie met gecontroleerde/levende polymerisatietechnieken hebben continue flow-processen heel wat te bieden voor het polymere vakgebied. Verschillende polymerisatietechnieken (anionisch, cationisch, vrij radicalair, ATRP, NMP, RAFT) zijn al eerder onderzocht in continue flow-reactoren. Het onderzoek in deze thesis focust op het ontwikkelen van een continue flow reactorcascade voor de synthese van specifieke polymere materialen voor biomedische toepassingen. Verdeeld in vijf aparte onderzoeksprojecten werden er dan ook vijf verschillende reactoropstellingen gebruikt. Complexe polymere materalen, zoals blokcopolymeren van poly(2-oxazoline)s, werden doelgericht gesynthetiseerd op kleine schaal door gebruik te maken van een continue flow reactorcascade (Figuur 8.1) (Hoofdstuk 2). Directe postmodificatiereacties werden onderzocht voor de synthese van functionele poly(fosfoëster)s (Figuur 8.2) (Hoofdstuk 3). Een opschaalbare productiemethode werd onderzocht voor het aanmaken van multiblokcopolymeren (Figuur 8.3) (Hoofdstuk 4). Een enzyme-geïmmobiliseerde reactor werd ontwikkeld en getest voor enzyme-gekatalyseerde radicalaire polymerizaties (Figuur 8.4) (Hoofdstuk 5). Tenslotte werd er ook een 'looped' reactor ontwikkeld om cyclische polymeren te maken (Figuur 8.5) (Hoofdstuk 6).

8.3 Outlook

After 4 years of PhD research, you should always ask yourself: have I done enough? To me, it just depends on the way you look at it. The world of continuous polymer synthesis changed tremendously during these 4 years. When I started my PhD, polymerizations in continuous flow reactors were generally investigated as proof of concept rather than for preparation purposes. Flow chemistry evolved, leading to the use of continuous flow processes as an effective tool to synthesize and produce tailor-made polymers for application-related purposes. The high industrial interest and multiple industrial projects in academia strongly support that thought. However, continuous flow processes can be so much more than just simply another production method. As illustrated here, continuous flow processes are an efficient toolbox for polymer synthesis by improving the control over the reaction and by reactor telescoping. Yet, continuous flow processes can also be used to design new functional polymers or to investigate novel polymerization protocols. Further development of online monitoring techniques will boost this innovative field, for research and for production purposes. It is only a matter of time. Or as stated by Frey and coworkers: "microreactor technology has only begun to show its eminent potential for controlled polymerizations".

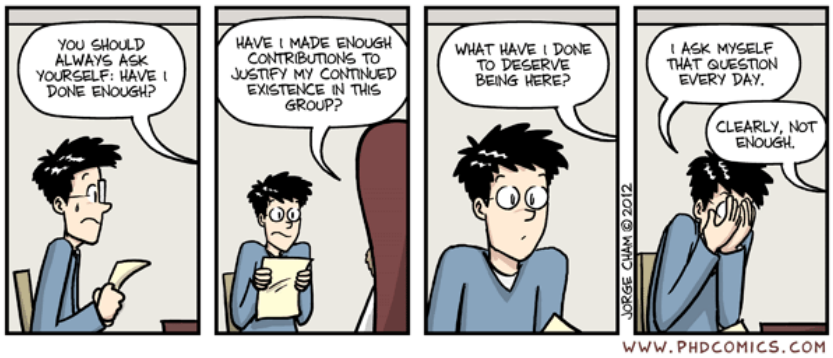

PUBLICATIONS

J. Vandenbergh, T. Tura, E. Baeten, T. Junkers, *Polymer end group modifications and polymer conjugations via "click" chemistry employing microreactor technology,* Journal of Polymer Science Part A: Polymer Chemistry, **2014**, *52*, 1263 – 1274.

E. Baeten, B. Verbraeken, R. Hoogenboom, T. Junkers, *Continuous poly(2-oxazoline) triblock copolymer synthesis in a microfluidic reactor cascade,* Chemical Communications, **2015**, *51*, 11701 – 11704.

N. Zaquen, E. Baeten, J. Vandenbergh, L. Lutsen, D. Vanderzande, T. Junkers, *Continuous synthesis and thermal elimination of sulfinyl-route poly(p-phenylene vinylene) in consecutive flow reactions*, Chemical Engineering and Technology, **2015**, *38*, 10, 1749 – 1757.

E. Baeten, S. Vanslambrouck, C. Jérôme, P. Lecomte, T. Junkers, *Anionic flow polymerizations toward functional polyphosphoesters in microreactors: polymerization and UV-modification*, European Polymer Journal, **2016**, *80*, 208 – 218.

J. J. Haven, E. Baeten, J. Claes, J. Vandenbergh, T. Junkers, *High-throughput polymer screening in microreactors: boosting the Passerini three component reaction*, Polymer Chemistry, **2017**, *8*, 2972 – 2978.

E. Baeten, J. J. Haven, T. Junkers, *RAFT multiblock reactor telescoping: from monomers to tetrablock copolymers in a continuous multistage reactor cascade*, Polymer Chemistry, **2017**, *8*, 3815 – 3824.

E. Baeten, M. Rubens, K. N. R. Wuest, C. Barner-Kowollik, T. Junkers, *Cyclic polymer preparation via a looped flow reactor*, in preparation.

CONFERENCE PRESENTATIONS

Oral Presentations

E. Baeten, S. Vanslambrouck, C. Jérôme, P. Lecomte, T. Junkers, *Green synthesis of polyphosphoesters: a promising class of bioinspired degradable materials*, Interuniversity Attraction Poles (IAP) Functional Supramolecular Systems (P7/05) **2015**, 11.09.2015, Hasselt, Belgium.

E. Baeten, T. Junkers, *Continuous flow synthesis towards complex macromolecular materials: one-step multiblock copolymer synthesis*, Flow Workshop **2016**, 18.01.2016 – 19.01.2016, Hasselt, Belgium.

E. Baeten, B. Verbraeken, R. Hoogenboom, T. Junkers, *Continuous flow synthesis towards complex macromolecular materials: one-step synthesis of poly(2-oxazoline) triblock copolymers*, Chemistry Conference for Young Scientists (ChemCYS) **2016**, 16.03.2016 – 18.03.2016, Blankenberge, Belgium.

Poster Presentations

E. Baeten, R. Hoogenboom, T. Junkers, *Polyoxazolines from cationic polymerization in continuous microflow reactors*, Chemistry Conference for Young Scientists (ChemCYS) **2014**, 27.02.2014 – 28.02.2014, Blankenberge, Belgium.

E. Baeten, B. Verbraeken, R. Hoogenboom, T. Junkers, *Continuous block copolymer synthesis via living cationic polymerization in microflow reactors*, Annual Meeting of the Belgian Polymer Group (BPG) **2014**, 19.05.2014 – 20.05.2014, Ghent, Belgium.

E. Baeten, B. Verbraeken, R. Hoogenboom, T. Junkers, *Poly(2-oxazoline) block copolymer synthesis in continuous microflow reactors*, Interuniversity Attraction Poles (IAP) Functional Supramolecular Systems (P7/05) **2014**, 19.09.2014, Louvain-La-Neuve, Belgium.

E. Baeten, B. Verbraeken, R. Hoogenboom, T. Junkers, *Triblock copolymer synthesis in microflow*, Network for Innovation and Learning on Microreactor Technology (NIL-MRT) symposium **2015**, 19.03.2015, Sittard-Geleen, Netherlands.

E. Baeten, B. Verbraeken, R. Hoogenboom, T. Junkers, *Poly(2-oxazoline) triblock copolymer synthesis in continuous microflow reactors*, Annual Meeting of the Belgian Polymer Group (BPG) **2015**, 18.05.2015 – 19.05.2015, Houffalize, Belgium.

E. Baeten, S. Vanslambrouck, C. Jérôme, P. Lecomte, T. Junkers, *Polymerization of cyclic phosphates in a continuous microflow reactor*, Interuniversity Attraction Poles (IAP) Functional Supramolecular Systems (P7/05) **2015**, 11.09.2015, Hasselt, Belgium.

E. Baeten, M. G. Bussinger, J. Haven, T. Junkers, *Towards multiblock copolymers via RAFT in a microfluidic reactor cascade,* Flow Workshop **2016**, 18.01.2016 – 19.01.2016, Hasselt, Belgium.

E. Baeten, B. Verbraeken, R. Hoogenboom, T. Junkers, *Continuous synthesis toward complex macromolecular materials*, 3rd Belgian-German Macromolecular Meeting (MacroBeGe) **2016**, 15.02.2016 – 16.02.2016, Houffalize, Belgium.

E. Baeten, T. Junkers, *Continuous flow synthesis towards complex macromolecular materials*, Annual Meeting of the Belgian Polymer Group (BPG) **2016**, 23.05.2016 – 24.05.2016, Hasselt, Belgium.

E. Baeten, T. Junkers, *One-step continuous flow synthesis towards functional multiblock copolymers*, Warwick Polymer Conference **2016**, 11.07.2016 – 14.07.2016, Warwick, United Kingdom.

E. Baeten, J. J. Haven, T. Junkers, *Continuous flow synthesis towards functional multiblock copolymers*, Interuniversity Attraction Poles (IAP) Functional Supramolecular Systems (P7/05) **2016**, 12.09.2016, Liège, Belgium.

E. Baeten, J. J. Haven, T. Junkers, *RAFT multiblock reactor telescoping: from monomer to tetrablock copolymers in a single step*, Annual Meeting of the Belgian Polymer Group (BPG) **2017**, 04.05.2017 – 05.05.2017, Houffalize, Belgium.

*** Best Poster Award ***

E. Baeten, J. J. Haven, T. Junkers, *RAFT multiblock reactor telescoping: from monomer to tetrablock copolymers in a single step*, Advanced Polymers via Macromolecular Engineering (APME) **2017**, 21.05.2017 – 25.05.2017, Ghent, Belgium.

DOCTORAL SCHOOL

SCIENCES AND TECHNOLOGY

Teaching Assignments

Chemie voor Levenswetenschappen 1, 09.2013 – 12.2013

Effective Scientific Communication, 05.2014 – 06.2014

Chemie voor Levenswetenschappen 1, 09.2014 – 12.2014

Chemie voor Levenswetenschappen 1, 09.2015 – 11.2015

Chemie voor Levenswetenschappen 1, 09.2016 – 11.2016

Studiereis bachelor Chemie, 11.2016

Modules on Education

Onderwijs en Examenreglement, 28.11.2013

Enhancing interaction with students through questions, 26.09.2014

Studenten in bijzondere omstandigheden, 18.12.2014

Coaching and evaluation in teamwork, 20.01.2015

Gebruik elektronische leeromgeving, 24.02.2015

Advanced courses

Masterclass Flow Chemistry, 09.09.2014

Microwave synthesis, Anton Paar, 08.01.2015

Flow Workshop, 18.01.2016 – 19.01.2016

General courses

IP & Valorisation: What makes an idea a good business idea?, 25.02.2014

Project management: managing my PhD, 02.2014 – 04.2014

Introduction to computational science: the supercomputer, 01.04.2014

Infosession ethics and research integrity, 05.05.2014

Studiedag Chemie en Wereldoorlog I, KVCV, 28.09.2014

Scientific and generic communication

Effective Scientific Communication, organized by Principae, 09.2013 – 10.2013

Academic English, 09.2014

Literature searching skills, 13.11.2014

Presentation skills – how to sell your project, 14.10.2014

Create an awesome poster, 09.2015 – 10.2015

Reviewing skills, 14.10.2015

How to write the impact of a Horizon 2020 proposal, 18.05.2016

Career and personal development

Gain insight into your talents and ambitions, 03.2016 – 06.2016

Individual Career Coaching, VDAB, 2015 – 2016

Grow your self-leadership, organized by Grow to Excel, 03.2017

Acknowledgements

Zo, het zit er bijna op. Hoewel, waarschijnlijk begint het nu… Mijn vier jaar doctoraat zijn omgevlogen. Vier jaar wetenschappelijk onderzoek voeren, in het labo staan en experimenten uitvoeren. Vier jaar vol ideeën, probeersels, ontdekkingen, mislukkingen en successen, gebundeld in dit boekje. Vier jaar om erachter te komen dat '42' ook het antwoord is op 'Flow' (en in uitbreiding op de hele wetenschap). Vier jaar om te ontdekken dat 'Flow Chemie' me kan blijven boeien en kan blijven verbazen.

Tanja, bedankt voor de kans die je me gegeven hebt om dit zelf te ontdekken tijdens een doctoraat. Bedankt voor de vrijheid, de discussies en het vertrouwen door de jaren heen. Bedankt om ons te tonen wat het is om moed te hebben en te tonen, niet alleen in de academische wereld, maar ook daarbuiten. Ik wens jou en de PRD groep dan ook alvast veel succes toe in het verre Australië.

Wouter, als deel van mijn doctoraatscommissie was je nooit veraf. Ook al was je nooit veel betrokken bij de projecten, toch polste je altijd even of alles wel in orde was. Bedankt voor je betrokkenheid, je motivatie en de enthousiaste interesse in al onze sociale OBPC-activiteiten. Dirk, tijdens mijn doctoraat kreeg je het steeds drukker en drukker. Als directeur van het IMO, kregen we je steeds minder en minder te zien. Toch maakte je regelmatig tijd om even bij te praten. Bedankt voor de interesse, je kritische blik en je gezelligheid.

Richard, Philippe and Nico, thank you all for being part of my jury and for your willingness to evaluate the manuscript. Richard, bedankt voor de toffe samenwerking bij het poly(2-oxazoline) project. Ik heb er enorm veel van bijgeleerd en heb me bij je onderzoeksgroep altijd erg welkom gevoeld. Bart, bedankt voor de uitgebreide uitleg, de vele GPC-tjes te meten die ik op zondag bij je thuis kon afzetten. Victor, thanks for the nice collaboration on the upscaling part – good luck with the company! Ook de rest van de Supramolecular Chemistry Group, bedankt voor de geweldige sfeer en de onvergetelijke feestjes op ChemCYS, BPG, en BeGe. Philippe, thanks for the nice collaboration on the polyphosphoesters. I learned a lot about this intriguing polymer class and about the importance of future applications. Merci beaucoup. Stephanie, thanks for all the procedures, your willingness to help and to synthesize again another monomer batch. Nico, thanks for the possibility to go abroad. I really enjoyed my stay at AMI and wished I could have stayed longer. Thanks for the excellent collaboration on the enzymatic polymerizations. Thanks for measuring confocal fluorescence microscopy during the late evening hours and for all the explanations. Bernadetta, thanks for helping me with the HRP polymerizations, too bad we could not get them to work at that time. Jonas, thanks for helping me around, for the Hb polymerizations and for providing me with cys-b-Hb. Also thanks to the rest of Macromolecular Chemistry people.

Christopher, thank you for the collaboration on the cyclic polymers. Eva, thank you for all practical details and explanations. Kilian, thanks for the synthetic part. Further, I would also like to thank some people for all the practical aspects and arrangements during my PhD. Laurence, thank you for all your help on the ordering and budget-wise aspects. Your work is often invisible for us, but you were

always there when we needed help with orders, payments, lab-equipment and so on. Peter, Gunter en Koen, bedankt voor de talrijke NMR metingen. De autosampler heeft nog nooit zo vol gestaan als tijdens mijn uitgebreide kinetica-experimenten. Erik, bedankt voor het onderhoud en de hulp bij de ESI-Orbitrap. Jenny, hartelijk bedankt voor de vele hulp bij de DMF-GPC. Zelfs bij de 'ontplofte' DMF-fles en de talrijke lekkages was je er telkens bij om het probleem op te lossen. Matthias C., Neomy, Joris en Gijs, bedankt voor het onderhoud en de calibratie van de GPC-toestellen. Huguette, bedankt voor het onderhoud en de hulp bij alle andere technische analyse-instrumenten. Eugène, Hilde en Iris, bedankt voor alle didactische ondersteuning. Ik kon altijd wel iets komen lenen als ik eventjes iets extra nodig had. Daarnaast wil ik ook graag de andere vaste personeelsleden van TANC bedanken voor de korte gesprekjes en het talrijke gebruik van de moffeloven, als mijn experimenten weer eens tegenzaten.

Thanks to the students who joined me in doing research: Tiago, Felipe, Mattheus, Vincent, Lauren and Axel. Daarnaast wil ik natuurlijk ook mijn talrijke collega's bedanken voor de leuke periode en voor hun steun. Dankjewel 'Oude Garde' voor de leuke sfeer toen ik hier begon: Joke, Toon, Tom, Inge & Wouter VN (succes met jullie eerste kindje!), Rafaël (succes met je nieuwe job!), Jurgen, Pieter en Neomy. Dankjewel jaargenootjes om hetzelfde proces te doorlopen en de steun onderweg: Sanne, Geert, Joris, Jasmine, Jeroen B., Mathias K. en Rebekka. Veel succes met het schrijven/de verdediging en veel geluk op jullie zoektocht naar een volgende uitdaging. Bedankt BDG voor het gebruik van jullie labo tijdens mijn enzymatische polymerizations: Erik, David, Brecht, Tien, Rebekka, Sofie en Ellie. Dankjewel DSOS voor jullie enthousiasme tijdens OBPC activiteiten, de leuke tijd in het lab en het gezever op bureau: Julija, Jurgen, Pieter, Sanne, Geert (de DSOS

flow expert), Jasmine, Jeroen B., Mathias K., Jorne, Ruben, Dries, Frederik, Tom en Sam. Dankjewel Roald en Wouter V.G., als aparte eenheid binnen OBPC. En natuurlijk een grote dankjewel aan de hele PRD groep: Inge, Matthias C., Veronique, Ya-Mi, Kayte, Benjamin (12 954 emails around midnight are still not funny), Luk, Joke (bedankt voor alle praktische hulp en de vele uitleg), Neomy (bedankt voor het gezellige geklets, de vele discussies en de leuke tijd – enjoy Australia!), Stephan (dankjewel om telkens weer naar mijn 'gezaag en geklaag' te luisteren en om elke keer een helpende hand te bieden), Joris (dankjewel voor de leuke congressen en het rijden ernaartoe, voor de vlotte samenwerkingen en je realistische kijk), Martijn, Joachim (do you know where the duckling is?), Gijs (snow is actually…), Erika, Nok, Svitlana, Kirsten, Maarten (dancing in the dark with cyclic polymers), Jeroen DN, Jeroen V, Lowie, Dries en Axel. Dankjewel allemaal voor de talrijke discussies, de leuke PRD-trips, alle hulp, feedback en verbeteringen.

Tenslotte wil ik ook graag mijn familie en vrienden bedanken voor hun steun tijdens deze periode. Dankjewel voor de steun en toeverlaat, voor het luisterend oor, voor de ontspanning in de vrije tijd en de leuke activiteiten, … Dankjewel!